

THE DETECTION, PREVENTION AND MITIGATION OF
CASCADING OUTAGES IN THE POWER SYSTEM

A Dissertation

by

HONGBIAO SONG

Submitted to the Office of Graduate Studies of
Texas A&M University
in partial fulfillment of the requirements for the degree of

DOCTOR OF PHILOSOPHY

December 2006

Major Subject: Electrical Engineering

THE DETECTION, PREVENTION AND MITIGATION OF
CASCADING OUTAGES IN THE POWER SYSTEM

A Dissertation

by

HONGBIAO SONG

Submitted to the Office of Graduate Studies of
Texas A&M University
in partial fulfillment of the requirements for the degree of

DOCTOR OF PHILOSOPHY

Approved by:

Chair of Committee,	Mladen Kezunovic
Committee Members,	Chanan Singh
	Aniruddha Datta
	William Lively
Head of Department,	Costas Georghiades

December 2006

Major Subject: Electrical Engineering

ABSTRACT

The Detection, Prevention and Mitigation of
Cascading Outages in the Power System. (December 2006)
Hongbiao Song, B.S., North China Electric Power University, China;
M.S., North China Electric Power University, China
Chair of Advisory Committee: Mladen Kezunovic

This dissertation studies the causes and mechanism of power system cascading outages and develops new methods and new tools to help detect, prevent and mitigate the outages. Three effective solutions: a steady state control scheme, a transient stability control scheme, and an interactive system-wide and local scheme have been proposed using those new methods and tools.

A steady state control scheme can help detect and prevent the possible cascading outage at its initial slow steady state progress stage. It uses new methods and new tools to solve the line overload, congestion or bus high/low voltage problems. New methods, such as vulnerability index (VI), margin index (MI), network contribution factor (NCF), topology processing and selected minimum load shedding (SMLS), and new tools, such as transmission network control based on a network contribution factor (NCF) method, generator control based on a generator distribution factor (GDF) method, and load control based on a load distribution factor (LDF) method have been proposed and developed.

A transient stability control scheme can help prevent and mitigate the possible cascading outage at its transient progress stage if there is enough time to take action. It uses one Lyapunov direct method, potential energy boundary surface (PEBS) method, and sensitivity analysis of transient energy margin for fast stabilizing control. The results are verified by the accurate time-domain transient stability analysis

method.

The interactive scheme takes advantage of accurate system-wide and local information and analysis results, uses some techniques from both steady state control and transient stability control, works at both the system-wide level and local substation level, monitors the system all the time, and takes actions when needed to help detect, prevent and mitigate the possible cascading outage.

Comprehensive simulation studies have been implemented using the IEEE 14-bus, 24-bus, 39-bus and 118-bus systems and promising results show the ability of the proposed solutions to help detect, prevent and mitigate cascading outages.

To my wife, Jing Zhang, and my parents, Jianting Song and Haimin Gao, for their love and support

ACKNOWLEDGMENTS

I would like to express my sincere gratitude to my advisor Dr. Mladen Kezunovic for his support and guidance throughout my studies at Texas A&M University. His knowledge and experience helped me a lot on my research work and in completion of this dissertation.

I am also grateful to my committee members Dr. Chanan Singh, Dr. Aniruddha Datta, and Dr. William Lively for their time, comments, and support.

My thanks also go to my great colleagues, Mr. Nan Zhang, Mr. Xu Luo, Mr. Yang Wu, Dr. Peichao Zhang, Mr. Satish Natti, Mr. Goran Latisko, Mr. Levi Portillo, Mr. Zarko Djekic, Ms. Maja Knezev, Ms. Anisha Jonas and other group members in our lab for their cooperation and assistance. It was an enjoyable experience in my life working with them.

Part of my research was sponsored by three projects, one from Electric Power Research Institute (EPRI): “Data Integration and Information Exchange: Impact on Future Substation and EMS Applications and Related Implementation Requirements”, the other two from NSF I/UCRC Power Systems Engineering Research Center (PSerc): “Detection, Prevention and Mitigation of Cascading Events”, and “Transient Testing of Protective Relays: Study of Benefits and Methodology”. I would like to acknowledge the financial support from all the sponsors.

TABLE OF CONTENTS

CHAPTER		Page
I	INTRODUCTION	1
	A. Problem Statement	1
	B. Causes and Consequences	4
	1. Non-technical Causes	4
	2. Technical Causes	5
	3. Consequences	8
	C. Current Research Efforts	9
	D. Research Objectives and Approach	13
	E. Summary	14
II	FUNDAMENTALS OF THE PROPOSED APPROACH	15
	A. Introduction	15
	B. Definitions of Terminologies	15
	C. Mechanism	17
	1. Stages of Cascading Outages	17
	2. Interaction Between the System-wide and Local Levels	18
	3. Case Studies	20
	D. Proposed Solution	25
	E. Summary	27
III	STEADY STATE CONTROL SCHEME	28
	A. Introduction	28
	B. Evaluation by Vulnerability Index and Security Margin Index	30
	1. Vulnerability Index and Margin Index for Generators	31
	2. Vulnerability Index and Margin Index for Buses	32
	3. Vulnerability Index and Margin Index for Branches	32
	4. Vulnerability Index for the Whole System	34
	5. Discussions about Vulnerability Index and Margin Index	35
	C. Identification of the Vulnerable Parts in the System	37
	1. Single-line Connection	37
	2. Single-line Connected Load Bus	37
	3. Double-line Connection	38

CHAPTER	Page
4. Network Contribution Factor (NCF) Method	39
a. Line Parameter Variance	39
b. Bus Parameter Variance	42
c. Flow Network Contribution Factor (FNCF) and Voltage Network Contribution Factor (VNCF)	43
5. Contingency Stiffness Index	44
6. Distance Relay Margin Index	45
D. Prediction of the Overload and Voltage Problems	45
E. Control Methods and Automatic Control Scheme	46
1. Network Contribution Factor (NCF) and NCF Control	46
2. Generator Distribution Factor (GDF) and GDF Control	46
3. Load Distribution Factor (LDF) and LDF Control . .	48
4. Selected Minimum Load Shedding (SMLS)	49
5. A Scheme for Detection and Prevention of Cascad- ing Outages	50
F. Case Study	53
G. Summary	59
IV TRANSIENT STABILITY CONTROL SCHEME	61
A. Introduction	61
B. Transient Stability Analysis Methods	62
C. Transient Stability Control Classification	69
D. Sensitivity Analysis of Transient Energy Margin	72
E. Transient Stability Control Scheme	74
F. Case Study	74
G. Summary	81
V INTERACTIVE SCHEME TO DETECT, PREVENT AND MITIGATE THE CASCADING OUTAGES	82
A. Introduction	82
B. Background of Interaction between System-wide and Local Levels	83
1. Static Analysis of Relay Behavior	83
2. Dynamic Analysis of Relay Behavior	86
C. System-wide Monitoring and Control	88
D. Local Monitoring and Control	89
E. Interactive Scheme	92
F. Case Study	95

CHAPTER	Page
G. Summary	99
VI EVALUATION OF STEADY STATE CONTROL SCHEME, TRANSIENT STABILITY CONTROL SCHEME AND IN- TERACTIVE SCHEME	101
A. Introduction	101
B. Study of Steady State Control Scheme	102
C. Study of Transient Stability Control Scheme	111
D. Study of Interactive Scheme	116
E. Summary	121
VII CONCLUSIONS	122
A. Summary of Achievements	122
B. Research Contribution	124
C. Suggestions for Future Research	125
REFERENCES	126
APPENDIX A	141
APPENDIX B	146
APPENDIX C	150
APPENDIX D	154
VITA	163

LIST OF TABLES

TABLE		Page
I	Summary of some cascading outages around the world	3
II	Vulnerability and margin indices of different conditions	56
III	Solution methods for lines L6(B3-9) & L27(B16-17) outages	57
IV	Solution methods for lines L25(B15-21) & L26(B15-21) outages	59
V	Admittance based control (ABC) means and associated parameters	72
VI	New transient energy margin after line switching	77
VII	New transient energy margin after TCSC switching	79
VIII	Vulnerable lines and their neighboring lines	96
IX	Transmission lines and their thermal limits (in MVA value)	104
X	Top 6 line outages ranked by vulnerability index and margin index	105
XI	Top 6 line outages ranked by vulnerability index based on NCF method (Part I: Total VI, VI at bus and generator parts)	105
XII	Top 6 line outages ranked by vulnerability index based on NCF method (Part II: VI at branch part)	105
XIII	Top 6 line outages ranked by vulnerability index based on PF method (Part I: Total VI, VI at bus and generator parts)	106
XIV	Top 6 line outages ranked by vulnerability index based on PF method (Part II: VI at branch part)	106
XV	Top 6 line outages ranked by margin index based on NCF method	106
XVI	Top 6 line outages ranked by margin index based on PF method	107
XVII	Top 6 line outages ranked by vulnerability index and margin index after L104(B65-68) is out-of-service	108

TABLE	Page
XVIII	Top 6 line outages ranked by vulnerability index and margin index after L126(B68-81) is out-of-service 108
XIX	Line flow before and after L116(B69-75) and L119(B69-77) outage (in p.u.) 109
XX	Generator contribution factors for L126(B68-81) and L127(B81-80) . 109
XXI	Generator contribution factors for L126(B68-81) and L127(B81-80) after adjustment 110
XXII	Solution methods for L126(B68-81) and L127(B81-80) overload . . . 111
XXIII	Sensitivity analysis and fast-valving for stability control 113
XXIV	Stability control means at B69 and their contribution to transient energy margin 116
XXV	Bus data of IEEE 14-bus system 143
XXVI	PV bus data of IEEE 14-bus system 143
XXVII	Line data of IEEE 14-bus system 144
XXVIII	Generator data of IEEE 14-bus system 144
XXIX	Exciter data of IEEE 14-bus system 145
XXX	Bus data of IEEE 24-bus system 146
XXXI	PV bus data of IEEE 24-bus system 147
XXXII	Line data of IEEE 24-bus system 148
XXXIII	Generator data of IEEE 24-bus system 149
XXXIV	Exciter data of IEEE 24-bus system 149
XXXV	PV bus data of IEEE 39-bus system 150
XXXVI	Bus data of IEEE 39-bus system 151
XXXVII	Line data of IEEE 39-bus system 152

TABLE	Page
XXXVIII Generator data of IEEE 39-bus system	153
XXXIX Exciter data of IEEE 39-bus system	153
XL Bus data of IEEE 118-bus system	154
XLI PV bus data of IEEE 118-bus system	157
XLII Line data of IEEE 118-bus system	158
XLIII Generator data of IEEE 118-bus system	161
XLIV Exciter data of IEEE 118-bus system	162

LIST OF FIGURES

FIGURE		Page
1	Basic structure of the electric power system	1
2	Basic structure of the North American Interconnections	2
3	FirstEnergy 345-KV line flows	21
4	Voltages on FirstEnergy's 345-KV lines: impacts of line trips	21
5	Cascade sequence	23
6	Rate of line and generators trips during the cascade	24
7	Sammis-Star 345-kV line trip	25
8	Basic flowchart for steady state control framework	29
9	Single-line connection and its connected load bus	38
10	Double-line connection	38
11	Flowchart of the control scheme	51
12	IEEE One Area RTS-96 24-bus system	54
13	PEBS crossing and controlling UEP	67
14	System trajectory in the rotor angle space	67
15	Flowchart of the transient stability control scheme	75
16	Modified IEEE 14-bus system	76
17	Machine angles when clearing fault at $t=0.1s$	77
18	Machine angles when switching line L4(B1-2) at $t=0.11s$	78
19	Machine angles when 5.5% load shedding at $t=0.11s$	79
20	Machine angles when 24.5% load shedding at $t=0.11s$	80

FIGURE	Page
21	Sammis-Star 345-kV line trip 84
22	Block diagram of system monitoring and control 90
23	Block diagram of local monitoring and control 92
24	Block diagram of interactive scheme 93
25	Potential infrastructure of the interactive scheme 94
26	IEEE 39-bus New England test system 96
27	Apparent impedance seen by distance relay at L29 during simulation 98
28	IEEE 118-bus system 103
29	Machine angles with fault clearing time at $t=0.149s$ 112
30	Machine angles with G13 fast-valving at $t=0.25s$ 114
31	Machine angles with G1 fast-valving at $t=0.25s$ 115
32	Machine angles with dynamic braking at G13 at $t=0.25s$ 117
33	Machine angles with shunt capacitor switching at B69 at $t=0.25s$. . 118
34	Normalized apparent impedance seen by distance relay at B69 of L108 119
35	Normalized apparent impedance seen by distance relay at B69 of L116 120

CHAPTER I

INTRODUCTION

A. Problem Statement

Electric power system is one of the biggest and most complex man-made systems. It is composed of thousands of generators, transformers, transmission lines, substations, loads and extensive infrastructure of measurement, communication and control equipment. It has been integrated into one big synchronous system (50 or 60 Hz) covering a large geographic area. Fig. 1 shows a basic structure of the electric system [1]. Fig. 2 shows a basic structure of the North American Interconnections covering USA, Canada and a part of Mexico [1].

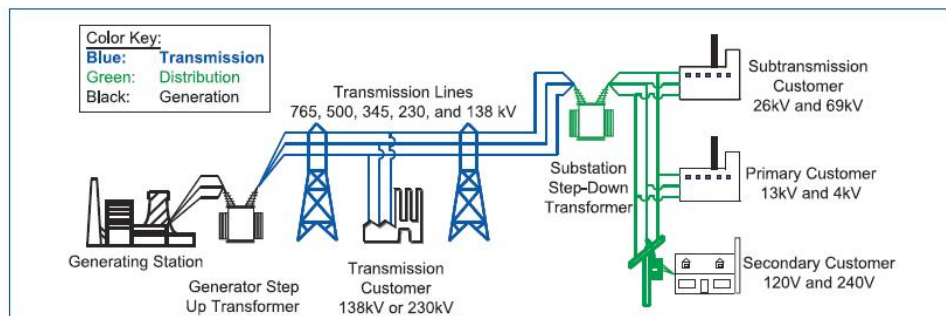


Fig. 1. Basic structure of the electric power system

Electric power system is exposed to all kinds of internal and external threats since it covers such a large geographic area. Too many factors, such as bad weather, natural disasters, human errors, tree/animal contacts, equipment malfunction, intentional intrusion, etc., can result in disturbances, i.e., faults and unplanned outages,

This dissertation follows the style of *IEEE Transactions on Automatic Control*.

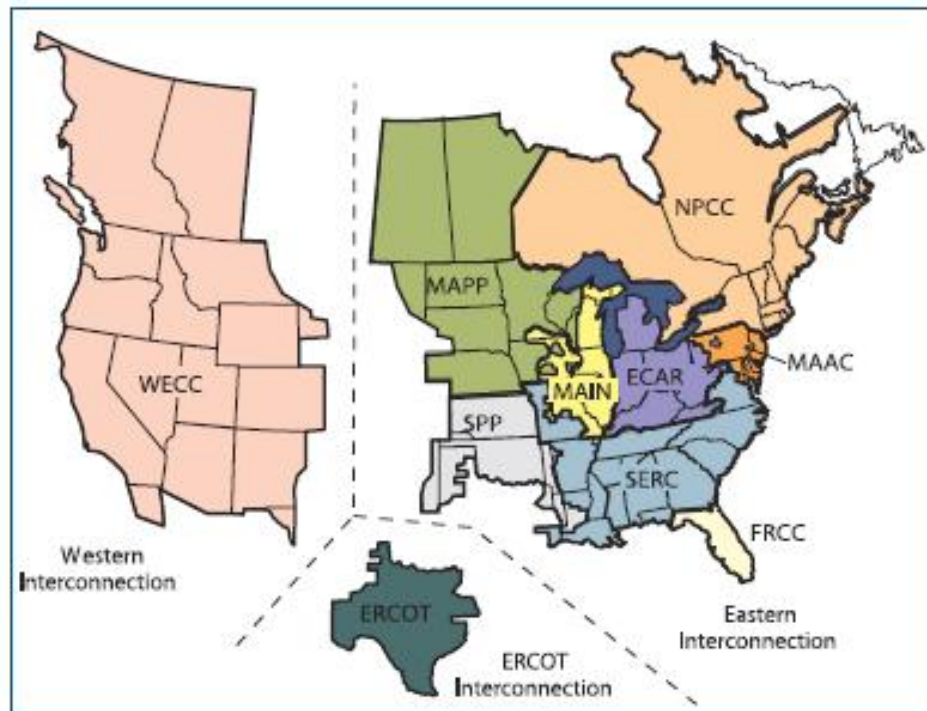


Fig. 2. Basic structure of the North American Interconnections

in the power system. Power system can withstand most disturbances without service interruption to customers through proper and timely protective relay and other control actions. Customers may even not feel the impact of disturbances. A small number of disturbances may have system impact such as service interruption, voltage reduction, demand reduction (load shedding). For example, there were about 28 to 63 disturbances with system impacts yearly in North America Power System from 1996 to 2002 [2].

We are interested in a more severe kind of system disturbances, cascading outages, which refers to the uncontrolled successive loss of system elements triggered by a disturbance [1]. Large area blackouts are always the final results of cascading outages.

Compared with hundreds of disturbances with local impact and dozens of distur-

Table I. Summary of some cascading outages around the world

Location	Date	Load loss (MW)	Affected People	Collapse Time	Restoration Time
US-Northeasten	Nov. 9, 1965	20000	30 million	13 mins	13 hrs
New York	July 13, 1977	6000	9 million	1 hr	26 hrs
France	Dec. 19, 1978	29000		26 mins	5 hrs
US-Western	Dec. 22, 1982	12350	5 million		
Sweden	Dec. 27, 1983	67% of load		53 secs	about 5 hrs
Tokyo	July 23, 1987	8200	2.8 million	20 mins	about 75 mins
US-Western	July 2, 1996	11850	2 million	36 secs	a few mins to several hrs
US-Western	Aug. 10, 1996	30500	7.5 million	>6 mins	a few mins to 9 hrs
Brazil	Mar. 11, 1999	25000	75 million	30 secs	30 mins to 4 hrs
US-Northeasten	Aug. 14, 2003	61800	50 million	>1 hr	up to 4 days
Denmark/Sweden	Sep. 23, 2003	6550	4.85 million	7 mins	average 2 to 4.3 hrs
Italy	Sep. 28, 2003	27700	57 million	27 mins	2.5 to 19.5 hrs
Greece	Jul. 12, 2004	9000	5 million	27 mins	3 hrs
Moscow	May 25, 2005	2500	4 million	2 hrs 20 mins	>6 hrs

bances with system impact yearly, cascading outages are relatively infrequent because power system owners, operators, engineers and researchers do the followings to ensure the secure and reliable operation: plan the operating studies, prepare for the worst fault scenarios and emergency conditions, enhance of quick response capability, design redundancy of generation and transmission capacity, provide backup capabilities, etc. [1].

However, cascading outages are not as few as people may assume. Lots of cascading outages with catastrophic social and economical impacts in history tell us that there is still a long way to solutions capable of detecting, preventing and mitigating cascading outages. Table I is a summary of some major cascading outages around the world [1,3–16].

There are two questions of interest in this study related to the cascading outages:

- Why cascading outages occur?

- How to detect, prevent and mitigate them?

B. Causes and Consequences

There are lots of factors making power system prone to cascading outages, which can be roughly classified into two groups: a) non-technical factors, such as change in operating procedures due to deregulation, aging infrastructure and lack of investment, and inadequate personnel training for new operating conditions, b) technical factors, such as operating difficulties, increased system complexity, more difficult protection setting coordination, inadequate traditional security analysis, lack of understanding of the cascades and unavailability of effective support tools.

1. Non-technical Causes

- *Change in operating procedures due to deregulation.* The original power system is designed to be operated in a vertically integrated and regulated environment. The power flow pattern and load can be predicted with some degree of confidence in such situations. Protection relay settings and transfer limits can be easily set and coordinated by off-line studies. With the deregulation and competition, load and generation are difficult to forecast and power flow transfer changes quickly due to the economic reason. In such instances, it is difficult to perform precise planning to provide adequate protection and security control. The power system has been operated closer to its short circuit and security limits due to economic reason.
- *Aging infrastructure and lack of investment.* Many generators, transmission lines, transformers, protective relays, etc., are 40 years, 50 years old or more. The failure rate increases for aged equipment. Compared with the steady in-

creasing load and generation, upgrading of transmission facility is pretty slow due to an uncertainty of the economic return from transmission investment. Lack of transmission becomes a "bottleneck" both to economic transfer and security concern. Combined, aging infrastructure and lack of investment lead to more vulnerable operation since the system is being stressed more now. Thus cascading outages are more probable.

- *Inadequate personnel training for new operating conditions.* The requirements on power system operators are much higher than before due to deregulation. Power system operators may lack training to be able to interpret system situational awareness and hence may not be able to make correct action to preserve the system during abnormal conditions. Inadequate training can also lead to human errors during the routine operation and maintenance work, which makes the system more vulnerable to contingencies. Operators' lack of situational awareness and failure to respond properly due to inadequate training was one direct causes for Aug 14, 2003 Northeastern Blackout [1].

2. Technical Causes

- *Operating difficulties.* Most electric power systems have been integrated into a big synchronous alternating current (AC) system covering a large area. The electricity has been generated by power plants, transmitted through transmission and distribution networks and consumed by loads (customers) almost simultaneously because of no power "storage". All AC generators must run at the same speed. The electricity flows through the networks "freely" close to the speed of light based on the laws of physics - along "paths of least resistance" [1]. The generation and load must be balanced to maintain the sched-

uled frequency. The reactive power supply and demand must be balanced to maintain the scheduled voltage. The transmitted power through each transmission line must be within the transfer limits, both thermal and security related. If there are congestions at the transmission lines, either load shedding, generation re-dispatching or generator rejection must be taken. The capacities of generation and transmission must be always larger than load demand for the possible disturbances. Those fundamental power system characters result in difficulties in safe and reliable operation. Traditional regulated utilities owned integrated systems, including generating plants, transmission and distribution networks. They considered those fundamental power system characters during their planning and operating practices. After deregulation, generation, transmission and distribution become separate entities and economy becomes their primary concern with potential sacrifice of the security.

- *Increased system complexity.* Power system is one of the biggest and most complex man-made systems. After deregulation, the original integrated utilities have been divided into different market participants and all of them seek their own economic interests. New technologies, i.e., flexible AC transmission systems (FACTS) [17–19], can increase the system security and reliability if they are applied properly. They also add operation and protection complexity. For example, series compensation capacitors may cause the subsynchronous resonance (SSR) problem [20] and difficulty in protection coordination because they change the transmission line impedance character. New energy sources such as wind energy, also add complexity and difficulty to the bulk power system operation because of their remote location and intermittent load characters [21]. From the large complex system point of view, cascading outage probability is

getting larger with the increase of the system size [22]. The system is lightly nonlinear and has many dynamic modes of operation which makes it almost impossible to determine all-inclusive control algorithm.

- *More difficult protection setting coordination.* Protective relays are the most important equipment to protect the power system elements from damage due to internal and external causes and isolate the faulted elements with minimum impact to other parts as soon as possible. Relay misoperation is believed to be a contributing factor in 75 percent of the major disturbances in North America [23]. Protection systems have been involved in 70 percent of the cascading outages [24]. Current power systems are operating closer to their short circuit limits. During abnormal conditions, the backup relays can not differentiate the faults from non-fault conditions such as overload and large power swing. Relay settings for the transmission lines, generators and under-frequency load shedding may not be appropriately coordinated to reduce the likelihood and consequence of cascading outages [1].
- *Inadequate traditional security analysis.* North American Electric Reliability Council (NERC) requires " $N - 1$ criterion" so that the power system can withstand the next worst contingency within 30 minutes (NERC Policy 2, Section A) [1]. " $N - K$ criterion" ($K \geq 2$) means the power system must withstand the concurrent loss of K elements. It is too difficult to perform " $N - K$ " security analysis because of the large number of possible contingency combinations. The normal practice is to do detailed " $N - 1$ " security analysis in off-line studies and fast and limited " $N - 1$ " contingency analysis in real-time operation. After outages of several facilities one by one during the abnormal conditions, the outage information might not be reported to the related or neighboring control

centers. The new contingency may neither be considered in real-time security analysis, nor be done by off-line studies. Therefore security analysis beyond traditional "N - 1" is needed.

- *Lack of understanding of the cascades and unavailability of effective support tools.*

Several common factors characterise the cascading outages [1]: over-estimation of reactive power support, inability to visualize events of the entire system, failure to ensure the power system within safe limits, lack of "safety nets". Real-time power system operators need support tools for understanding power system cascade mechanism, performing off-line studies and controlling power systems. With dynamicly changing conditions, the real-time operating condition may be totally different from off-line study and the complex hardware and software infrastructure may fail to excute their desired functions. Thus power system operators may operate their system in an insecure state unknowingly, just like it was the case in the Aug 10, 1996 US-Western Blackout [10] and Aug 14, 2003 US-Northeastern Blackout [1].

3. Consequences

Cascading outage often causes large area blackouts and difficulties for system restoration because it is a very slow process for all the generators to re-start and re-synchronize and all the loads to be re-connected through transmission and distribution networks. As a result, millions of people may not have power supply for long time. The economic losses may be huge. The loss of Aug 10, 1996 US-Western Cascading Outages was over \$1.5 billion [1]. The estimated loss of Aug. 14, 2003 US-Northeast Cascading Outages was between \$4 billion and \$10 billion in US, and \$2.3 billion in Canada [1]. Besides the economic losses, the modern society also faces

disorders, crimes, loss of lives, living difficulties, mental sufferings, etc. due to the loss of power supply.

Due to the above mentioned reasons, finding solutions to detect, prevent and mitigate cascading outages is one of the most difficult and challenging tasks for power system engineers and researchers, especially under current deregulated operating constraints.

C. Current Research Efforts

The current power systems are operating in a mode for which they have not been designed. Combined with the aging infrastructure, lack of investment, and inadequate training of operating personnel, current power systems are more prone to cascading outages. To mitigate the non-technical factors, more investments in both economic and human resources are needed.

For the technical factors, different research efforts are aimed at understanding and finding ways to prevent and mitigate cascading outages. For example, new technologies of superconductivity [25–27] and flexible AC transmission systems (FACTS) [17–19] try to overcome the operating difficulties due to power system fundamental characters. Dynamic and probabilistic study of the cascade model [28] tries to study the system complexity. To try to solve the protection problem, relay hidden failure analysis [23, 29, 30], wide area back-up protection expert system [31], and wide area monitoring, protection and control [32–38] are proposed. To overcome the inadequate traditional security analysis, dynamic decision-event tree analysis [39] is proposed. To overcome lack of understanding of the cascades and unavailability of effective support tools, different methods are proposed and used, such as visualization of power system operating conditions [40], special protection scheme (‘safety

nets') [41], self-healing system with the aid of multi-agent technology [42, 43], steady state simulation method [44, 45], etc. However, they are still far from being mature and being readily used to solve the cascading outage problem.

Superconducting technologies [25–27] can be used in following applications: superconducting magnetic energy storage (SMES), cables, fault current limiters, transformers, generators, motors, etc. They can provide improved efficiency, smaller size, reduced weight and increased system reliability compared with existing technologies. Flexible AC transmission system (FACTS) [17–19] controllers can control important power system variables such as: voltage, angle and impedance easily. They can provide benefits such as increased transfer capability, added power flow control, improved power system stability, increased system security and reliability, etc. Those new technologies can provide some good solutions regarding the power system fundamental characteristics and increase the system security and reliability. They are still constrained from large commercial useage by the maturity of technologies, complexity and costs.

Dynamic and probabilistic study of the cascade model tries to understand the power system cascade from probability, statistics and large complex system point of view [28]. It analyzes the influence of load increase, number of line outage and system size on blackout size and gives some probabilistic results. However, it does not give useful solutions for the detection, prevention and mitigation of cascading outages.

Relay hidden failure analysis aims at exploring the undetected relay defect that results in relay misoperation [23, 29, 30]. It can give some risk assessment. Relay hidden failure is only one part of protection problems. Many relay misoperations are not caused by relay hidden failure. To detect, prevent and mitigate cascading outages much more work than relay hidden failure analysis is needed.

Wide area back-up protection expert system method takes advantage of the

communication technology and artificial intelligence [31]. When it gets a solid decision and identifies the faulted component, it blocks the conventional backup protection to avoid unnecessary trip. However, it is difficult to make the solid decision and find the exact faulted element during the complex situations and stressed conditions.

Wide area monitoring, protection and control tries to utilize advanced technologies of GPS synchronization, communication, computer, protection, control devices and engineering practice to provide wide-area disturbance monitoring and emergency control [32–38]. It can act as decentralized subsystems making local decisions based on local measurements and remote information and/or send preprocessed information to higher hierarchical levels. The concept is still at its early stage.

Dynamic decision-event tree analysis is trying to find a rapid response scheme for the N-K event with a low probability in advance [39]. It also finds some dependent N-K events with probability close to N-1 event. For any initial events, it tries to find all subsequent possible events, make event trees and then store them. When such events occur, it identifies if they match the stored event tree and activates the associated emergency control to mitigate the events. Compared with the fixed special protection scheme (or 'safety nets'), it is more flexible and can adapt to the dynamic changing conditions. However, it is time consuming to create all possible dynamic event trees and update them after conditions have changed. Another problem is associated with the simulation model it uses. If the model is too simple, the method may be a bit faster but the control results are not reliable thus it can not prevent or mitigate the cascading outage. If the model is not simple, the method is very time consuming.

Visualization of power system operating conditions utilizes new technology to represent complex power system operating conditions and conventional analysis results [40]. It helps power system operators to improve the situational awareness and readiness for the alert and emergency conditions. However, visualization in itself does

not bring any new technical solutions for the prevention and mitigation of cascading outage.

Special protection scheme (or "safety net") activates automatically if a pre-specified, significant contingency occurs [41]. When activated, such scheme involves certain costs and inconvenience, but it can prevent some disturbances from getting out of control. It is hardware based and responds to a limited set of conditions with a limited number of possible actions. When the conditions are different from the pre-studied conditions, the special protection scheme may not be suitable.

Self-healing system with the aid of multi-agent technology wants to use the multi-agent technology to provide self-healing and adaptive reconfiguration capabilities for the power system based on the wide-area system vulnerability analysis [42, 43]. It uses the multi-layer structure with independent multi-agent to fulfill its self-healing goal. However, it is still at its conceptual design stage.

Steady state method has been used successfully in simulating the cascading sequence of 2003 US-Northeastern blackout [44] and the terrorist attack plan aimed at finding the vulnerability of a power system [45]. It is also used by the Task Force to benchmark the pre-cascade conditions of the Northeastern power system and make important conclusion that the system was secure at 15:05EDT before the loss of Harding-Chamberlin 345-KV line [1]. Such methods can give some promising results for the steady state and long term voltage and frequency stability problems. For the dynamic conditions, the transient stability analysis is still needed.

As a summary, there is no comprehensive solution to the overall problem: to detect, prevent and mitigate the cascading outages. The catastrophic social and economical impacts of cascading outages, the high complexity of the cascading outage problem, and the immature research efforts and engineering practices urge engineers and researchers to try their best to find solutions to help detect, prevent and mitigate

cascading outages.

D. Research Objectives and Approach

To detect, prevent and mitigate cascading outages, one must know why and how cascading outages occur so that some techniques and tools can be found to deal with them. The causes of cascading outages and current research efforts have been described in previous sections. One important reason for the insufficiencies of current research efforts is that they do not investigate the mechanism of cascading outages completely so they can not provide effective tools accordingly.

This dissertation has two major objectives: a) to investigate the mechanism of cascading outages to be able to point out effective techniques, b) to apply those techniques in detection, prevention and mitigation of cascading outages. A breakdown of research issues addressed in this dissertation is listed as follows:

- Investigate the mechanism of cascading outages.
- Develop a steady state control scheme for the early detection and prevention of cascading outages based on the steady state progress character of cascading outages.
- Develop a transient stability control scheme based on the transient progress character of cascading outages.
- Develop an interactive scheme between system-wide and local monitoring and control based on the interactive character of cascading outages.
- Evaluate the performance of the proposed control schemes.

E. Summary

This dissertation works on one of the most difficult and challenging problems in the power system: detection, prevention and mitigation of cascading outages. The causes and consequences of cascading outages have been discussed. The mechanism has been investigated. Effective schemes and tools based on the mechanism to help detect, prevent and mitigate cascading outages have been proposed in this dissertation.

The dissertation is organized as follows. The fundamentals of the proposed approach are provided in Chapter II. Chapter III describes the comprehensive steady state control scheme for early detection and prevention of cascading outages. The whole procedure for evaluation, identification, prediction, control and applications of associated tools are provided. The transient stability control scheme and its methods are presented in Chapter IV. Chapter V describes the interactive scheme between system-wide and local monitoring and control. The details of system monitoring and control tool are introduced. Evaluation of those schemes is given in Chapter VI. The conclusions of the dissertation are given in Chapter VII. References and Appendices are attached in the end.

CHAPTER II

FUNDAMENTALS OF THE PROPOSED APPROACH

A. Introduction

An overview of this dissertation is given in the first chapter. This chapter presents the fundamentals of the proposed approach for detection, prevention and mitigation of the power system cascading outages. In Section B, the definitions of frequently used terminologies are given. Section C describes some mechanism of cascading outages. The proposed solution based on the assumed mechanism is given in Section D. A summary is given in Section E.

B. Definitions of Terminologies

In this section, we will give some definitions of frequently used terminologies in this dissertation [1].

- Disturbance: *"An unplanned event that produces an abnormal system condition"*.
- Contingency: *"An unexpected failure or outage of a system component, such as a generator, transmission line, circuit breaker, switch, or other electrical element. A contingency may also include multiple components, leading to simultaneous component outages"*.
- Outage: *"The period during which a generating unit, transmission line, or other facility, is out of service"*. A power outage is the loss of the electricity supply to an area, irresponsive how small or big.

- Cascade: *"The uncontrolled successive loss of system elements triggered by an incident"*.
- Stability: *"The ability of an electric system to maintain a state of equilibrium during normal and abnormal system conditions or disturbances"*.
- Transient stability: *"The ability of an electric system to maintain synchronism between its parts when subjected to a large disturbance and to regain a state of equilibrium following that disturbance"*.
- Reliability: *"The degree of performance of the elements of the bulk electric system that results in electricity being delivered to customers within accepted standards and in the amount desired. Reliability may be measured by the frequency, duration, and magnitude of adverse effects on the electric supply. Electric system reliability can be addressed by considering two basic aspects of the electric system: Adequacy and Security"*.
- Adequacy: *"The ability of the electric system to supply the aggregate electrical demand and energy requirements of customers at all times, taking into account scheduled and reasonably expected unscheduled outages of system elements"*.
- Security: *"The ability of the electric system to withstand sudden disturbances such as electric short circuits or unanticipated loss of system elements"*.
- Blackout: A large-scale disruption in electricity supply, which is often a result of cascading outages.

Vulnerability can be taken as a measure opposite to security. The system is vulnerable if contingencies lead to an interruption of service to a part or the entire

system. The element is vulnerable if contingencies or changing conditions lead to violation of the limit, outage or mal-function of the element.

C. Mechanism

In general, cascading outages are not sudden events that human being can not detect, prevent or mitigate. From the temporal framework, there is a process from slow successive events to fast cascading outages. From the spatial framework, there are interactions between the system-wide and local levels: local disturbances, i.e., faults or relay misoperations stress the system condition, weak system condition causes more local disturbances, further stressed system condition, till the cascading outages unfold.

1. Stages of Cascading Outages

Normally there are two stages of cascading outages [46]. The first stage is steady state progress stage: a period of slowly evolving successive events. The system operating conditions may get worse with several new disturbances following one another. It can be approximated with steady state analysis. This stage is a very important stage because the system operators may have enough time to evaluate the system condition, identify some vulnerable contingencies, take some control to increase the security level and prevent the possible cascading outages. The control cost is minimal compared with the huge cost of cascading outages.

The second stage is transient progress stage: a fast transient process resulting in cascading outages and finally the collapse of the entire system. System dynamics needs to be carefully considered. The common practice is to do transient stability analysis. If faults occur and are not cleared within their critical clearing time (CCT),

they will cause the transient stability problem. Some generators may run faster and others may run slower. Thus the system synchronism is lost. Some generators and transmission lines may be tripped by protective relays. If there were no effective transient stability control scheme, cascading outages would occur.

Some cascading outages may only have fast transient progress stage, like the Dec. 27, 1983 Sweden Blackout [6], July 2, 1996 US-Western Backout [10], and Mar. 11, 1999 Brazil Blackout [9]. The transient stability analysis and control must be executed in such cases immediately.

2. Interaction Between the System-wide and Local Levels

There are interactions between the system-wide and local levels, especially system security and local protection. The unfavorable interaction can go as follows: Local disturbances, i.e., faults or relay misoperations, occur first and stress the system condition. The stressed system condition may cause more local disturbances, either faults because overloaded transmission lines sag to trees or relay misoperations due to wrong settings, hidden failure, or being "fooled" by the non-fault conditions as faults. More local disturbances stress the system condition more severely. Following this interactive chain, cascading outages would occur. The favorable interaction can be like this: Local disturbances have been contained within minimum impacted area. For example, faults have been cleared timely and correctly. Any relay misoperations have been prevented or corrected. Exact local disturbances information has been reported to the control center. After local disturbances, the system security level decreases. System-wide security analysis starts and identifies some vulnerable contingencies and vulnerable parts. Possible control actions have been taken to enhance system security level and some commands may be sent to vulnerable relays to increase relay security, i.e., to block the backup protection from acting on power swing and overload condi-

tions. After those proper system-wide and local interaction and control actions, the power system goes to another secure operating state.

Protective relays take measurements from local current and voltage transformers and from the remote end of the lines through communication channels. They work locally and independently, without knowing or considering the entire system condition. They work in primary and backup modes to obtain redundancy in protection. If one relay fails, another should detect the fault and trip the appropriate circuit breakers. Some backup relays have significant "reach". Thus they may see non-fault conditions such as line overloads, low voltage or stable swings as faults and trip the healthy line [1]. That is one kind of relay misoperations. Another misoperation is that relays refuse to operate when there is a fault within its primary reach, which occurs much less than the former case. Relay settings are made by off-line studies. They are not updated frequently. With the changing of load level, power flow pattern, and network topology, those relay settings may not be proper unknowingly. For example, In 1965 US Northeastern Blackout, a backup relay misoperated to open one of five 230-KV lines taking power north from a generating plant in Ontario to the Toronto area. That was the direct cause of the following power swings resulting in a cascading outage that blacked out much of the Northeast. It was because of a wrong setting which was set 9 years earlier [30].

The system security analysis takes information, such as voltages, currents, topology, controllers, etc., and does analysis for the whole system. It can know system security level, identify the vulnerable contingencies and vulnerable parts within the system, make proper control actions to increase system security level. It can also give local relays guidance to prevent their misoperations when the system is in abnormal condition .

If there were any control scheme making use of interaction between the system-

wide and local levels, some cascading outages might have been prevented. However, it is still an immature research field and only a few references have discussed this [47–52].

3. Case Studies

We can take the Aug. 14, 2003 US-Northeastern Cascading Outages as an example [1]. Let us look at both the cascading outage stages and interactions between system-wide and local levels.

- Stage 1: steady state progress
 - 12:08-14:14EDT, several transmission lines and one generator outage;
 - 15:05-15:41EDT, three First Energy (FE) 345-KV line outage;
 - 15:39-15:59EDT, collapse of 138-KV system;
 - 16:05EDT, trigger issue: outage of Sammis-Star 345-KV line, started the cascade;
 - 16:05-16:09EDT, loss of two 345-KV lines and numerous 138-KV lines;
- Stage 2: transient progress
 - 16:09-16:10EDT, loss of multiple generators;
 - 16:10-16:13EDT, fully cascading outages

For the steady state progress stage, we can take the FirstEnergy System as an example. Before the first 345-KV line (Harding-Chamberlin) was tripped at 15:05EDT, the whole system was "N-1" secure eventhough the outages of several lines and one generator reduced the security level. After Harding-Chamberlin line was tripped, the system was "N-1" insecure. For the three 345-KV lines outage, after each line outage, line loading increased at other lines and voltages decreased. We can see this from Fig. 3 and Fig. 4 [1]. The collapse of 138-KV system was also one direct result.

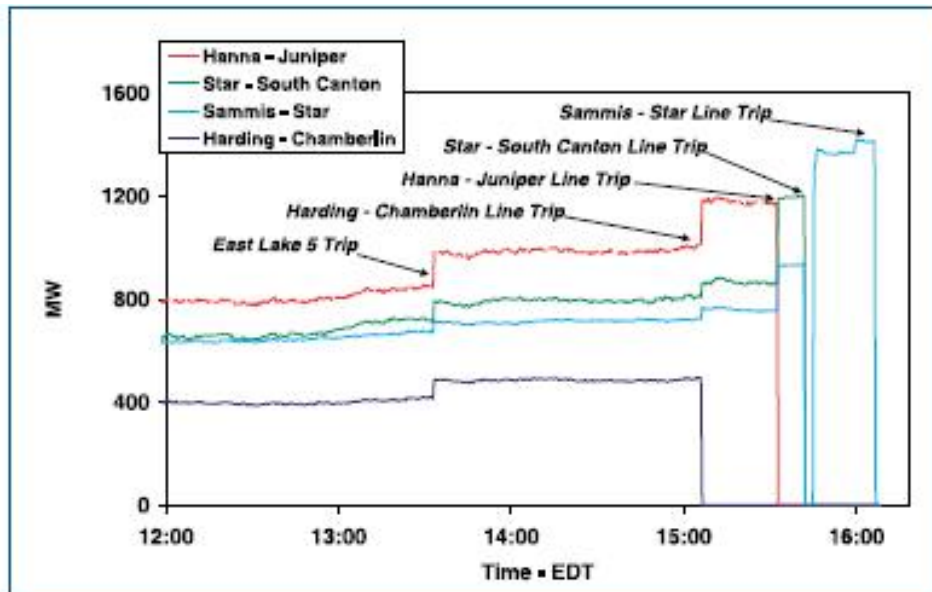


Fig. 3. FirstEnergy 345-KV line flows

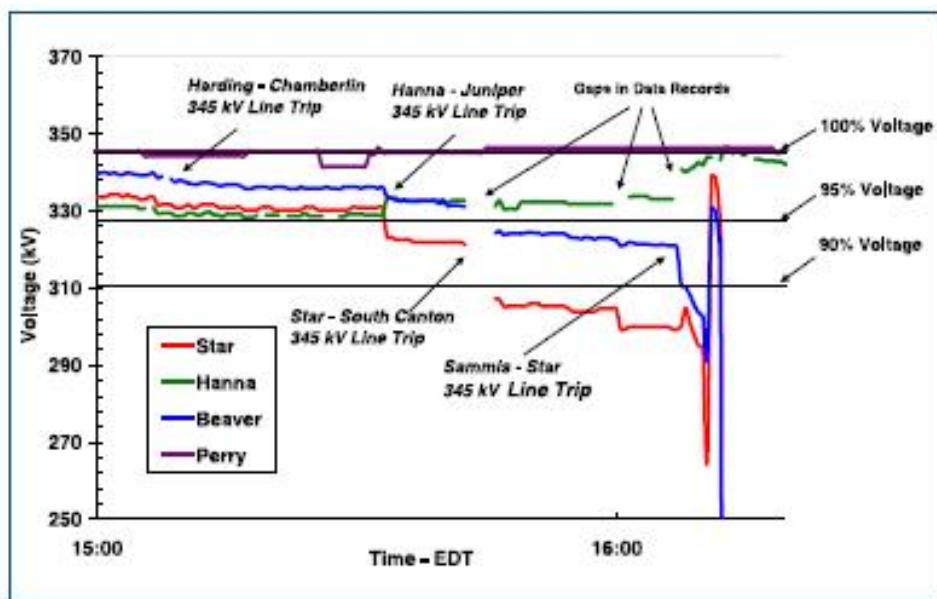


Fig. 4. Voltages on FirstEnergy's 345-KV lines: impacts of line trips

The outage of Sammis-Star 345-KV line at 16:05EDT triggered the cascade. But the system still remained stable till the trip of East Lima-Fostoria Central line at 16:09EDT. After that, big power swing occurred and fast transient progress started. We can see lots of tripping of lines, transformers and generators and fast spread of the blackout area from the Fig. 5 and Fig. 6 [1]:

From Fig. 3 to Fig. 6 we can see that the steady state progress stage has a comparatively longer period. If there were any early detection and prevention scheme, it would detect and prevent the possible cascading outage at its early stage. This would be the best choice to detect, prevent and mitigate cascading outages.

The investigation team found that the following control could have prevented the blackout [1].

- At 15:41EDT, if 1000 MW load were shed in Cleveland-Akron area before the third 345-KV line: Star-South Canton line tripping, it would have prevented the subsequent tripping of the Sammis-Star line at 16:05:57EDT.
- At 16:05EDT, if 1500MW load were shed within Cleveland-Akron area before the loss of Sammis-Star 345-KV line, the blackout could have been prevented. Loss of the Sammis-Star line was the critical event leading to the widespread cascade in the Northeastern system.

We can also analyze the interactions between system-wide and local levels. Outage of several transmission lines and one generator between 12:08EDT and 14:14EDT stressed the system condition but did not put the system into "N-1" insecure state. The outage of Harding-Chamberlin line at 15:05EDT put the system into "N-1" insecure state. It was caused by tree contact within normal line rating due to lack of tree trimming. The following two 345-KV lines outages at 15:32EDT and 15:41EDT were also caused by tree contact. Those disturbances stressed the system in abnormal

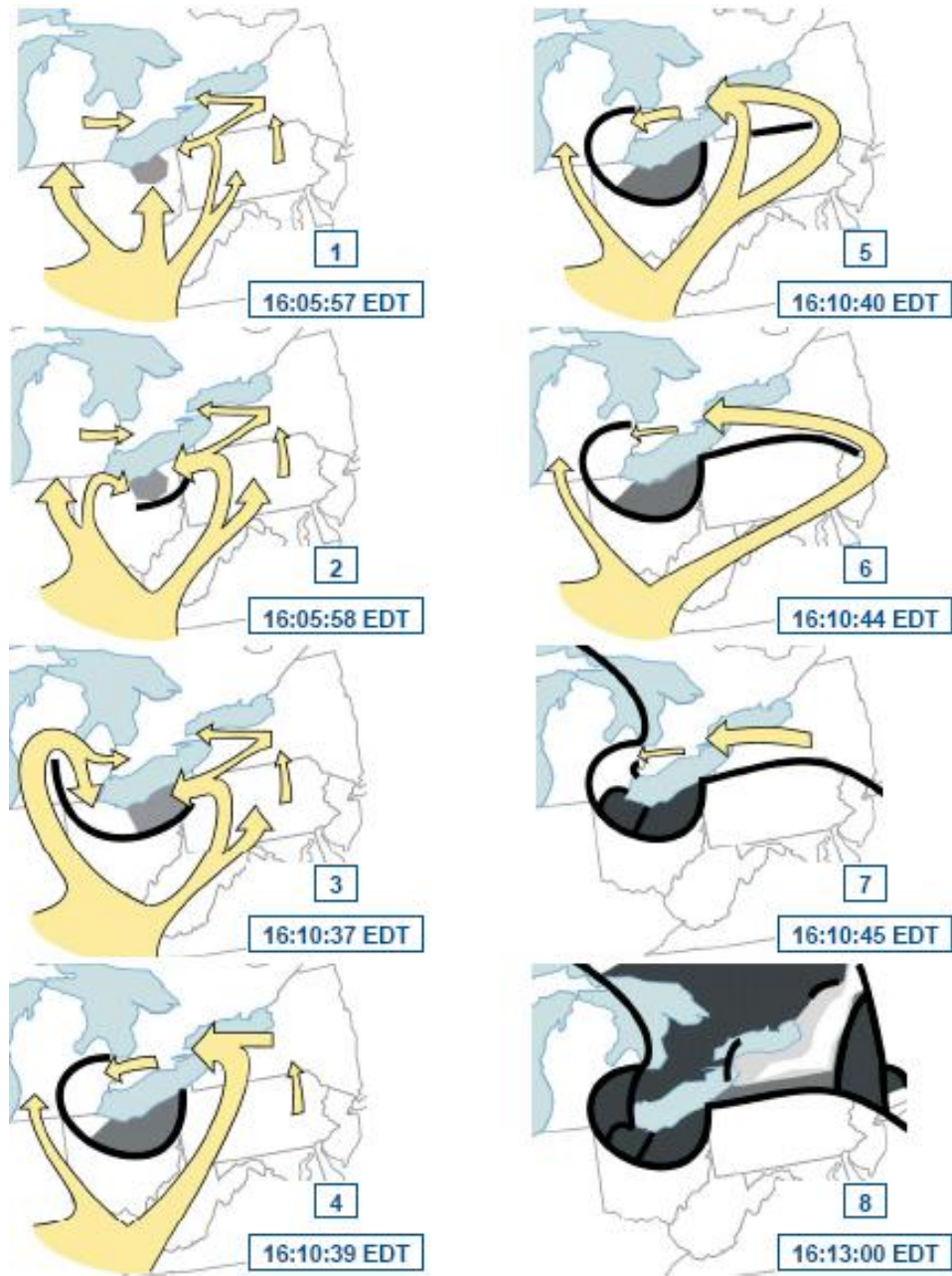


Fig. 5. Cascade sequence

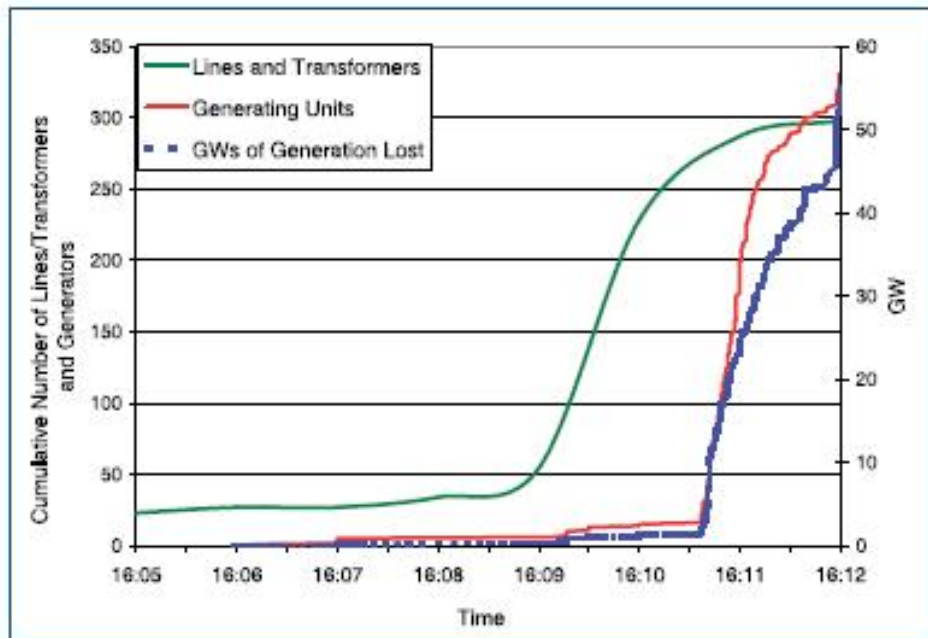


Fig. 6. Rate of line and generators trips during the cascade

conditions. The underlying 138-KV lines were overloaded and tripped. The heavy loading and low voltage condition caused Sammis-Star 345-KV line distance relay to see a "zone 3" fault even though there was no fault, trip that line and trigger the cascading outage. This can be seen from Fig. 7. As discussed above, proper load shedding would have prevented the relay misoperation at Sammis-Star line and averted the cascading outage.

We can also look at examples of July 2 & 3, 1996 US Western Disturbances [10]. On July 2, a protective relay on a parallel healthy 345-KV transmission line incorrectly tripped that line, resulting in the loss of both lines which triggered the subsequent cascading outage. On July 3, the same relay misoperated again. The possible cascading outage was prevented because of operators' appropriate load shedding action.

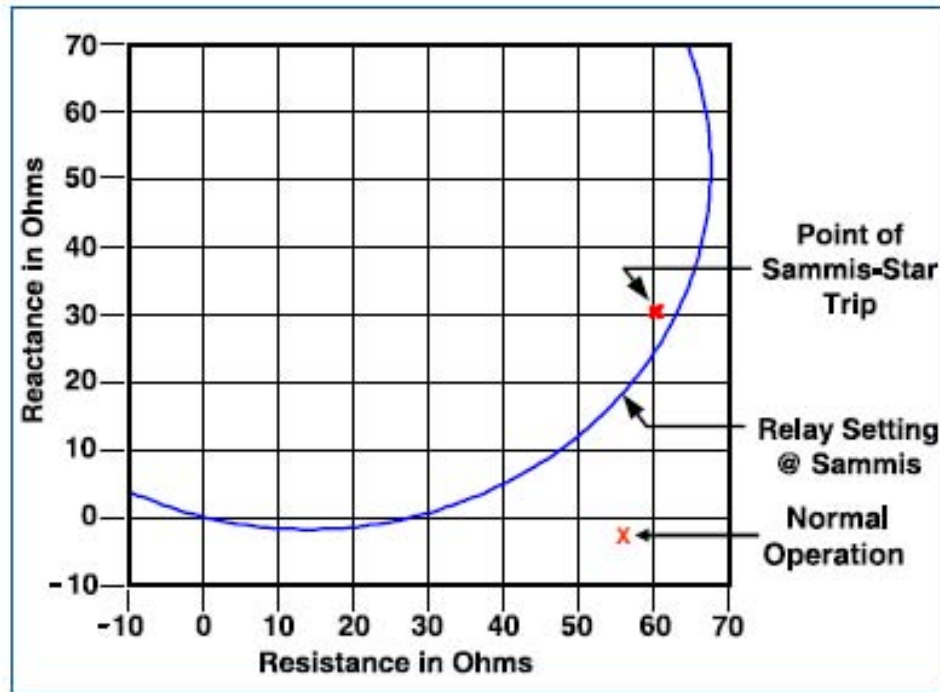


Fig. 7. Sammis-Star 345-kV line trip

D. Proposed Solution

From the study of the cascading mechanism, we can confirm that from the temporal framework, there are two stages of cascading outages: steady state progress stage and transient progress stage. From the spatial framework, there are interactions between system-wide and local levels. In this dissertation, we propose three effective control schemes to help detect, prevent, and mitigate the cascading outages.

Aimed at solving problems in the slow steady state progress stage, a steady state analysis and control scheme is proposed in Chapter III. It is a new steady state analysis method and control scheme for early detection and prevention of power system cascading outages. It uses the Vulnerability Index (VI) and Margin Index (MI) to evaluate the vulnerability and security of the individual system parts and the operating condition of the entire system. For the given disturbance, it calculates

the power flow, evaluates the vulnerability and security, identifies the vulnerable part, finds the transmission line overload and bus voltage problems, and predicts the possible successive events. The approach uses the control means based on methods of Network Contribution Factor (NCF), Generator Distribution Factor (GDF), Load Distribution Factor (LDF), and Selected Minimum Load Shedding (SMLS) for early detection and prevention of cascading outages.

Aimed at handling system dynamic problems in transient progress stage, a transient stability control scheme based on potential energy boundary surface (PEBS) method and analytical sensitivity of transient energy margin is proposed in Chapter IV. It classifies the stability control means into two categories, admittance-based control (ABC) and generator-input-based control (GIBC), and uses a comprehensive method to analyze the contribution of each control means. The scheme can get the optimal control from all the available transient stability control means by sensitivity analysis and then verify it in the time-domain transient stability program. Fast and accurate control goal can be obtained from this stability control scheme.

Aimed at making better use of interactions between system-wide and local levels, an interactive scheme of system-wide and local monitoring and control is proposed in Chapter V. This interactive scheme coordinates the system-wide and local monitoring and control to fulfill this task. The proposed system tool is intended for installation at the control center. It consists of routine and event-based security analyses, along with security control schemes for expected and unexpected events. Routine security analysis includes vulnerability analysis, and static and dynamic contingency analysis. For the routine static and dynamic contingency analysis, contingencies which can lead to an overload condition, voltage problem, transient stability, etc., will be found and taken care of. Either preventive control actions need to be taken to prevent such problems or emergency control needs to be activated if such contingencies have really

happened. Vulnerability and security margin analysis of operating condition of the entire system and individual element can be implemented. Vulnerable elements will be identified and their relays need to be closely monitored. The event-based security analysis is triggered when an unexpected disturbance occurs. It will indicate whether the emergency control is needed to mitigate the transient stability problem or not. The local monitoring and control tool is intended for installation at local substations. It can provide system tool with correct local disturbance information and diagnostic support. Thus, the system tool can have correct local information and take better control to ensure the secure operation. The local tool can get the system security status and monitoring command from the system tool.

E. Summary

The power system cascading outages are complex. Many factors can cause cascading outages. There are some mechanism of cascading outages, which can give researchers clues where focus research efforts aimed at detecting, preventing and mitigating them. Steady state control scheme, transient stability control scheme, and interactive scheme of system-wide and local monitoring and control are proposed in this dissertation to help detect, prevent, and mitigate the cascading outages. They will be described in detail in the rest chapters.

CHAPTER III

STEADY STATE CONTROL SCHEME*

A. Introduction

In general, cascading outages are not sudden events that human being can not detect, prevent or mitigate. As described in Chapter II, normally there are two stages of cascading outages. First, a period of slowly evolving successive events that can be approximated with steady state analysis. The system operating conditions may get worse with several new disturbances following one another. Second, after succession of several major disturbances, there is a fast transient process resulting in cascading outages and finally the system collapses.

Steady state method has been used successfully to simulate the cascading sequence of 2003 US-Northeastern Blackout using rough information [44]. It was also used by the Task Force to benchmark the pre-cascade conditions of the Northeastern power system and make important conclusion that the system was secure at 15:05EDT before the loss of Harding-Chamberlin line [1]. A similar method is used to simulate terrorist attack plan to find the vulnerability of the system [45].

There are several successful cases of early detection and prevention of cascading outages [10]: for example, on July 3, 1996, the Western Coast system operators manually shed load to avoid the possible cascading outages when conditions were similar to July 2. On Aug 26 and Oct 30, 1996, there were disturbances resulting in line flow above the transfer limit in New York Power Pool. The appropriate control prevented the possible cascading outages if the next contingency had occurred.

*Part of the material in this chapter is reprinted from “A new analysis method for early detection and prevention of cascading events” by Hongbiao Song and Mladen Kezunovic, *Electric Power Systems Research*, doi:10.1016/j.epsr.2006.09.010, ©2006 Elsevier B.V., with permission from Elsevier.

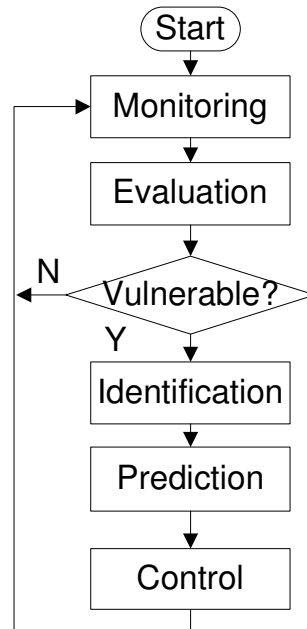


Fig. 8. Basic flowchart for steady state control framework

This chapter gives a new approach for analysis of cascading outages, as well as early detection and prevention scheme based on steady state analysis method for the slow steady state progress stage. This method can be implemented to work automatically or with operator supervision, and can serve as a decision-support tool for real time operation or operator training purpose. The basic flowchart of this approach can be seen in Fig. 8.

The proposed method framework is discussed as follows: First, the power system is monitored to see whether there are any events or changing conditions during the system normal operation. Second, the system conditions are evaluated by computing the vulnerability index and margin index. Those indices can give specific quantitative measure of system vulnerability and security margin. Third, if the system is determined to be secure (not vulnerable), the monitoring of the system continues. Otherwise, the vulnerable parts of the system and vulnerable conditions are identi-

fied, the possible voltage and overload problems if those vulnerable conditions occur are predicted, the suitable control means to prevent or mitigate the problems are identified, and the control means are activated when needed.

In Section B, comprehensive vulnerability index and margin index for generators, buses and branches are provided to evaluate the power system operation, both at the individual component and system level. In Section C, the topology processing and operation index methods are given to identify the vulnerable parts of the power system. A list of vulnerable system parts that need careful monitoring or special study is created. In Section D, fast network contribution factor (NCF) method is used to predict the line overload and bus voltage problems for a given network event or assumed contingency. Its results are verified by the full AC load flow method. In Section E, steady state control scheme based on network contribution factor (NCF), generator distribution factor (GDF), load distribution factor (LDF), and selected minimum load shedding (SMLS) methods to prevent and mitigate possible cascading outages is provided. Case Study and Summary are given in Section F and G respectively.

B. Evaluation by Vulnerability Index and Security Margin Index

Power system operators need to know as precisely as possible the security condition of the system operation. Thus they can take some control actions when the system security is being or has been threatened.

"Security of a power system refers to the degree of risk in its ability to survive imminent disturbances (contingencies) without interruption of customer service. Stability of a power system refers to the continuance of intact operation following a disturbance" [53]. Vulnerability can be taken as a measure opposite to security. The

system is vulnerable if contingencies lead to an interruption of service to a part or the entire system. The element is vulnerable if contingencies or changing conditions lead to violation of the element limit, outage or mal-function of the element.

Before the power system faces interruption of service or the element faces outage or mal-function, some indices can be used to represent the degree of vulnerability and security. Vulnerability index (VI) and margin index (MI) are proposed to represent comprehensive and quantitative vulnerability and security information of the individual part and whole system [54]. Given a system with m generators, n buses, p lines and q loads, we define the vulnerability index (VI) and Margin Index (MI) sets as follows:

1. Vulnerability Index and Margin Index for Generators

$$VI_{Pg,i} = \frac{W_{Pg,i}}{2N} \left(\frac{Pg_i}{Pg_{i,max}} \right)^{2N} \quad (3.1)$$

$$VI_{Qg,i} = \frac{W_{Qg,i}}{2N} \left(\frac{Qg_i}{Qg_{i,max}} \right)^{2N} \quad (3.2)$$

$$VI_{gen.loss,i} = W_{gen.loss,i} k_{gen.loss,i} \quad (3.3)$$

$$VI_{gen} = \sum_{i=1}^m (VI_{Pg,i} + VI_{Qg,i} + VI_{gen.loss,i}) \quad (3.4)$$

$$MI_{Pg,i} = 1 - \frac{Pg_i}{Pg_{i,max}} \quad (3.5)$$

$$MI_{Qg,i} = 1 - \frac{Qg_i}{Qg_{i,max}} \quad (3.6)$$

2. Vulnerability Index and Margin Index for Buses

$$VI_{V,i} = \frac{W_{V,i}}{2N} \left(\frac{V_i - V_i^{sche}}{\Delta V_{i,lim}} \right)^{2N} \quad (3.7)$$

$$VI_{Loadab,i} = \frac{W_{Loadab,i}}{2N} (r_{Loadab,i})^{2N} \quad (3.8)$$

$$VI_{load.loss,i} = W_{load.loss,i} k_{load.loss,i} \quad (3.9)$$

$$VI_{bus} = \sum_{i=1}^n (VI_{V,i} + VI_{Loadab,i} + VI_{load.loss,i}) \quad (3.10)$$

$$MI_{V,i} = 1 - \left| \frac{V_i - V_i^{sche}}{\Delta V_{i,lim}} \right| \quad (3.11)$$

$$MI_{Loadab,i} = 1 - r_{Loadab,i} \quad (3.12)$$

3. Vulnerability Index and Margin Index for Branches

$$VI_{Pf,i} = \frac{W_{Pf,i}}{2N} \left(\frac{Pf_i}{S_{i,max}} \right)^{2N} \quad (3.13)$$

$$VI_{Qf,i} = \frac{W_{Qf,i}}{2N} \left(\frac{Qf_i}{S_{i,max}} \right)^{2N} \quad (3.14)$$

$$VI_{Qc,i} = \frac{W_{Qf,i}}{2N} \left(\frac{Qc_i}{Q_\Sigma} \right)^{2N} \quad (3.15)$$

$$VI_{line_angle,i} = \frac{W_{line_angle,i}}{2N} \left(\frac{La_i}{La_{i,max}} \right)^{2N} \quad (3.16)$$

$$VI_{Relay,i} = \frac{W_{Relay,i}}{2N} \left(\left(\frac{1}{d_{sr,i}} \right)^{2N} + \left(\frac{1}{d_{rs,i}} \right)^{2N} \right) \quad (3.17)$$

$$VI_{line.loss,i} = W_{line.loss,i} k_{line.loss,i} \quad (3.18)$$

$$VI_{line} = \sum_{i=1}^p (VI_{Pf,i} + VI_{Qf,i} + VI_{Qc,i} + VI_{line.angle,i} + VI_{Relay,i} + VI_{line.loss,i}) \quad (3.19)$$

$$MI_{Sf,i} = 1 - \frac{Sf_i}{S_{i,max}} \quad (3.20)$$

$$MI_{line.angle,i} = 1 - \frac{La_i}{La_{i,max}} \quad (3.21)$$

$$MI_{Relay,i,sr} = d_{sr,i} - K_z |\sin(\pi/2 - \alpha + \theta_{d,sr})| \quad (3.22)$$

$$MI_{Relay,i,rs} = d_{rs,i} - K_z |\sin(\pi/2 - \alpha + \theta_{d,rs})| \quad (3.23)$$

where

VI_{xx} : vulnerability index for different parameters,

MI_{xx} : margin index for different parameters,

W_{xx} : weighting factor for different parameters, based on the system operating practice. If the operators are more concerned with one part, they can assign larger weight to that part.

$k_{x.loss,i}$: loss ratio, between 0 and 1. 0: no loss; 1: complete loss;

N : 1 in general,

$r_{Loadab,i}$: bus loadability,

$$r_{Loadab,i} = \frac{Z_{th,i}}{Z_{L0,i}},$$

$Z_{th,i}$: Thevenin equivalent system impedance,

$Z_{L0,i}$: equivalent load impedance at steady state,

Pf_i, Qf_i, Sf_i : line real, reactive and apparent power,

Qc_i : individual line charging,

Q_Σ : total reactive power output of all generators, or total reactive power of the whole system,

La_i : individual bus voltage angle difference at each line,

$La_{i,max}$: bus voltage angle difference limit at each line,

$d_{sr,i}, \theta_{d,sr}$: magnitude and angle of normalized apparent impedance seen by distance relay located at the sending end of that line and looking at the receiving end,

α : line impedance angle,

K_z : zone setting,

$MI_{Relay,i,sr}, MI_{Relay,i,rs}$: defined as the distance from the apparent impedance seen by transmission line distance relay to the relay protection zone circle; zero or negative values mean the apparent impedance is at or within the protection zone circle.

4. Vulnerability Index for the Whole System

The aggregate system vulnerability index (VI) can be presented by

$$VI = W_{gen}VI_{gen} + W_{bus}VI_{bus} + W_{line}VI_{line} \quad (3.24)$$

The larger the vulnerability index value, the more vulnerable the system condition. We can learn about the system-wide vulnerability and security of individual system elements from different VI and MI values computed for various system conditions.

5. Discussions about Vulnerability Index and Margin Index

System Performance Index (PI) was originally proposed for automatic contingency selection by ranking transmission line outages and generator outages in [55]. It only considers the influences of line/generator outages on bus voltage and line real power flow, similar to Eq. 3.7 and 3.13.

Current power systems are being operated closer to its security limit due to economic reasons. The influences of more parameters must be considered. The proposed vulnerability index and margin index are more comprehensive because they are modeling more parameters than traditional Performance Index. We just give some simple explanations for some new parameters, such as loadability, line charging, bus voltage angle difference, distance relay, etc.

To maintain the scheduled voltage, loadability and reactive power supply need to be considered besides the voltage magnitude. Loadability is often associated with voltage stability limit. There are good methods and references for loadability analysis in [56]. Loadability is computed in this paper by using the Thevenin equivalent impedance method [57].

The line charging influence is also considered by the proposed vulnerability index. Some lightly loaded lines with high charging capacitance may contribute significantly to the reactive power and voltage support. Their outages may decrease the reactive power support or need generators to generate more reactive power. Outages of several lightly loaded transmission lines may reduce the system security, which was one of the key factors in the August 10, 1996 US-Western Blackout [10].

The bus voltage angle difference at each line is also an important index. We can see this from the line power flow and apparent impedance seen by line distance relay.

For example, from the simplest lossless line model (represented with L only), real power flow through the transmission line can be represented by $P_{sr} = \frac{V_s V_r}{x_{sr}} \sin \theta_{sr}$.

A larger bus voltage angle difference means larger power transfer through that line. If the lossless line model or short line model (represented with R & L) is used, we can find that the normalized apparent impedance is only associated with the bus voltages along the line.

$$Z_{d,sr} = \frac{V_s}{I_{sr}} = \frac{V_s}{(V_s - V_r)/Z_{sr}} \quad (3.25)$$

$$\bar{Z}_{d,sr} = \frac{Z_{d,sr}}{Z_{sr}} = \frac{V_s}{V_s - V_r} = \frac{|V_s|}{|V_s - V_r|} \angle \theta_{d,sr} = d_{sr} \angle \theta_{d,sr} \quad (3.26)$$

The larger the bus voltage angle difference, the smaller the normalized apparent impedance, the more possible the case that the apparent impedance may fall into the distance relay backup zone (zone 3 or zone 2 acting as backup) during non-fault conditions such as power swing, overload and low voltage. The heavy loading and low voltage condition caused the Sammis-Star 345-KV line distance relay to "see" a zone 3 fault and trigger the Aug 14, 2003 Northeastern Blackout [1].

The selection of the weight factors can be based on the power system operating practice. If the operators are more concerned with one part, they can assign larger weight value to that part. For example, important tie-lines can be assigned larger values than other transmission lines. Larger generators can be given larger values than smaller generators.

Vulnerability index and margin index can be used for contingency ranking. They can also be used to judge whether the system condition is vulnerable or not. For example, for a normal ("N-1 secure") operating state, we can increase the system loading till it is "N-1 insecure". We define the system vulnerability index value at this point as the threshold for vulnerable criterion. If the system vulnerability index

value is larger than this threshold, the system is vulnerable. This threshold will also change with the changes in the network topology and generation/load pattern. The fast network contribution factor (NCF) method will be used to approximate power flow results and calculate the vulnerability index and margin index.

C. Identification of the Vulnerable Parts in the System

After the system operating condition is identified as being vulnerable by examining the vulnerability index and margin index, the topology processing method and operation index method can be used to identify the vulnerable parts of the system.

The single-line connection, single-line connected load bus, and double-line connection can be identified from the topology processing method through bus-branch incidence matrix A . The operation index method, including network contribution factors, contingency stiffness index, and distance relay margin index, can be obtained by the base power flow condition and network information.

1. Single-line Connection

If one line is out, one or several buses will be isolated from the main part of the system. This specific line is called single-line connection, as represented with the line i - j in Fig. 9a and lines i - j and j - k in Fig. 9b. Those single-line connections are used to identify single-line connected load buses and avoid N-1 analysis at those lines.

2. Single-line Connected Load Bus

If the load bus is connected by one single-line, as represented with the bus j in Fig. 9a and bus k in Fig. 9b, or if it is connected by more than one line but all of them are single-line connections, as represented with the bus j in Fig. 9b, the load bus is

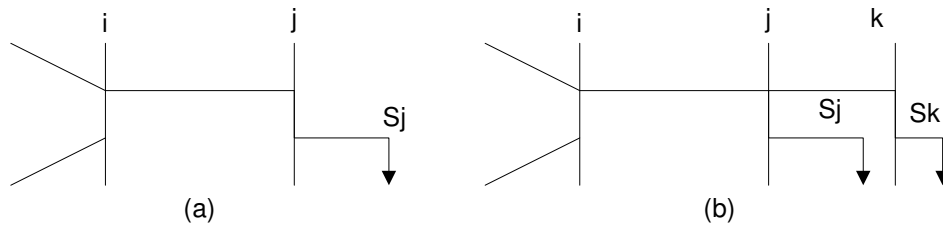


Fig. 9. Single-line connection and its connected load bus

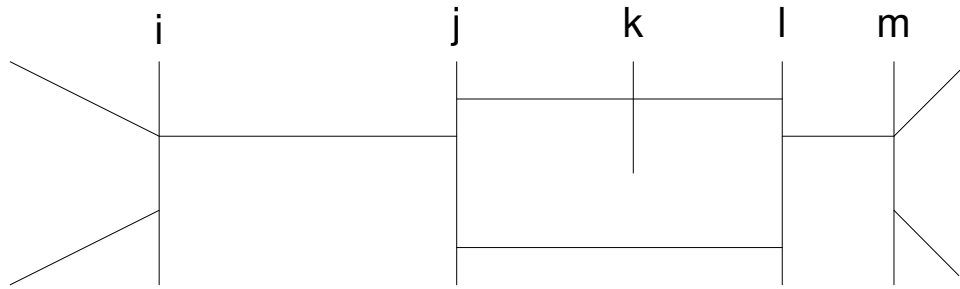


Fig. 10. Double-line connection

called single-line connected load bus. For those single-line connected load buses, the maximum load is limited by the voltage drop along the line. This method is used for voltage control and selected minimum load shedding (SMLS).

3. Double-line Connection

If two lines are out, one or several buses will be isolated from the main part of the system. Those two specific lines are called double-line connections. We can see them represented in Fig. 10 where the outage of lines $j-k$ and $k-l$ isolates the bus k , and outage of lines $i-j$ and $l-m$ isolates buses j , k and l . They are used to identify single-line connections after one line outage and avoid the $N-2$ analysis at those two-line outage combinations.

4. Network Contribution Factor (NCF) Method

The Network contribution factor (NCF) method was first proposed in [58]. Flow network contribution factor (FNCF) and voltage network contribution factor (VNCF) are obtained from the base flow condition and network information. After a network parameter variance, such as line on/off, TCSC on/off, SVC on/off, etc., the branch flow and bus voltage variances can be obtained from FNCF and VNCF in a fast and approximate way.

a. Line Parameter Variance

Given an n -bus- l -branch system, A is the node-branch incidence matrix, Y_p is the primitive branch admittance matrix, Y_{bs} is the node shunt capacitance matrix,

$$Y_p = \text{diag}[y_1 \cdots y_l] \quad (3.27)$$

$$Y_{bs} = \text{diag}[y_{s1} \cdots y_{sn}] \quad (3.28)$$

$$A_{ij} = \begin{cases} 1 & \text{if } i \text{ is the sending node of branch } j \\ -1 & \text{if } i \text{ is the receiving node of branch } j \\ 0 & \text{others} \end{cases} \quad (3.29)$$

From the fast decouple power flow (FDPF) [59], we know the approximate real power equation,

$$\frac{P}{E} = B' \theta \quad (3.30)$$

where,

P , E , θ are the node real power injection, magnitude and angle of the bus voltage respectively.

Assign

$$Y_1 = -imag(Y_p) \quad (3.31)$$

Approximate the line real power flow,

$$P_{line} \cong Y_1 A^T (E\theta) \quad (3.32)$$

Node real power injection,

$$P_{node} \cong AP_{line} \quad (3.33)$$

Bus voltage angle variance due to line parameter variance,

$$\Delta\theta = -(A(Y_1 + \Delta Y_1)A^T)^{-1}(A\Delta Y_1 A^T)\theta \quad (3.34)$$

Rewrite as

$$\Delta\theta = -X_1(A\Delta Y_1 A^T)\theta \quad (3.35)$$

where

$$X_1 = (A(Y_1 + \Delta Y_1)A^T)^{-1} \quad (3.36)$$

for single parameter variance at branch i ,

$$\Delta Y_1 = diag[0 \cdots \Delta y_i \cdots 0]$$

for multi-parameter variance, here only assume at branches i and j , more variances are similar,

$$\Delta Y_1 = diag[0 \cdots \Delta y_i \cdots \Delta y_j \cdots 0]$$

Line real power flow variance,

$$\Delta P_{line} = \Delta Y_1 A^T (E\theta) + (Y_1 + \Delta Y_1) A^T (E\Delta\theta) \quad (3.37)$$

Therefore, for single line i parameter variance,

for the line k , $k \neq i$, real power flow change,

$$\Delta P_{line,k} = -[A_{1k} \cdots A_{nk}]X_1 K_i (y_k \Delta y_i) \quad (3.38)$$

where

$$K_i = [A_{1i} \cdots A_{ni}]^T \sum_{j=1}^n (A_{ji} E_j \theta_j) \quad (3.39)$$

for the line i real power flow change,

$$\Delta P_{line,i} = \left(\sum_{j=1}^n A_{ji} E_j \theta_j / y_i' - [A_{1i} \cdots A_{ni}]X_1 K_i \right) (y_i' \Delta y_i) \quad (3.40)$$

For single line outage, simply assign

$$\Delta P_{line,i} = -P_{line,i} \quad (3.41)$$

For multi-parameter variance, here we only two parameters variance for simple example, assume lines i, j ,

for line k , $k \neq i, j$, real power flow change,

$$\Delta P_{line,k} = -[A_{1k} \cdots A_{nk}]X_1 (K_i \Delta y_i + K_j \Delta y_j) y_k \quad (3.42)$$

where

$$K_i = [A_{1i} \cdots A_{ni}]^T \sum_{l=1}^n (A_{li} E_l \theta_l) \quad (3.43)$$

$$K_j = [A_{1j} \cdots A_{nj}]^T \sum_{l=1}^n (A_{lj} E_l \theta_l) \quad (3.44)$$

For the line i, j real power flow change,

$$\Delta P_{line,i} = \sum_{l=1}^n A_{li} E_l \theta_l \Delta y_i - [A_{1i} \cdots A_{ni}]X_1 (K_i \Delta y_i + K_j \Delta y_j) y_i \quad (3.45)$$

$$\Delta P_{line,j} = \sum_{l=1}^n A_{lj} E_l \theta_l \Delta y_j - [A_{1j} \cdots A_{nj}] X_1 (K_i \Delta y_i + K_j \Delta y_j) y_j \quad (3.46)$$

for lines i, j outages, simply assign

$$\Delta P_{line,i} = -P_{line,i} \quad (3.47)$$

$$\Delta P_{line,j} = -P_{line,j} \quad (3.48)$$

b. Bus Parameter Variance

By the fast decoupled power flow (FDPF),

$$\frac{\Delta Q}{E} = B'' \Delta E \quad (3.49)$$

$$\Delta E = (B'')^{-1} \frac{\Delta Q}{E} = X_2 \Delta B_s E \quad (3.50)$$

where,

$$X_2 = (B'')^{-1} \quad (3.51)$$

$$\Delta Q = \Delta B_s E^2 \quad (3.52)$$

for single bus parameter variance at bus i ,

$$\Delta B_s = [0 \cdots \Delta y_{bs,i} \cdots 0]^T$$

bus k voltage variance

$$\Delta E_k = X_{2,ki} E_k \Delta y_{bs,i} \quad (3.53)$$

for bus multi-parameter variance at buses i, j

$$\Delta B_s = [0 \cdots \Delta y_{bs,i} \cdots \Delta y_{bs,j} \cdots 0]^T$$

bus k voltage variance

$$\Delta E_k = X_{2,ki} E_k \Delta y_{bs,i} + X_{2,kj} E_k \Delta y_{bs,j} \quad (3.54)$$

- c. Flow Network Contribution Factor (FNCF) and Voltage Network Contribution Factor (VNCF)

For single parameter variance at line i , Flow Network Contribution Factor (FNCF) can be defined as follows:

for line k , $k \neq i$, FNCF is

$$N_{f,k} = -[A_{1k} \cdots A_{nk}]X_1K_i \quad (3.55)$$

for line k , $k = i$, FNCF is

$$N_{f,k} = \sum_{j=1}^n A_{ji}E_j\theta_j/y'_i - [A_{1i} \cdots A_{ni}]X_1K_i \quad (3.56)$$

where X_1 and K_i as defined in Eq. 3.36 and Eq. 3.39 respectively

Line k flow variance

$$\Delta P_{line,k} = N_{f,k}y_k\Delta y_i \quad (3.57)$$

For multi-parameter variance, here only take 2 parameters (lines i, j) variance as simple example,

Line k flow variance

$$\Delta P_{line,k} = N_{f,k}y_k(\Delta y_i + \frac{K_j}{K_i}\Delta y_j) \quad (3.58)$$

where K_i and K_j as defined in Eq. 3.43 and Eq. 3.44 respectively.

For single parameter variance at bus i , Voltage Network Contribution Factor (VNCF) can be defined as follows:

for bus k , VNCF is

$$N_{v,ki} = X_{2,ki} \quad (3.59)$$

bus k voltage variance is

$$\Delta E_k = N_{v,ki} E_k \Delta y_{bs,i} \quad (3.60)$$

where X_2 is defined in Eq. 3.51.

For multi-parameter variance, here only take 2 parameters (buses i, j) variance as simple example,

bus k voltage variance

$$\Delta E_k = N_{v,ki} E_k \Delta y_{bs,i} + N_{v,kj} E_k \Delta y_{bs,j} \quad (3.61)$$

The approximate variance for line k reactive power flow is

$$\Delta Q_{f,k} \approx P_{f,k} \Delta \theta_k \quad (3.62)$$

where $\Delta \theta$ can be obtained from Eq. 3.35.

By using the FNCF and VNCF, we can find variance of the line flow and variance of the bus voltage due to network parameter change. Thus, line overload and bus low voltage problems due to parameter change can be predicted.

5. Contingency Stiffness Index

The contingency stiffness index is proposed to represent the maximum disturbance at buses directly affected by a line outage contingency, normalized by the bus equivalent admittance [60]. It is also used in this dissertation to identify vulnerable lines whose outages may impact the security of the system. For the outage of line k connecting buses i and j , it is defined as

$$SI_k = Max \left\{ \frac{S_{ij}}{Y_i^{eq}}, \frac{S_{ji}}{Y_j^{eq}} \right\} \quad (3.63)$$

where

S_{ij}, S_{ji} : apparent power flow at the two ends of line k ,

Y_i^{eq}, Y_j^{eq} : equivalent admittance of buses i and j .

The contingencies with the stiffness index values higher than a pre-determined threshold need more attention.

6. Distance Relay Margin Index

Eq. 3.22 and 3.23 define the distance relay margin indices from both ends of the line. If either one is negative, that means, the apparent impedance phasor falls into the relay protection zone. The single-line connection, single-line connected load bus, and double-line connection can be identified from the topology processing method through bus-branch incidence matrix A . The flow and voltage network contribution factors, contingency stiffness index, and distance relay margin index can be obtained by the base power flow condition and network information.

D. Prediction of the Overload and Voltage Problems

For a given network event or assumed network contingency, we can first use fast network contribution factor (NCF) method to get approximate power flow results. Then associated margin and vulnerability indices can be obtained. If the operation condition is judged vulnerable, the vulnerable elements will be identified by the topology processing and operation index methods. Line overload or voltage problems can be predicted by the flow and voltage network contribution factor method. The final results will be verified by the full AC power flow method. If the contingency is a loss of generator or load, new AC power flow needs to be run instead.

E. Control Methods and Automatic Control Scheme

If line overload and/or low voltage problems occur after the event, associated control needs to be taken to solve such problems. The proposed steady state control scheme is based on methods of network contribution factor (NCF), generator distribution factor (GDF), load distribution factor (LDF) and selected minimum load shedding (SMLS). GDF and LDF are proposed in [61] for supplemental charge allocation in the transmission open access. In this dissertation, they are used for line overload relief based on their contribution to the line flow. Here we give the brief description of those methods and related automatic control scheme.

1. Network Contribution Factor (NCF) and NCF Control

For a given system, there are some available network control means [53,62–65], such as line switching, TCSC control, SVC control, shunt capacitor/reactor switching, etc. For the line overload problem, choose Eq. 3.57 or 3.58 to get the wanted overload relief. For the bus voltage problem, choose Eq. 3.60 or 3.61 to get the bus voltage adjustment.

2. Generator Distribution Factor (GDF) and GDF Control

Let the gross nodal power P_i^g flowing through node i (when looking at the inflows) be defined by

$$P_i^g = \sum_{j \in \alpha_i^u} |P_{ij}^g| + P_{Gi} \quad \text{for } i = 1, 2, \dots, n \quad (3.64)$$

where

α_i^u is the set of nodes supplying power and directly connected into node i , and

P_{Gi} is the power generation injected into node i . Rewrite it as:

$$A_u P_{gross} = P_G \quad (3.65)$$

where A_u is the upstream distribution matrix with its $(ij)^{th}$ element defined by

$$[A_u]_{ij} = \begin{cases} 1 & \text{for } i = j \\ -|P_{ji}/P_j| & \text{for } j \in \alpha_i^u \\ 0 & \text{others} \end{cases} \quad (3.66)$$

where

P_{ji} is the real power flow from node j to node i in line $j - i$; P_j is the total real power injected into node j . Then we have

$$P_i^g = \sum_{k=1}^n [A_u^{-1}]_{lk} P_{Gk} \quad \text{for } i = 1, 2, \dots, n \quad (3.67)$$

Finally the contribution of each generator k to line $i - j$ flow can be calculated by

$$P_{ij}^g = \sum_{k=1}^n D_{ij,k}^g P_{Gk} \quad \text{for } j \in \alpha_i^u \quad (3.68)$$

$$D_{ij,k}^g = P_{ij}^g [A_u^{-1}]_{ik} / P_i^g \quad (3.69)$$

$D_{ij,k}^g$ can be called the generation distribution factor (GDF). They are always positive or zero. For the line i - j overload problem, simply choose the most and least contributing generator pair, decrease the output of the most contributing generator and increase that of the least contributing one. The generator adjustment amount will be restricted by generator upper/lower limit and the line transfer limit. When those limits are hit and the line overload problem still exists, the second most and least contributing generator pair will be chosen till the overload problem is solved.

3. Load Distribution Factor (LDF) and LDF Control

Similarly, let the gross nodal power P_i^n (looking from outflows) be defined by

$$P_i^n = \sum_{j \in \alpha_i^d} |P_{ij}^n| + P_{Li} \quad \text{for } i = 1, 2, \dots, n \quad (3.70)$$

where

α_i^d is the set of nodes supplied directly from node i , and P_{Li} is the load at node i . Similarly, rewrite it as:

$$A_d P_{net} = P_L \quad (3.71)$$

where

A_d is the downstream distribution matrix with its $(ij)^{th}$ element defined by

$$[A_d]_{ij} = \begin{cases} 1 & \text{for } i = j \\ -|P_{ji}/P_j| & \text{for } j \in \alpha_i^d \\ 0 & \text{others} \end{cases} \quad (3.72)$$

$$P_i^n = \sum_{k=1}^n [A_d^{-1}]_{lk} P_{Lk} \quad \text{for } i = 1, 2, \dots, n \quad (3.73)$$

Finally the contribution of each load k to line $i - j$ flow can be calculated by

$$P_{ij}^n = \sum_{k=1}^n D_{ij,k}^n P_{Lk} \quad \text{for } j \in \alpha_i^d \quad (3.74)$$

$$D_{ij,k}^n = P_{ij}^n [A_d^{-1}]_{ik} / P_{Lk} \quad (3.75)$$

$D_{ij,k}^n$ can be called the load distribution factor (LDF). They are always positive or zero. If the load can be reduced by an agreement, it can be taken into the LDF control. For the overload line, simply choose one or several most contributing loads to shed to solve the overload problem.

4. Selected Minimum Load Shedding (SMLS)

If the power flow diverges due to a line outage but without loss of system integrity, normally some load shedding scheme needs to be activated to make the power flow converge. If the power flow converges, some bus voltages are lower than their lower limits. Load shedding also needs to be taken if other control means can not solve the problem. The following are the steps for SMLS.

Step 1. Check whether the system has single-line connected load buses or not. If bus j is the single-line connected load bus, calculate the approximate voltage drop along line $i - j$:

$$dV_{ij} \approx P_{ij}R_{ij} + Q_{ij}X_{ij} \quad (3.76)$$

where

P_{ij}, Q_{ij} : real and reactive part of line $i - j$ flow,

R_{ij}, X_{ij} : resistance and reactance of line $i - j$.

If $dV_{ij} > dV_{ij,lim}$, check whether there is shunt reactor or capacitor at this bus. If there is a shunt reactor, switch off the shunt reactor. If there is a shunt capacitor, switch on the capacitor. Then recalculate the dV_{ij} . If the voltage difference is still larger than the limit, shed the load at this bus.

$$k_{ratio} = dV_{ij,lim}/dV_{ij} \quad (3.77)$$

$$k_{shed} = 1 - k_{ratio} \quad (3.78)$$

After the load shedding at single-line connected load buses is performed, run power flow. Check whether power flow converges or not. If it diverges, increase the load shedding ratio. Otherwise, check whether there is low voltage problem. If yes, go to Step 2. If no, stop.

Step 2. Check whether the low voltage bus is single-line connected load bus, and if so, continue load shedding at this bus. If it is not a single-line connected load bus, choose the neighboring buses and voltage sensitive buses to shed their loads to bring the bus voltage within the limit.

Step 3. Choose the control area or system-wide load shedding based on an available control scheme.

Step 4. Compare different load shedding results, and choose the minimum load shedding as the final control means.

5. A Scheme for Detection and Prevention of Cascading Outages

The conventional approach is for the lines experiencing overload conditions for a long time to be tripped off by relays. Under frequency load shedding will be activated when the demand is larger than supply and the system frequency keeps decreasing. So will the under voltage load shedding during low voltage conditions if there exists such control scheme.

During the stressed system conditions, if the line outage decreases the security level and causes more cascading outages and low voltage problem, that line should not be tripped. Other overload relief means should be activated. We have defined the steady state control scheme combined with network contribution factor (NCF) and generator distribution factor (GDF) methods. If these two methods can not solve the overload condition, load control based on load distribution factor (LDF) method and selected minimum load shedding (SMLS) will be inacted. For the low bus voltage problem, the minimum load shedding will be undertaken instead of the control area or system-wide load shedding. Fig. 11 is the flow chart for the proposed automatic control scheme.

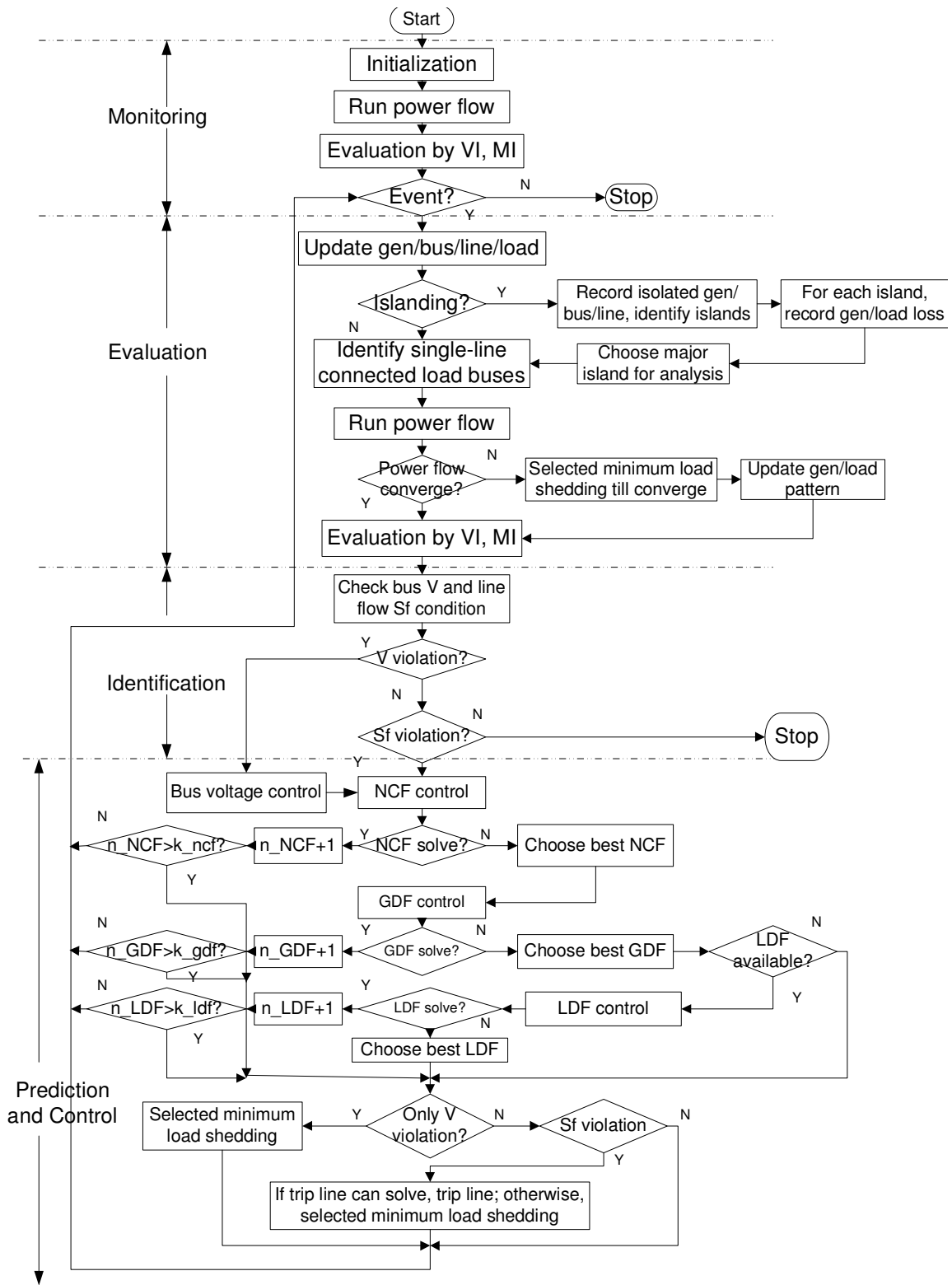


Fig. 11. Flowchart of the control scheme

The basic procedure is explained as follows.

- Step 1. Initialize the computation;
- Step 2. Run the base power flow;
- Step 3. Evaluate system vulnerability and security by VI and MI indices;
- Step 4. Check whether an event has occurred or not. If no event occurs, Stop; if an event occurs, update system information;
- Step 5. Check whether system islands have been formed or not. If system islands are not formed, go to Step 8;
- Step 6. Otherwise, identify the islands, record isolated bus/generator/branch, and record generator/load loss in each island;
- Step 7. Choose major island for analysis, update system information;
- Step 8. Identify the single-line connected load buses;
- Step 9. Run the power flow;
- Step 10. If power flow converges, go to Step 12;
- Step 11. Otherwise, use selected minimum load shedding (SMLS) scheme to make power flow converge, and update generator/load pattern;
- Step 12. Evaluate vulnerability and security by VI and MI;
- Step 13. Check whether there is any bus voltage V and line flow S_f violation. If there is no V violation, go to Step 15;
- Step 14. Otherwise, activate bus voltage control;

- Step 15. Check whether there is line flow violation, if not, stop;
- Step 16. Otherwise, executed associated NCF control to solve the violation problem;
- Step 17. If NCF method solves the problem, $n_NCF = n_NCF + 1$, if $n_NCF < k_NCF$, go to Step 4, else, go to Step 19; if NCF does not solve the problem, choose the best available NCF control;
- Step 18. Execute GDF control. If GDF method solves the problem, $n_GDF = n_GDF + 1$, if $n_GDF < k_GDF$, go to Step 4, else, go to Step 19; if GDF does not solve the problem, choose the best available GDF control, go to Step 19;
- Step 19. Check whether LDF control is available or not. If not, go to Step 20; Otherwise, check if LDF method solves the problem, if yes, $n_LDF = n_LDF + 1$, if $n_LDF < k_LDF$, go to Step 4, else, go to Step 20; if LDF does not solve the problem, choose the best available LDF control, go to Step 20;
- Step 20. Final control. If the original violation is only voltage (V) violation, use the selected minimum load shedding scheme to bring V within limit; otherwise, check whether removing overloaded line can solve the overload problem or not, if yes and there is no other violations, remove the line; otherwise, use the selected minimum load shedding scheme to eliminate any violation.

Note: k_NCF , k_GDF and k_LDF are pre-defined numbers. If n_NCF , n_GDF and n_LDF are larger than those values, the final control is used. Otherwise, the associated NCF, GDF and LDF control are used.

F. Case Study

We use the IEEE One Area 24-bus system as the study system [66]. Fig. 12 gives the system configuration. Detailed system data is shown in Appendix B.

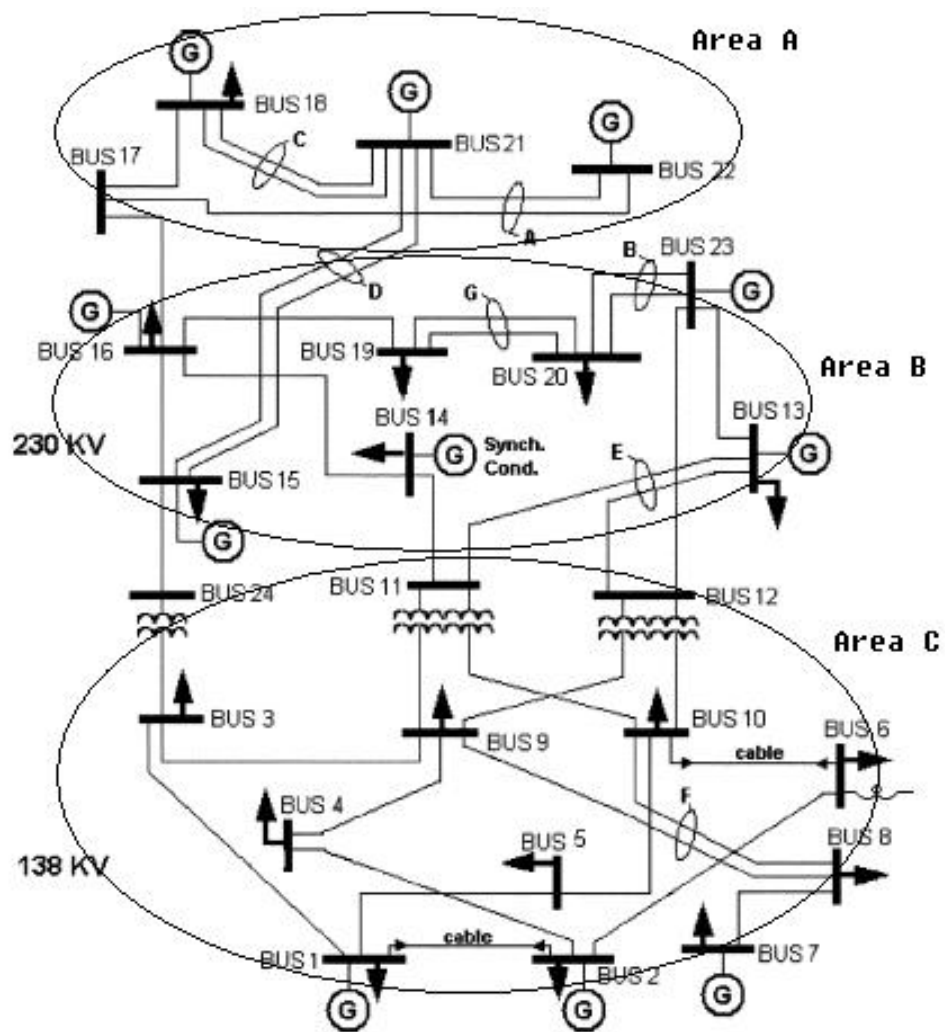


Fig. 12. IEEE One Area RTS-96 24-bus system

For the vulnerability index calculation, we simply assign all weights as 1, the line bus voltage angle difference limits as 40 degrees, PQ bus voltage magnitude limits as 1.0 p.u., the base power as 100MVA. Then we sum all individual vulnerability index values of generators, buses and lines and get the separate summary of vulnerability index values.

Bus voltage magnitude lower limit is 0.9 p.u.. The transmission line thermal limit is assumed to be the line rate A setting in the standard IEEE power flow data. Bus voltage drop limit along the transmission line is 0.10 p.u.. For the margin index, we just choose margin indices of generator real and reactive power outputs, bus voltage, bus loadability, line flow, line angle, and line distance relay for simple demonstration.

Here we give three study cases. The Case 1 is the outage of special cable line L10 (B6-10). There will be a serious low voltage problem if the compensation reactor at bus 6 is not switched off. In reality, the system can not operate at such a low voltage level. That means, voltage collapse may happen and the system may have cascading event if no appropriate control. The Case 2 is the outage of lines L6 (B3-9) and L27 (B16-17) which results in power flow divergence. Voltage collapse and cascading event may happen before the power flow divergence. The Case 3 is the outage of lines L25 (B15-21) and L26 (B15-21) which results in an overload on two other lines. System islanding and cascading outage may occur if there is no appropriate control. The proposed automatic cascading events prevention and mitigation scheme gives very good results for these cases.

Case 1. Outage of cable line 10 (B6-10)

If the reactor at bus 6 is not switched off, the bus 6 voltage magnitude is 0.6726 p.u. Load shedding is taken to increase the bus 6 voltage. Even if 99% of the total system load is shed, the bus 6 voltage magnitude is still as low as 0.8701 p.u.. If the reactor at bus 6 is switched off, its voltage magnitude is 0.8555 p.u.. If 16.2% of the

Table II. Vulnerability and margin indices of different conditions

	Case 1A	Case 1B	Case 1C	Case 1D	Case 1E
VI values	7.863	23.369	12.122	14.773	12.059
MI values	4.063	3.619	3.800	3.981	3.807

total system load, that is, $461.7 + j93.96$ MVA, is shed, the bus 6 voltage magnitude is increased to 0.90 p.u..

The new control scheme first finds that bus 6 is a single-line connected load bus by L5 (B2-6). Second, it searches whether there is an available shunt reactor or capacitor at that bus. Then it finds and switches off the shunt reactor. Third, it calculates the approximate voltage drop along this single line L5 (B2-6) based on the original load level at bus 6. $\Delta V_{26} = P_{26}R_{26} + Q_{26}X_{26} = 1.36 \times 0.05 + 0.28 \times 0.192 = 0.122 > 0.10$ p.u. To bring the bus 6 voltage within limit, the selected minimum load shedding (SMLS) is run and shedding 6.84% of the original load at bus 6 can bring the bus 6 voltage be 0.90 p.u.. Thus, only $9.3 + j1.92$ MVA load is shed. Compared with the total system load shedding of $461.7 + j93.96$ MVA obtained by the conventional method, the proposed approach is only about 2.02% of the conventional method.

Table II gives a simple summary of vulnerability and margin indices for different conditions. The Case 1A is the base power flow case without L10 outage. The Case 1B is with L10 outage. The Case 1C is the L10 outage with reactor switched off at B6. The Case 1D is the L10 outage, reactor switched off, and 16.2% system load shedding. The Case 1E is similar as the Case 1D but with only 6.84% load shedding at B6. Here we take 100MVA load loss as 1.00 in the VI calculation.

The base Case 1A has the smallest VI and largest MI. The Case 1B has the largest VI and smallest MI. The Case 1C decreases the vulnerability and increases the security level compared with the Case 1B after the shunt reactor is switched off.

Table III. Solution methods for lines L6(B3-9) & L27(B16-17) outages

	Procedure	Result
Method 1	(191.52+j38.976) MVA system load shedding	Power flow converges, with B3 & B24 voltage as 0.6122 p.u. and 0.6032 p.u.
Method 2	(1311.6+j266.92) MVA system load shedding	Power flow converges, with B3 & B24 voltage as 0.9135 p.u. and 0.90 p.u.
Proposed Method	(82.836+j17.027) MVA load shedding at B3	Same results as Method 2, but only 6.32% shedding amount of Method 2.

The Case 1D increases the security level but increases vulnerability because of large load shedding. The Case 1E is the optimal one because it increases the security while requiring a minimum load shedding.

Case 2. Outage of lines L6 (B3-9) and L27 (B16-17)

Power flow diverges because of the outage of those two lines. By the conventional method, after 6.72% of the total system load (191.52+j38.976 MVA) is shed, the power flow converges. But the bus voltage magnitudes at bus 3 and 24 are 0.6122 p.u. and 0.6032 p.u. respectively. Then 46.02% of the total system load (1311.6+j266.92 MVA) needs to be shed to make the voltages at bus 3 and 24 to be 0.9135 p.u. and 0.90 p.u. respectively.

The new scheme first identifies that bus 3 is a single-line connected load bus although it is connected by two lines. Second, it concludes that there is no available shunt reactor or capacitor at bus 3. Third, it determines that the approximate voltage drop along this line is 0.177 p.u., which is larger than the 0.1 p.u. limit. Fourth, it runs the selected minimum load shedding and finds that if 46.02% of the load (82.836+j17.027 MVA) is shed at bus 3, the power flow will converge and there is no any limit violation. The amount of load to be shed determined by the new method is only 6.32% of what was determined by the conventional method. The results of those methods can be shown in Table III.

Case 3. Outage of lines L25 (B15-21) and L26 (B15-21)

Assume that line L25 is tripped due to a fault and the parallel line L26 is also tripped due to relay misoperation, which is a possible case. The apparent flows at L28 (B16-17) and L30 (B17-18) are 7.4453 p.u. and 5.6395 p.u. respectively. The two lines will be overloaded because both of their thermal limits are 5.00 p.u..

L28 and L30 will be tripped due to an overload. Area A will be disconnected from the main part of the system. Before the islanding, there is a total of $7.57+j1.446$ p.u. flow transferred from Area A to Area B through three tie-lines: L25, L26 and L28. From the steady state analysis viewpoint, to make the balance between power demand and supply, at least 7.57 p.u. of real power generation needs to be reduced at Area A. At Area B and Area C, the load shedding amount of $698.72+j142.13$ MVA, which constitutes 27.76% of the total load, is needed to make the power flow converge without any limit violation. If we consider the system dynamics, the system may lose the stability and cascading outage may occur.

The new method first finds the L28 and L30 overload after outage of L25 and L26. Second, it tries to use the NCF and GDF control methods to solve the overload problem instead of tripping L28 and L30. Since there is no contributing NCF method available, GDF control method is pursued. GDF method finds two generator pairs which contribute most and least to the overload of L28 and L30 respectively, G10 (at B22) and G1 (at B1) for L28, and G8 (at B18) and G2 (at B2) for L30. In Step 1, GDF control chooses to increase the real power output of G1 and decrease that of G10 by the same amount to solve the L28 overload. GDF control increases the real power output of G2 and decreases that of G8 to solve the L30 overload. The outputs of G1 and G2 can only be increased to their upper limits 2.304 p.u.. By this step, the flow at L30 is 4.7971 p.u. and the overload is solved. But the flow at L28 is 6.332 p.u., which is still larger than 5.00 p.u. thermal limit. In Step 2, generator pair G10

Table IV. Solution methods for lines L25(B15-21) & L26(B15-21) outages

	Procedure	Result
Base condition	L28 & L30 overload (7.4453 p.u. & 5.6395 p.u. vs. their 5 p.u. limit)	Outage of L28 & 30, system islanding and cascading; or (698.72+j142.13) MVA load shedding to save the system
Step 1	Down G10 & Up G1 to solve L28 overload; Down G8 & Up G2 to solve L30 overload;	L30 overload solved, L28 overload decreased because of G1 upper limit
Step 2	Down G10 & Up G3 to solve L28 overload;	L28 overload decreased because of L11 transfer limit
Step 3	Down G10 & Up G4 to solve L28 overload;	Solve
Step 4	Verified with AC load flow	Solve, no violation.

(at B22) and G3 (at B7) is chosen to solve the L30 overload. There is a thermal limit of 1.75 p.u. at L11 (B7-8). Thus the increase of G3 has a limit. By taking this step, the flow at L28 is brought to 5.764 p.u., which is larger than 5.00 p.u. limit. In Step 3, generator pair G10 and G4 (at B13) is chosen and L28 overload is finally solved. By applying the steady state analysis method, the overload problem is solved by using the NCF and GDF methods. The possible cascading outage is prevented. The results of those methods can be shown in Table IV.

G. Summary

This chapter proposes a new approach to detect and prevent cascading outages at their initial stage that can be assessed using the steady state analysis method. For each operating state, the system vulnerability and security are evaluated based on the vulnerability and margin indices. The vulnerable parts of the system can be identified based on the topology processing and operational index methods. The next possible event can be predicted based on the analysis. If there are any problems of islanding, transmission line overload, bus voltage violation, or distance relay misoperation, new control means based on network contribution factor (NCF), generator distribution

factor (GDF), load distribution factor (LDF) and selected minimum load shedding (SMLS) methods will be taken to prevent the possible cascading events. Case studies using the IEEE 24-bus test system show good results of the proposed approach.

The proposed approach is based on the steady state analysis method. It gives an understanding how cascading outages progress in early stages and provides control means for preventing further unfolding of the cascade. The power system cascading events are very complex and a comprehensive analysis needs also to consider the system dynamics, which will be included in the following chapters.

CHAPTER IV

TRANSIENT STABILITY CONTROL SCHEME*

A. Introduction

The steady state control scheme in Chapter III gives promising results for early detection and prevention of cascading outages in their early stage. For the transient progress stage and system dynamic conditions during and after big disturbances (i.e., faults), transient stability analysis must be executed. If it finds that the system will lose the stability before it can move to a new steady state operation point, transient stability control must be used to preserve the system.

Transient stability control is more difficult in current deregulated environment than before. This is due to the frequently changing generation/load patterns and network topology during normal power system operations. Competitive market, steady increasing load, and limited transmission capacity stress the power system closer to the security margin. Several unexpected disturbances may put the system into an emergency state, resulting in cascading outages or system collapse if there are no fast and appropriate stability controls in action. Conventional off-line study and pre-defined stability control scheme can no longer adapt to the fast changing conditions. The need for fast and adaptive stability analysis and stability control is more visible.

Lyapunov-like direct methods have the advantages of speed and security margin information. Therefore, many good results have been obtained by many researchers' continuous efforts. There are some useful investigations in the transient stability analysis by using analytical sensitivity of the transient energy margin [67–69]. How-

*Part of the material in this chapter is reprinted with permission from “Stability control using PEBS method and analytical sensitivity of the transient energy margin” by Hongbiao Song and Mladen Kezunovic, *Presented in 2004 IEEE PES Power Systems Conference and Exposition*, New York, Oct. 2004, vol. 2, pp. 1153-1158. ©2004 IEEE.

ever, these interesting papers focus more on the stability analysis by using sensitivity information. Stability control is discussed less.

This chapter proposes the transient stability control scheme using PEBS method and analytical sensitivity of the transient energy margin. It classifies current stability control means into two categories, admittance-based control (ABC) means and generator-input-based control (GIBC) means. The proposed method can quickly find the parameter variance of each stability control means for the transient stability analysis. Analytical sensitivity of the transient energy margin is used to find the most suitable control to make the possibly unstable system stable. One of the Lyapunov methods, potential energy boundary surface (PEBS) method, is used. Some simulation results are provided.

In Section B, the background of transient stability analysis methods is given. The proposed transient stability control classification is discussed in Section C. The sensitivity analysis of transient energy margin is presented in Section D. Section E describes the transient stability control scheme. Case Study and Summary are provided in Sections F and G respectively.

B. Transient Stability Analysis Methods

As defined in Chapter II, transient stability refers to the ability of an electric power system to maintain synchronism between its parts when subjected to a disturbance and to regain a state of equilibrium following that disturbance. Transient stability problem is one of the most important problems to ensure the stable and secure operation of power systems. It has been the dominant stability problem on most power systems and many power system cascading outages have been caused by transient instability [70]. There are lots of books and papers covering transient

stability analysis and control [5, 51, 53, 67, 68, 70–92].

In general, the dynamics of the power system state can be described by a set of differential equations (power swing equations):

$$\dot{x} = f(x, u) \quad (4.1)$$

where

x is a vector of state variables, including variables associated with generators and excitation systems.

u is an input vector, including stator and field voltages, and mechanical power input of each generator in the system.

The objective is to study the stability of the dynamic system described by the differential equations from the steady state operating point as the starting point. It can provide time-domain information related to variances in rotor angles, speeds, torques, voltages, currents, and powers of generators as well as the variances in voltages and power flows in the transmission network during and after the disturbance, depending on the modeling details of the system.

Normally there are three types of solution methods: time-domain methods, Lyapunov-like direct methods and hybrid methods. Time domain methods have the advantages of handling any type of power system modeling, providing time-wise description of the dynamic information, and having the highest accuracy. Their disadvantages are time-consuming aspect and lack of sensitivity analysis. Lyapunov-like direct methods eliminate most of the time domain simulations, by inferring information about transient stability from the system when entering its post-fault phase. They can also provide stability margin and sensitivity analysis for preventive control. The results of direct methods are not as accurate and reliable as time-domain methods. Hybrid methods try to incorporate the transient energy calculation into the time-domain

simulations. They are not used as frequently as the former two methods.

In this dissertation, we use one direct method, potential energy boundary surface (PEBS) method, and analytical sensitivity of transient energy margin for transient stability analysis and control. Its results will be verified by the most accurate time-domain method. First, we will introduce the Lypunov-like transient energy function. PEBS method will be described next.

Let us use the classical model of machine for an example, in the Center of Angle (COA) reference [67], power swing equations can be written as:

$$\dot{\theta}_i = \tilde{\omega}_i \quad (4.2)$$

$$M_i \dot{\tilde{\omega}}_i = P_i - P_{ei} - \frac{M_i}{M_T} P_{COI} \quad (4.3)$$

where

$$P_{ei} = \sum_{j=1, j \neq i}^n [C_{ij} \sin(\theta_i - \theta_j) + D_{ij} \cos(\theta_i - \theta_j)] \quad (4.4)$$

$$P_i = P_{mi} - E_i^2 G_{ii} \quad (4.5)$$

$$P_{COI} = \sum_{i=1}^n (P_i - P_{ei}) \quad (4.6)$$

$$M_T = \sum_{i=1}^n M_i \quad (4.7)$$

$$C_{ij} = E_i E_j B_{ij} \quad (4.8)$$

$$D_{ij} = E_i E_j G_{ij} \quad (4.9)$$

C_{ij} , D_{ij} : real and reactive parts of the admittance matrix. They change at pre-fault, during-fault and post-fault conditions.

By linear path-dependence assumption, we can get the transient energy function as follows:

$$V_{\theta, \tilde{\omega}} = V_{KE} + V_{PE} \quad (4.10)$$

The kinetic energy function is:

$$V_{KE} = \frac{1}{2} \sum_{i=1}^n M_i \tilde{\omega}_i^2 \quad (4.11)$$

The potential energy function is:

$$V_{PE} = - \sum_{i=1}^n P_i^{pf}(\theta_i - \theta_i^s) - \sum_{i=1}^{n-1} \sum_{j=i+1}^n [C_{ij}^{pf}(\cos \theta_{ij} - \cos \theta_{ij}^s) - \beta_{ij} D_{ij}^{pf}(\sin \theta_{ij} - \sin \theta_{ij}^s)] \quad (4.12)$$

As for the transient stability, the critical energy is the potential energy at the controlling unstable equilibrium point (Controlling UEP) since it represents the maximal energy that the system can absorb. If the total energy at the clearing time is larger than this one, the associated machine(s) will lose the synchronism. Thus, transient energy margin can be calculated by following equation:

$$\Delta V = V(\theta^u, \tilde{\omega}^u) - V(\theta^{cl}, \tilde{\omega}^{cl}) \quad (4.13)$$

Since at Controlling UEP, we assume $\tilde{\omega}^u = 0$, we can get transient energy margin ΔV by following equation:

$$\begin{aligned} \Delta V = & - \frac{1}{2} M_{eq} (\tilde{\omega}_{eq}^{cl})^2 - \sum_{i=1}^n P_i^{pf}(\theta_i^u - \theta_i^{cl}) - \\ & \sum_{i=1}^{n-1} \sum_{j=i+1}^n [C_{ij}^{pf}(\cos \theta_{ij}^u - \cos \theta_{ij}^{cl}) - \beta_{ij} D_{ij}^{pf}(\sin \theta_{ij}^u - \sin \theta_{ij}^{cl})] \end{aligned} \quad (4.14)$$

where,

$$\beta_{ij} = \frac{\theta_i^u + \theta_j^u - \theta_i^s - \theta_j^s}{\theta_{ij}^u - \theta_{ij}^s} \text{ (in linear dependence direction),}$$

θ^{cl} : rotor angle positions at the end of disturbance (fault clearing time),

θ^u : rotor angle positions of Controlling UEP,

$$M_{eq} = M_{cr} M_{sys} / (M_{cr} + M_{sys}),$$

$$\tilde{\omega}_{eq}^{cl} = \tilde{\omega}_{cr}^{cl} - \tilde{\omega}_{sys}^{cl},$$

M_{eq} : inertia constants of the equivalent generator,

M_{cr} : inertia constants of the critical generators,

M_{sys} : inertia constants of the rest generators,

$\tilde{\omega}_{eq}$: speed of inertia centers of the equivalent generator at the end of a disturbance,

$\tilde{\omega}_{cr}$: speed of inertia centers of the critical generators at the end of a disturbance,

$\tilde{\omega}_{sys}$: speed of inertia centers of the rest of generators at the end of a disturbance.

Potential energy boundary surface (PEBS) method is based on physical intuition [74]. From the post-fault stable equilibrium point (SEP) draw a number of rays in each direction in the angle space with Center of Angle (COA) as reference. Along each ray, search for the first point where the potential energy achieves a local maximum. Join those points of θ to form the boundary surface of interest (stability boundary). Mathematically, PEBS can be obtained by setting the directional derivative of the potential energy $V_p(\theta)$ to zero, as follows:

$$[f(\theta)]^T \bullet (\theta - \theta^s) = 0 \quad (4.15)$$

It can be rewritten as:

$$\sum_{i=1}^n (\theta_i - \theta_i^s) f_i(\theta) = 0 \quad (4.16)$$

$$f_i(\theta) = -\frac{\partial V_{PE}(\theta)}{\partial \theta_i} = P_i - P_{ei} - \frac{M_i}{M_T} P_{COI} \quad (4.17)$$

Eq. 4.17 uses the post-fault configuration (admittance matrix).

Inside the PEBS, the $[f(\theta)]^T \bullet (\theta - \theta^s)$ is smaller than 0 and outside the PEBS it is larger than 0. So $[f(\theta)]^T \bullet (\theta - \theta^s)$ changing sign from '-' to '+' is the indication of PEBS crossing. Detailed description can be found in [73].

Fig. 13 gives the relationship among unstable equilibrium point (UEP), PEBS crossing point, exit point, Controlling UEP [76]. Fig. 14 gives a simple example of

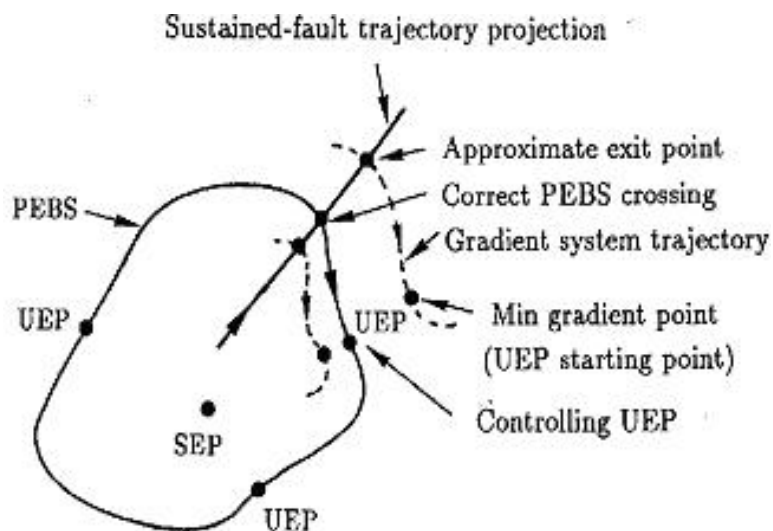


Fig. 13. PEBS crossing and controlling UEP

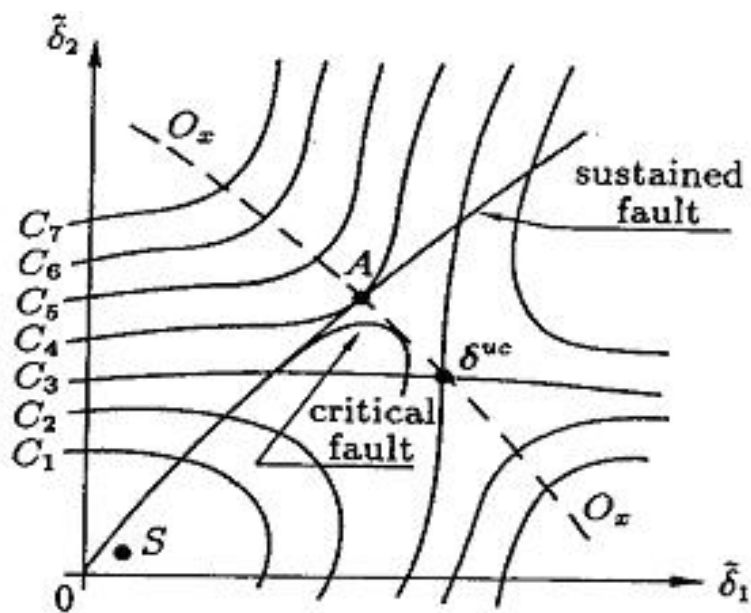


Fig. 14. System trajectory in the rotor angle space

the system trajectory in the rotor angle space [74].

PEBS method assumes that the system critical energy value is equal to the system potential energy maximum value along the system trajectory. We can see from Fig. 13

and Fig. 14 that when the system is not very ill-conditioned, the controlling UEP, and the PEBS crossing points of fault-on and critical trajectories are very close. Therefore, PEBS method can get an accurate approximation of critical clearing time (CCT). The advantage of PEBS method is that it does not need the Controlling UEP calculation, which is very complex and time consuming. The system post-fault trajectory path is not known before the CCT solution. It may give either an optimistic or pessimistic estimate of the CCT. Iterative PEBS [74] and Corrective PEBS [77] are proposed to give more accurate solution of CCT. Their procedures are going as follows:

Step 1. Integrate the fault-on trajectory, use the fault-on θ and post-fault admittance matrix Y to get the first PEBS crossing point θ_{cross} , that is, at time T , $[f(\theta)]^T \bullet (\theta - \theta^s)$ changes the sign from '-' to '+', and V_{PE} gets its local maximum which is the first estimate of V_{cr} .

Step 2. Use the fault-on θ , $\tilde{\omega}$ and Y to find the transient energy V equal to V_{PE} . That time point T_u is the estimate of the CCT.

Step 3. Integrate the post-fault trajectory from T_u to T .

Step 4. If $[f(\theta)]^T \bullet (\theta - \theta^s)$ doesn't change the sign, that T_u is the CCT, stop. Else, find the new V_{PE} and θ_{cross} , go to Step 2 to find new T_u , say it is T_{u2} . If $|T_{u2} - T_u| \leq \varepsilon$, stop, either T_u or T_{u2} is the CCT. Else, let $T_u = T_{u2}$, go to Step 3.

From this iterative or corrective PEBS method, we can get the more accurate results of the CCT.

For the transient energy margin, we can use θ_{cross} as the approximate θ_u , and then use Eq. 4.14 to get the energy margin. If we do not use PEBS method, we can use other Lyapunov-like methods, i.e., the MOD method [67, 74], to get the real

Controlling UEP and finally get the energy margin. But it may be much slower than PEBS method because the grouping pattern of the machines at instability is fairly complex and also arriving at the Controlling UEP may be very difficult.

C. Transient Stability Control Classification

There are many fast stability control means in the literature and real practice [18, 19, 53, 93–101]. From the generator side, we have the generator tripping, fast valving, dynamic braking, etc. From the load side, we have the load reduction (by voltage reduction), load shedding, etc. From the network side, we have FACTS controllers (TCSC, SVC, etc.), shunt reactors and capacitors, switching on/off lines, etc. For all the above control means, there are two comprehensive ways: either change the P_m (fast valving), or change the admittance matrix Y . The generator tripping is the combination of the two. Therefore, we can define two stability control categories, generator-input-based control (GIBC) means, and admittance-based control (ABC) means.

For generator-input-based control (GIBC) means, the variance of P_m can be easily obtained. For admittance-based control (ABC) means, the variances of admittance matrix Y can be obtained as follows:

For a g -generator- l -bus system, the augmented admittance matrix:

$$\hat{Y} = \begin{bmatrix} Y_{gg} & Y_{gl} \\ Y_{lg} & Y_{ll} \end{bmatrix} \quad (4.18)$$

where

$$Y_{ll} = Y_{bus} + Y_{gen} + Y_{load},$$

Y_{bus} : load flow node admittance matrix,

Y_{gen} : generator node admittance matrix, at generator-connected bus, admittance

of generator branch; others, 0

Y_{load} : load node admittance matrix, at load bus, constant admittance of load;
others, 0

Y_{ll} : $l \times l$ bus admittance matrix

Y_{gg} : $g \times g$ generator admittance matrix

Y_{lg} : $l \times g$ bus-generator admittance matrix

Y_{gl} : $g \times l$ generator-bus admittance matrix

The reduced admittance matrix is:

$$Y = Y_{gg} - Y_{gl}(Y_{ll})^{-1}Y_{lg} \quad (4.19)$$

For all the single admittance-based control (excluding generator tripping), from fast decoupled power flow method [59], we know that:

$$Y_{ll,new} = Y_{ll} - b * M^T * M \quad (4.20)$$

$$(Y_{ll,new})^{-1} = (Y_{ll})^{-1} - c * X * M * (Y_{ll})^{-1} \quad (4.21)$$

where

$$c = (-1/b + M * X)^{-1},$$

$$X = (Y_{ll})^{-1} * M^T.$$

Therefore, we get the reduced admittance matrix variance for each control means,

$$\Delta Y = Y_{new} - Y_{old} = Y_{gl}[(Y_{ll})^{-1} - Y_{ll,new}^{-1}]Y_{lg} = Y_{gl}[cXM(Y_{ll})^{-1}]Y_{lg} \quad (4.22)$$

There are different network control means to change the reduced admittance matrix as follows:

- (1). One line $i - j$ outage or switching off

M : row vector which is null except for $M_i = a$ and $M_j = -1$

a : off-nominal turns ratio referred to the bus corresponding to column i , for a transformer; 1, for a line

b : line or nominal transformer series admittance

(2). One line $i - j$ switching on

M : row vector which is null except for $M_i = -a$ and $M_j = 1$

a, b are the same as above.

(3). Inserting TCSC at line $i - j$, compensation ratio k , $0 < k < 1$

M : row vector which is null except for $M_i = a$ and $M_j = -a$,

$$a = \sqrt{1/k - 1},$$

b is the same as above.

(4). Switching on shunt reactor, capacitor, braking-resistor, SVC at bus i

M : row vector which is null except for $M_i = 1$

b : admittance of shunt reactor, capacitor, braking-resistor, SVC

(5). Switching off shunt reactor, capacitor, braking-resistor, SVC, load reduction at bus i

M : row vector which is null except for $M_i = -1$

b : admittance of shunt reactor, capacitor, braking-resistor, SVC,

for load reduction or shedding, $b = k$, $0 \geq k \leq 1$.

They are represented in Table V.

Table V. Admittance based control (ABC) means and associated parameters

ABC Control Means	M_i	M_j	b
Line Outage	a : Transformer:off-nominal ratio; Line:1	-1	Line or nominal transformer series admittance
Line On	$-a$	1	Same as above
TCSC Insertion	$a = \sqrt{1/k - 1}$, k : compensation capacity, $0 < k < 1$	$-a$	Same as above
Shunt reactor, capacitor, or braking-resistor On	1	N/A	Admittance of shunt reactor, capacitor or resistor
Shunt reactor, capacitor, braking-resistor Off	-1	N/A	Same as above
Load Reduction or Shedding	-1	N/A	Admittance of reduced load

D. Sensitivity Analysis of Transient Energy Margin

For the transient energy margin, its sensitivity to a change in any parameter $\alpha_k(\theta^{cl}, \theta^u, \tilde{\omega}^{cl}, P_i^{pf}, B_{ij}^{pf}, G_{ij}^{pf})$, can be given by the partial derivative of ΔV with respect to α_k .

$$\Delta V = \sum_{k=1}^m \frac{\partial \Delta V}{\partial \Delta \alpha_k} \Delta \alpha_k \quad (4.23)$$

For our control means, since the clearing time is known, we only consider the changes of θ_u , P_i^{pf} , B_{ij}^{pf} , G_{ij}^{pf} . We can get the change of energy margin by

$$\begin{aligned} \Delta V = & \sum_{i=1}^n \frac{\partial \Delta V}{\partial P_{mi}} \Delta P_{mi} + \sum_{i=1}^n \frac{\partial \Delta V}{\partial G_{ii}} \Delta G_{ii} + \\ & \sum_{i=1}^{n-1} \sum_{j=i+1}^n \frac{\partial \Delta V}{\partial G_{ij}} \Delta G_{ij} + \sum_{i=1}^{n-1} \sum_{j=i+1}^n \frac{\partial \Delta V}{\partial B_{ij}} \Delta B_{ij} + \sum_{i=1}^n \frac{\partial \Delta V}{\partial \theta_i^u} \Delta \theta_i^u \end{aligned} \quad (4.24)$$

where,

$$\frac{\partial \Delta V}{\partial P_{mi}} = -(\theta_i^u - \theta_i^{cl}) \quad (4.25)$$

$$\frac{\partial \Delta V}{\partial G_{ii}} = E_i^2(\theta_i^u - \theta_i^{cl}) \quad (4.26)$$

$$\frac{\partial \Delta V}{\partial G_{ij}^{pf}} = \beta_{ij} E_i E_j (\sin \theta_{ij}^u - \sin \theta_{ij}^c l) \quad (4.27)$$

$$\frac{\partial \Delta V}{\partial B_{ij}^{pf}} = -E_i E_j (\cos \theta_{ij}^u - \cos \theta_{ij}^c l) \quad (4.28)$$

$$\frac{\partial \Delta V}{\partial \theta_i^u} = -P_i^{pf} + \sum_{j=i+1}^n (E_i E_j B_{ij}^{pf} \sin \theta_i^u + \beta_{ij} E_i E_j G_{ij}^{pf} \cos \theta_i^u) \quad (4.29)$$

ΔG_{ij} and ΔB_{ij} are real and imaginary parts of ΔY_{ij} obtained from Eq. 4.22.

For big parameter change (i.e., additional network topology change), Controlling UEP may change. From [69] we get

$$(A)(\Delta \theta_i^u) = R_i \quad (4.30)$$

where

$$A_{ii} = \left(1 - 2 \frac{M_i}{M_T}\right) \sum_{j=1, j \neq i}^n C_{ij} \cos \theta_{ij}^u \quad (4.31)$$

$$A_{ij} = \left(2 \frac{M_j}{M_T}\right) \sum_{l=1, l \neq j}^n D_{lj} \sin \theta_{lj}^u + C_{ij} \cos \theta_{ij}^u - D_{ij} \sin \theta_{ij}^u \quad (4.32)$$

$$R_i = E_i^2 \Delta G_{ii} - \frac{M_i}{M_T} \sum_{j=1}^n E_j^2 \Delta G_{jj} - \frac{M_i}{M_T} \sum_{l=1}^n \sum_{j=1, j \neq l}^n E_l E_j \cos \theta_{lj} \Delta G_{lj} + \sum_{j=1, j \neq i}^n (E_i E_j \sin \theta_{ij}^u \Delta B_{ij} + E_i E_j \cos \theta_{ij}^u \Delta G_{ij}) \quad (4.33)$$

Therefore, we can get

$$\Delta \theta^u = A^{-1} R \quad (4.34)$$

$$\theta_{i,new}^u = \theta_i^u + \Delta \theta_i^u \quad (4.35)$$

if $\max(\Delta \theta^u) < \varepsilon$, we can assume Controlling UEP does not change and ignore the 5th item of Eq. 4.24.

E. Transient Stability Control Scheme

After a big disturbance (fault) and its clearing, first we do the transient stability study (i.e., use PEBS method) to see if the system is stable or not. If yes, keep monitoring the system. If not, check all available control means being considered or not. If all control means have not been analyzed, use the sensitivity analysis of transient energy margin to find the suitable control to make the system stable, then check the solution in the time-domain transient stability program to make sure it will work. Finally, issue the control command to stabilize the system and keep monitoring the system. If all control means are analyzed and the system is still unstable, warning will be given and the process will stop. In general, as the last defense, load shedding and islanding may be deployed to try to keep the loss as minimal as possible to make the system stable. Fig. 15 is the flowchart of the transient stability control scheme.

F. Case Study

Given a modified IEEE 14-bus system (modified load and generation conditions), assume the following control means are available: all generators have fast valving (decrease up to 20% capacity), braking resistors (up to 50% capacity), line switching, TCSC (up to 50% compensation capacity of that line), SVC (up to 50MVA capacity), all buses have shunt reactors and capacitors (up to 50MVA capacity), load shedding. Simply use the classical machine model as described in Eq. 4.2 and 4.3 for the step-by-step (SBS) time-domain method and PEBS method. Fig. 16 gives the modified IEEE-14 bus system configuration. The system parameters are given in Appendix A.

Assume that at $t = 0s$, a three-phase-to-ground-fault occurs at 95% of line 9–14. The critical clearing time (CCT) of step-by-step (SBS) method is 0.06s, and the CCT of PEBS method is 0.09s. There is a small difference between the SBS and PEBS

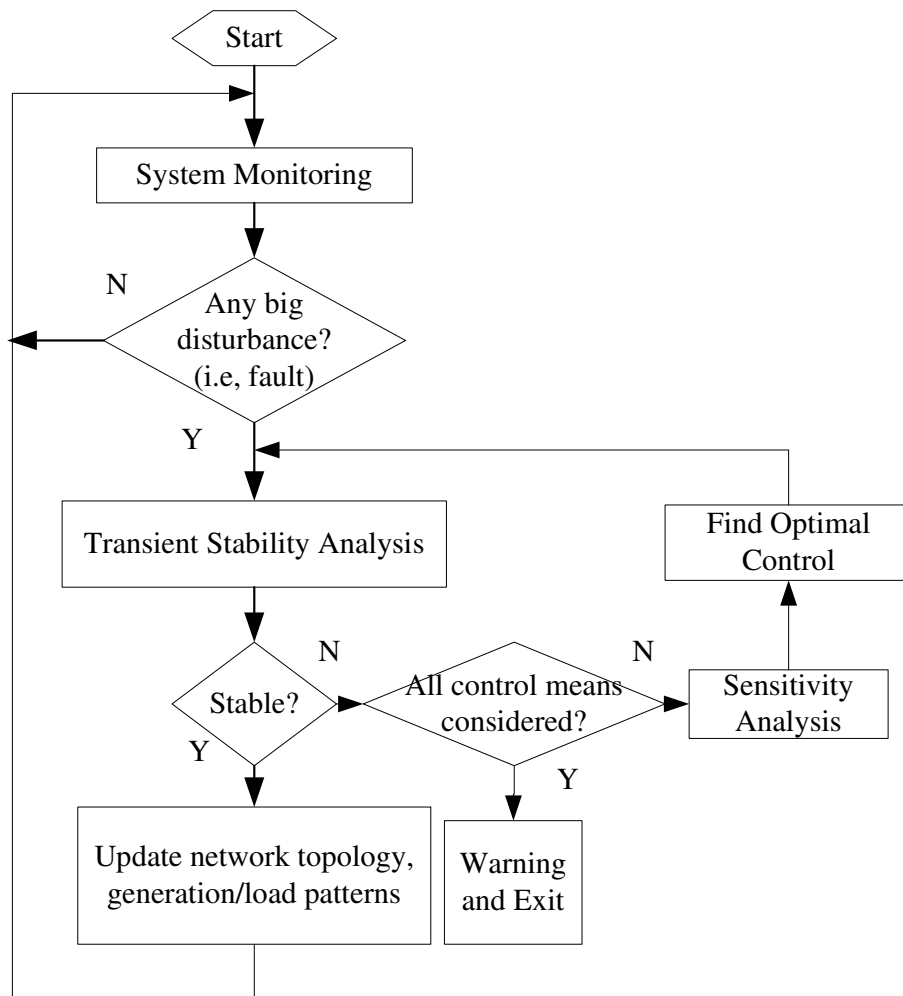


Fig. 15. Flowchart of the transient stability control scheme

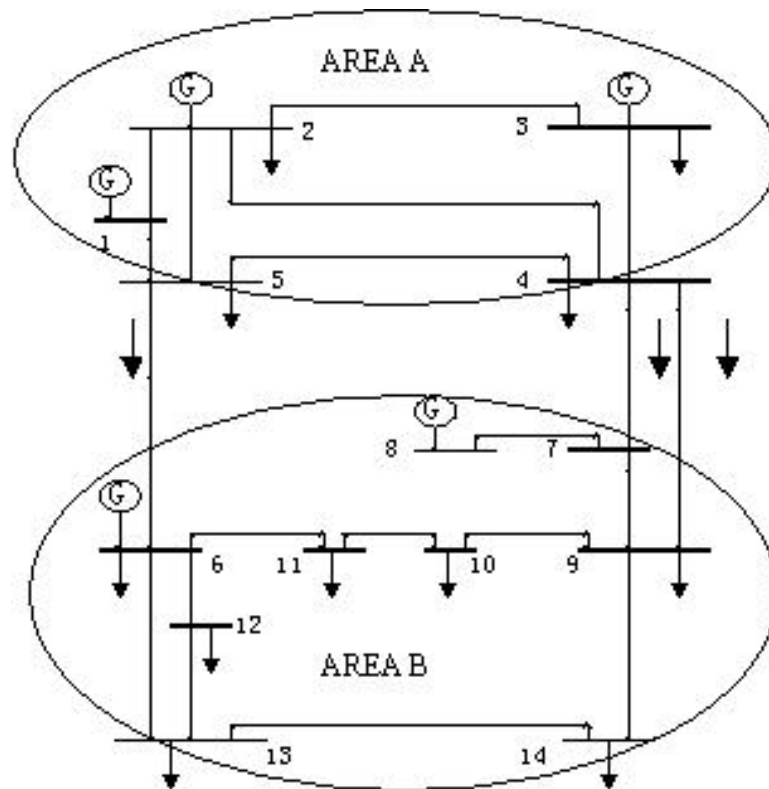


Fig. 16. Modified IEEE 14-bus system

methods due to numerical reason. When the fault is cleared at $t = 0.1s$, we get the machine rotor angle curve given in Fig. 17, where generator G1's angle goes upward and all other generators' angles go downward. The transient energy margin is -0.042 by PEBS method, as described in Eq. 4.14.

All rotor angles in Fig. 17 to 20 are in degrees. Total simulation time is 3s. The maximal angle difference is chosen as the angle stability criterion. If the maximal angle difference among all machines is bigger than 90° at $t = 3s$, the system is unstable. Otherwise, the system is stable.

Assume stability control can be activated at $t=0.11s$ with the aid of the sensitivity analysis. Four kinds of stability control means are chosen: line switching, TCSC switching, load shedding, shunt capacitor and reactor switching.

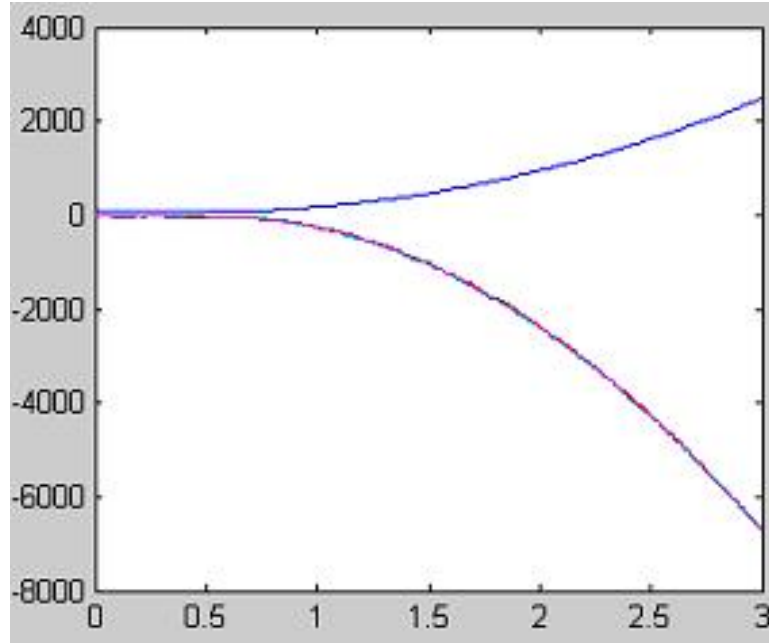


Fig. 17. Machine angles when clearing fault at $t=0.1s$

Table VI. New transient energy margin after line switching

Line switching	L4(B1-2)	L12(B7-9)	L2(B4-7)	L3(B4-9)	L1(B5-6)
Energy margin	-0.007	-0.025	-0.027	-0.028	-0.033

Case 1. Line switching

We get the new transient energy margin after switching additional single line as given in Table VI.

We only list the top 5 lines, which contribute positively for stabilizing the system. Besides these 5 lines, the switching of line L5(B2-3), L14(B6-11), L20(B13-14) also contributes positively to stability. Switching line L11(B7-8) will result in islanding. The switching of other lines contributes negatively to stability. The sensitivity analysis is not very accurate because of the first order approximation. Thus, we need to check with the time-domain transient stability program. Take the example of line

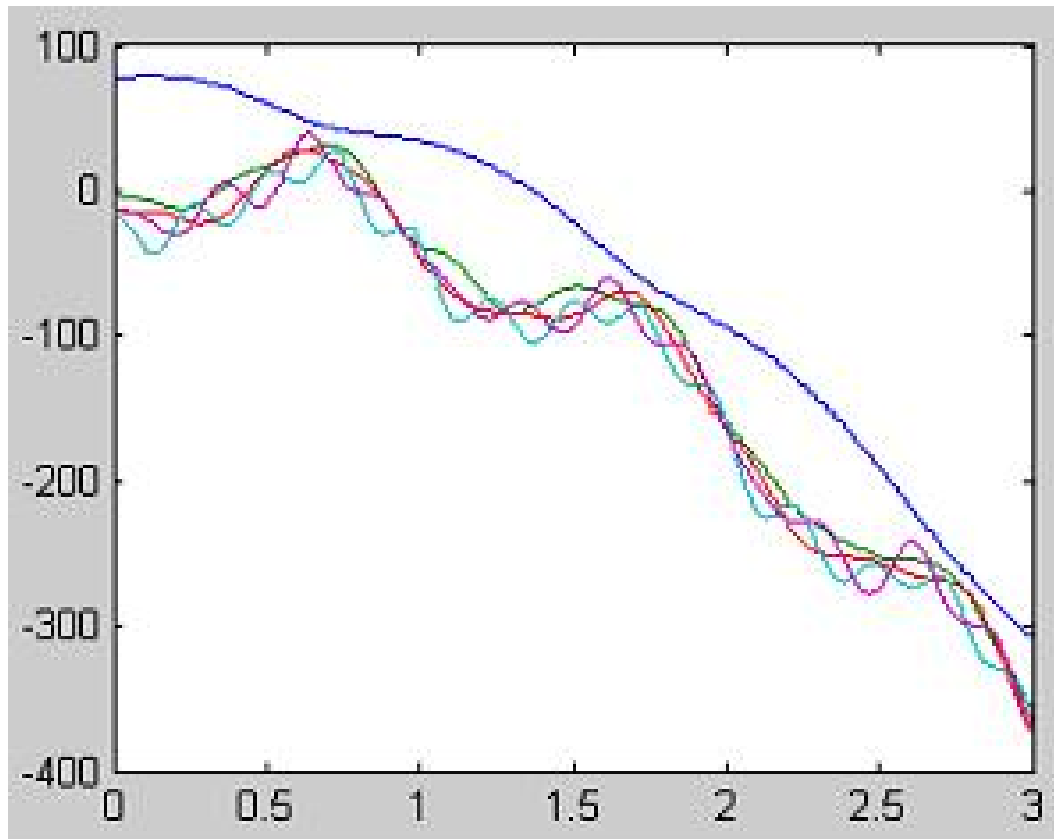


Fig. 18. Machine angles when switching line L4(B1-2) at $t=0.11s$

L4(B1-2) switching, which contributes the most to stability, as described in Fig. 18. We can see the energy margin after this switching is -0.007. That means the system is still unstable after this control. However, by the angle difference criterion in the time-domain transient stability program, the system can be judged as stable.

Case 2. TCSC switching

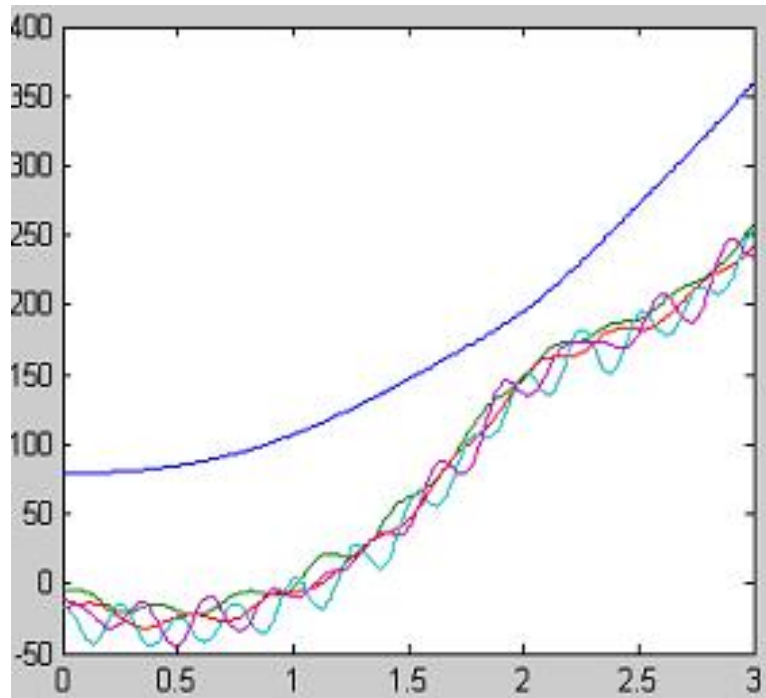
Similarly, we get the top 5 lines by TCSC switching with compensation capacity of 50%, as described in Table VII.

If we check with the time-domain transient stability program, the system is still unstable.

Case 3. Load shedding

Table VII. New transient energy margin after TCSC switching

Line switching	L1(B5-6)	L2(B4-7)	L3(B4-9)	L7(B1-5)	L9(B3-4)
Energy margin	-0.017	-0.034	-0.034	-0.037	-0.037

Fig. 19. Machine angles when 5.5% load shedding at $t=0.11s$

Assume the constant impedance model and the area load can be shed simultaneously with the same ratio. From the analytical sensitivity of the transient energy margin, we can get that the 24.5% load shedding is needed for the energy margin changing from negative to positive value. In fact, by the transient stability program, only 5.5% load shedding can make the system stable. Fig. 19 is the rotor angle curve obtained by shedding 5.5% load. Fig. 20 is the rotor angle curve obtained by shedding 24.5% load.

Case 4. Shunt capacitor and reactor switching

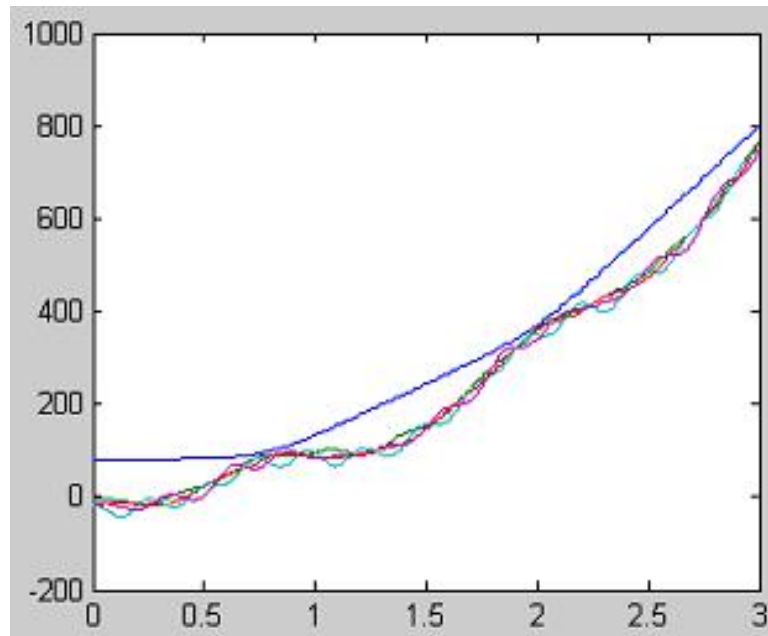


Fig. 20. Machine angles when 24.5% load shedding at $t=0.11s$

In general, when switching on shunt capacitor or reactor at the same bus, their contributions for the energy margin are opposite. For this modified IEEE 14-bus system, when switching on shunt capacitors with 50 MVA capacity at buses 1, 2, 3 and 14 respectively, the energy margin will increase. While doing it at other buses, the energy margin will decrease. When switching on shunt reactors at these buses, their contributions are opposite. When switching on shunt reactor with 50 MVA capacity at buses 4 to 13 respectively, the energy margin will increase. For switching shunt capacitor and reactor at buses by 50 MVA capacity, the most contributing shunt capacitor switching is at bus 1, and the new transient energy margin is -0.038; the most contributing shunt reactor switching is at bus 9, and the new transient energy margin is -0.036. If we check with the time-domain transient stability program, both cases are still unstable.

G. Summary

This chapter presents a transient stability control scheme based on the potential energy boundary surface (PEBS) method and analytical sensitivity of the transient energy margin. If the system is judged unstable after the disturbance, it calculates the new transient energy margin by analyzing the contribution of each control means. Suitable control to stabilize the system will be found to stabilize the system. The time-domain transient stability program is used as a reference. Two categories of the stability control means are given: admittance-based control (ABC) and generator-input-based control (GIBC). A modified IEEE 14-bus system is used to test the methodology. Some simulation results are provided. It needs to be considered that the PEBS method has limits, i.e., the assumption that the PEBS crossing point and Controlling UEP are close to each other for normal system. For some special cases, the error of this method may be a bit bigger. For example, if we find a solution by sensitivity analysis, the system may be stable after this control. However, in the time-domain transient stability program, it may still be unstable. On the other hand, the system may be judged unstable by sensitivity analysis after the control action. But it may be stable by the time-domain transient stability program. The accuracy of the first order sensitivity analysis may be influenced by a big parameter change, which results in the change of Controlling UEP. We can also see from the results that the sensitivity analysis method can give good direction for the control but the final contribution needs to be verified using the time-domain transient stability program.

CHAPTER V

INTERACTIVE SCHEME TO DETECT, PREVENT AND MITIGATE THE
CASCADING OUTAGES*

A. Introduction

As mentioned in Chapter II, there is an interaction between the system-wide and local levels of power system, especially the interaction between system security and local relay action. The relay misoperation or unwanted operation is either the trigger factor or accelerating factor for the large area cascading outages [1, 23]. The research on the interaction between power system security and protective relay is not as strong as the research on security and protection individually [47, 49, 51, 102–105].

In this chapter, an interactive scheme between system-wide and local monitoring and control based on the previous research results in [52, 106] is developed and explained in details to help detect, prevent and mitigate the cascading outages. The background of interaction between system-wide and local levels is given in Section B. The system-wide monitoring and control is discussed in Section C, followed by the simple description of the local monitoring and control tool in Section D. The interactive scheme is explained in Section E. Case Study and Summary are given in Section F and G respectively.

*Part of the material in this chapter is reprinted with permission from “New monitoring and control scheme for preventing cascading outage” by Nan Zhang, Hongbiao Song and Mladen Kezunovic, *Presented in 2005 Proceedings of the 37th Annual North American Power Symposium*, Ames, Iowa, Oct. 2005, pp. 37-42. ©2005 IEEE.

B. Background of Interaction between System-wide and Local Levels

Traditional system transient stability analysis assumes the protection system can clear the fault within expected time. It does not take into account the relay misoperation or unwanted operation. From the local side, the relay settings are based on fault analysis results under prevailing worst case system operating conditions and consider time and protection zone coordination. When fault occurs within their protection zone, most relays use local information and act independently as fast as possible without considering the system information. The relay settings based on off-line studies that may not meet the requirements of the dynamic changing system conditions. The relay behavior impact the system transient stability performance. From the historical record, 75% of the US major power system disturbances is related to protection problems [23]. There are two kinds of relay misoperation: 1) fail to clear the fault or clear the fault in a delayed time, 2) trip the healthy element while the fault is at another element, or operate undesirably at the non-fault conditions, such as power swing and overload/low voltage conditions. More work needs to be done on interaction between the system transient stability and relay behavior. In recent years, wide area monitoring and control system (WAMS) [32–38] using synchronized phasor measurement (PMU) tries to fulfill this gap. It is still in its early development stage.

1. Static Analysis of Relay Behavior

Relay behavior needs to be monitored carefully from the system side. The competitive market operation causes steady state changing conditions, where change of the generation pattern and change of the transfer between generator and load are frequent. This results in frequent changes of power flow patterns through the

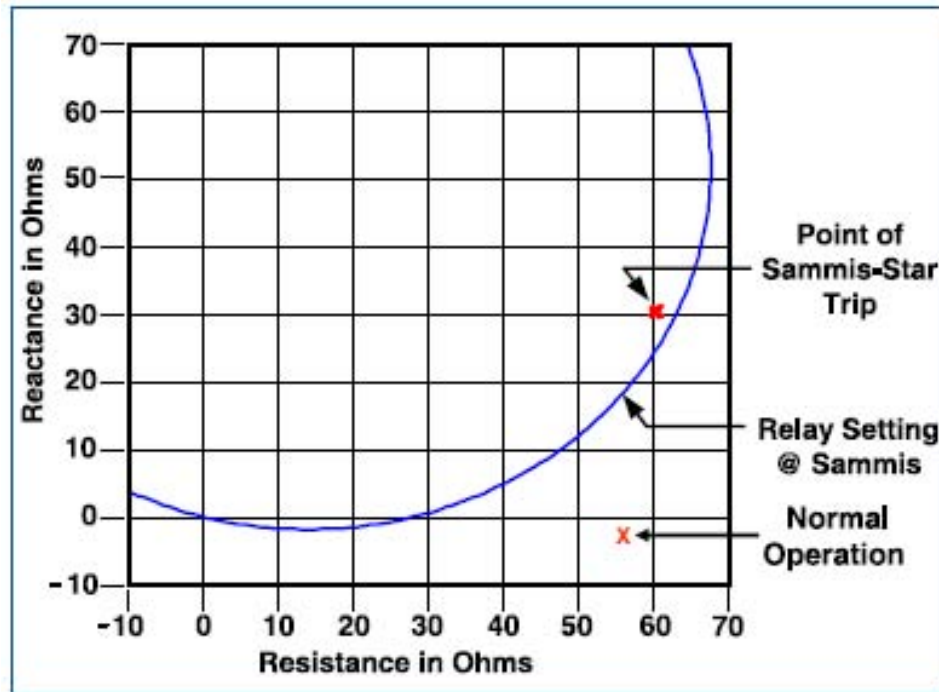


Fig. 21. Sammis-Star 345-kV line trip

transmission network and significant changes of the bus voltages and line currents. During the normal operation condition, the behavior is still within the system security limit and there is no problem with the protective relay. However, after some outages, the system operating security has been degraded. Some transmission lines may have overload conditions and their connected buses may have low voltage problems. The apparent impedance seen by distance relays may fall into their backup protection zones. They may trip the healthy lines if the lasting time is longer than the setting time period and may further trigger the cascading outage. As described in Chapter II, the tripping of the Sammis-Star 345KV line during the August 14, 2003 Northeastern blackout is one of these examples [1].

Voltages and currents obtained from the power flow method or state estimation or phasor measurements are used to calculate the apparent impedance seen by distance

relay, similar as vulnerability index calculation in Chapter III for line distance relay:

$$z_{d,ij} = \frac{V_i}{I_{ij}} = \frac{V_i}{(V_i - V_j)/z_{ij}} \quad (5.1)$$

$$\bar{z}_{d,ij} = \frac{z_{d,ij}}{z_{ij}} = \frac{V_i}{V_i - V_j} = \frac{|V_i|}{|V_i - V_j|} \angle \theta_{d,ij} = d_{ij} \angle \theta_{d,ij} \quad (5.2)$$

$$D_{ij} = d_{ij} - K_z |\sin(\pi/2 - \alpha_{ij} + \theta_{d,ij})| \quad (5.3)$$

where,

V_i, V_j : voltage of buses i and j ,

I_{ij} : line current from bus i to bus j ,

z_{ij} : impedance of line $i - j$,

$z_{d,ij}$: apparent impedance seen by distance relay from bus i to bus j of line $i - j$,

$\bar{z}_{d,ij}$: normalized apparent impedance seen by distance relay from bus i to bus j ,

$d_{ij}, \theta_{d,ij}$: magnitude and angle of normalized apparent impedance $\bar{z}_{d,ij}$,

α_{ij} : line $i - j$ impedance angle,

K_z : zone setting,

D_{ij} : defined as the distance from the apparent impedance seen by transmission line distance relay to the relay protection zone circle, zero or negative values mean the apparent impedance is at or within the protection zone circle.

For the static line distance relay (with *mho* characteristic), it will operate if

$$|z_{d,ij} - \rho| \leq |\rho| \quad (5.4)$$

where,

$$\rho = \beta z_{ij}/2 \quad (5.5)$$

Normalize as

$$|\bar{z}_{d,ij} - \beta/2| \leq \beta/2 \quad (5.6)$$

For typical relay settings, for zone 1, choose $\beta = 0.8$; for zone 2, choose $\beta = 1.2$. Zone 3 relay settings are power system dependent, here we can simply choose 2.4 or choose settings to protect the full length of next longest neighboring line.

During the system normal operation or dynamic changing conditions, normalized apparent impedance and distance relay margin can be calculated for the monitoring of distance relay performance. If the apparent impedance is close to relay protection zone, warning information will be given and careful monitoring of the associated distance relay is required.

2. Dynamic Analysis of Relay Behavior

Dynamic apparent impedance can be calculated from the retrieved dynamic voltage phasors from time-domain transient stability analysis [47, 102]. They can be used for approximate dynamic analysis of relay behavior.

Let us use the two-axis generator model (assumption: $x'_d = x'_q$), constant impedance load model, and IEEE type I voltage regulator [75]. The system dynamics can be represented by:

$$T'_{q0}\dot{E}'_{di} = -E'_{di} + (x_{qi} - x'_{qi})I_{qi} \quad (5.7)$$

$$T'_{d0}\dot{E}'_{qi} = -E'_{qi} + (x_{di} - x'_{di})I_{di} + E_{fdi} \quad (5.8)$$

$$\dot{\delta}_i = \omega_0(\omega_i - 1) \quad (5.9)$$

$$2H_i\dot{\omega}_i = -(E'_{di}I_{di} + E'_{qi}I_{qi}) - D_i(\omega_i - 1) + P_{mi} \quad (5.10)$$

$$T_{Fi}\dot{R}_{fi} = -R_{fi} + \frac{K_{Fi}}{T_{Fi}}E_{fdi} \quad (5.11)$$

$$T_{Ei}\dot{E}_{fdi} = -(K_{Ei} + S_{Ei})E_{fdi} + V_{Ri} \quad (5.12)$$

$$T_{Ai}\dot{V}_{Ri} = K_{Ai}(R_{fi} - \frac{K_{Fi}}{T_{Fi}}E_{fdi} - \frac{1}{K_{Ai}}V_{Ri} - V_{ti} + V_{ref,i}) \quad (5.13)$$

where,

V_{ti} : phase voltage at the generator bus, $V_{ti} = \sqrt{V_{di}^2 + V_{qi}^2}$,

V_{di} : d-axis voltage, $V_{di} = x'_{qi}I_{qi} + E'_{di}$,

V_{qi} : q-axis voltage, $V_{qi} = x'_{di}I_{di} + E'_{qi}$,

The algebraic equations for an m -machine- n -bus network are described by:

$$\begin{bmatrix} I_g \\ I_l \end{bmatrix} = \begin{bmatrix} Y_{gg} & Y_{gl} \\ Y_{lg} & Y_{ll} \end{bmatrix} \begin{bmatrix} V_g \\ V_l \end{bmatrix} \quad (5.14)$$

$$I_g = (I_{di} + jI_{qi})e^{j(\delta_i - \pi/2)} \quad (5.15)$$

$$V_g = (E'_{di} + jE'_{qi})e^{j(\delta_i - \pi/2)} \quad (5.16)$$

We can get the time domain V_g , I_g phasors easily, and the Y matrix will change due to the pre-fault, during-fault and post-fault periods.

If we use the classical generator model (one-axis) and constant impedance load model, as described by Eq. 4.2 and 4.3 in Chapter IV, it is more simple. After we get the δ from swing equations, generator voltage phasor is $V_{g,i} = E_i e^{j\delta_i}$ since E_i is constant.

By assuming constant impedance load model, that is, $I_l = 0$, we can get bus voltage phasors:

$$V_l = -(Y_{ll})^{-1}Y_{lg}V_g \quad (5.17)$$

After the dynamic voltage phasors are obtained from the time-domain simulation, the apparent impedance $z_{d,ij}$, normalized apparent impedance $\bar{z}_{d,ij}$, relay margin D_{ij} , and the conclusion of whether apparent impedance falling into protection zone can be obtained from Eq. 5.1, 5.2, 5.3, 5.6.

By this method, we can check whether the dynamic apparent impedance falls into the distance relay protection zones or not. For example, it may appear that the system is stable because fault clearing time is smaller than critical clearing time (CCT) from the transient stability viewpoint. However, distance relay may "see" apparent impedance falling into its protection zone so it may trip the line. Cascading outage may occur if there is no effective means to prevent relay misoperation.

C. System-wide Monitoring and Control

The system-wide monitoring and control tool is intended for installation at the control center. It consists of security analysis and security control. Security analysis includes routine and event-based security analyses for expected and unexpected events. Security control includes emergency control means obtained from the steady state control scheme discussed in Chapter III and transient stability control scheme discussed in Chapter IV for those expected and unexpected events.

Routine security analysis includes vulnerability analysis, static contingency analysis and dynamic contingency analysis. Vulnerability analysis of operating condition of the whole system and individual element is performed by the topology processing method and operation index (vulnerability index, margin index, stiffness index, distance relay margin index, etc.) method. Vulnerable elements can be identified and their associated relays need to be closely monitored. System security information will be defined. Static contingency analysis uses the fast approximate network contribution factor (NCF) method and full AC power flow method to do the contingency analysis and finds vulnerable contingencies. Dynamic contingency analysis studies the transient stability performance of the contingency. The static analysis of relay behavior will be included in the static contingency analysis. The dynamic analysis

of relay behavior will be obtained during the the dynamic contingency analysis. For the routine static and dynamic contingency analysis, contingencies which can lead to an overload condition, voltage problem, angle stability, voltage stability, etc., will be found and taken care of. Either preventive control actions need to be taken to prevent such problems or emergency control needs to be activated if such contingencies have already happened.

Event-based security analysis is triggered when a disturbance occurs. If it is studied by the routine security analysis, its results are made available. If it is not studied by the routine security analysis, the transient stability analysis and steady state analysis will be taken. If the disturbance drives the system into emergency state or more vulnerable conditions, associated emergency control means will be found and activated to keep the system secure.

Security control handles both the expected vulnerable contingencies obtained from the routine security analysis and the unexpected real-time events. It uses the steady state control scheme and transient stability control scheme to find control means to solve the steady state line overload and bus low/high voltage problems and transient stability problem.

The block diagram of detailed system-wide monitoring and control and simple relationship with local tool and system-wide tool is shown in Fig. 22.

D. Local Monitoring and Control

Exact local information is very useful for the system analysis and control. For example, when the transmission lines are tripped during the abnormal conditions, the system operators at the control center may not know whether there is a fault or not. If there is a fault, they may not know the exact fault location, which is important for

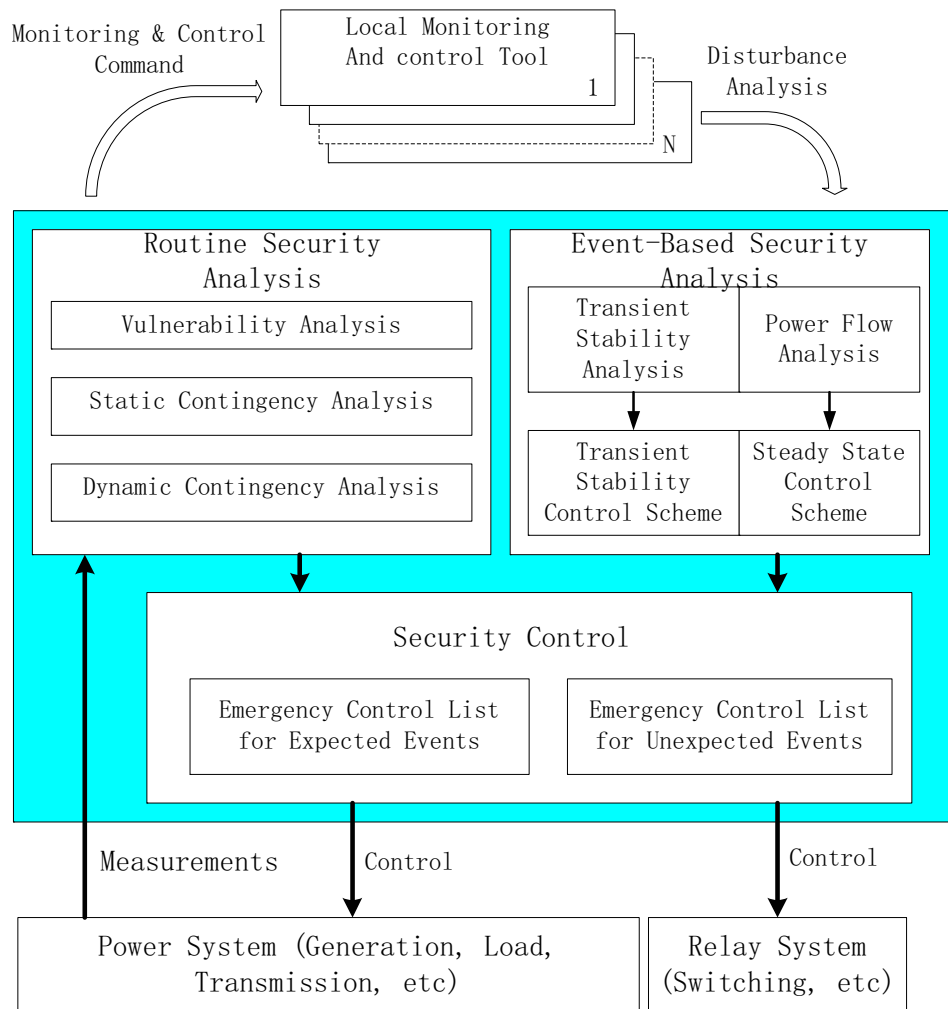


Fig. 22. Block diagram of system monitoring and control

operators' situational awareness and correct action to keep the system secure. When the system tool finds vulnerable elements in the system based on extensive simulation and analysis, it will be a great help if there are local monitoring and control tools installed at those locations to enhance the security. On one side, the local tool can provide exact disturbance information and analysis results to the control center when needed. On the other side, the system tool can send monitoring and control commands to the local tools based on wide-area measurement and system analysis.

Such a local monitoring and control tool is proposed in [107]. The neural network based fault detection and classification (NNFDC), synchronized sampling based fault location (SSFL), and event tree analysis (ETA) can be combined into an advanced real time fault analysis tool and relay monitoring system. This will provide detailed information about disturbance and relay operations for each related local substation. The proposed local monitoring and control tool [107] is described in Fig. 23. It can be installed locally at substations.

Neural network based fault detection and classification (NNFDC) provides a more accurate fault detection and classification by using the same data inputs as distance relay. Synchronized sampling based fault location (SSFL) provides a very high accuracy in fault location using data from two ends of the line. Event tree analysis (ETA) provides an efficient way for real time observation of relay operations and an effective local disturbance diagnostic support.

The system tool can work together with any kind of local tools to help detect, prevent and mitigate cascading outages.

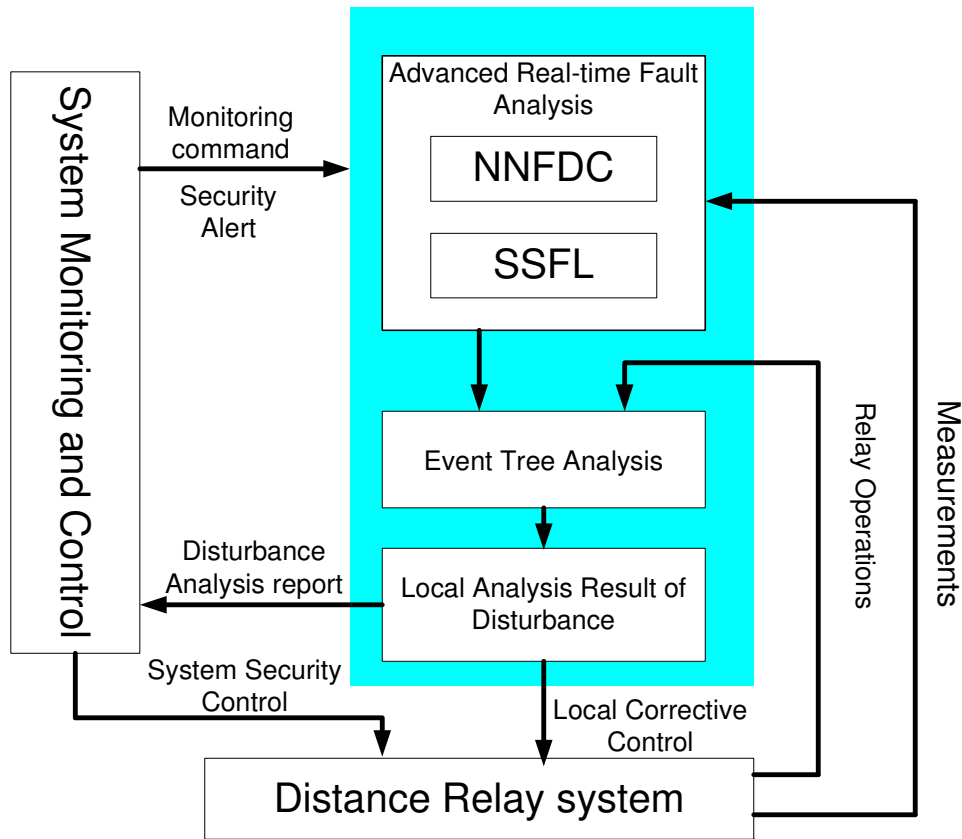


Fig. 23. Block diagram of local monitoring and control

E. Interactive Scheme

The steps of an interactive scheme of system-wide and local monitoring and control can be described as follows:

Step 1. Routine security analysis performed by the system tool at the control center:

- (a) decides security level and finds vulnerable elements, then sends system security status and monitoring command to the local tool at substations; (b) identifies critical contingencies, and starts associated control schemes to find the control means for those expected events.

Step 2. Local monitoring performed by the local tool at substations: (a) starts anal-

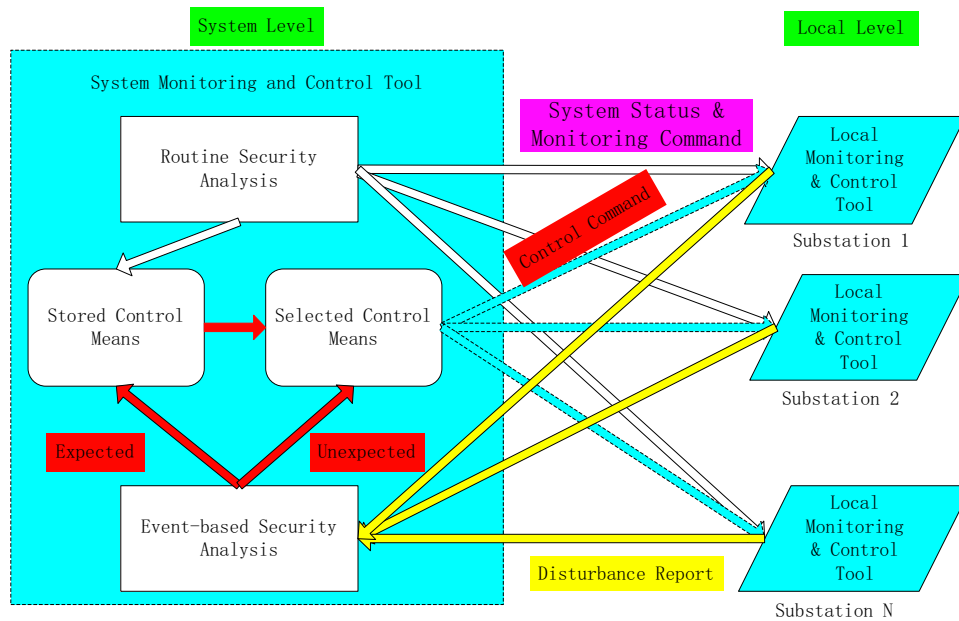


Fig. 24. Block diagram of interactive scheme

ysis when disturbance occurs; (b) if it finds relay misoperation, it makes correction or receives system control command for better control; (c) reports disturbance information and analysis results to the system tool.

Step 3. Event-based security analysis performed by the system tool at the control center: (a) if it finds a match with expected event, activates the emergency control if the disturbance is harmful; (b) if it does not find a match, analyzes if the system is secure or not; (c) if the system is not secure, it finds new emergency control and activates it.

Step 4. Update information and go to Step 1.

The block diagram of the interactive scheme is represented by Fig. 24.

The potential infrastructure of the interactive scheme is described in Fig. 25.

The interactive scheme between the system-wide and local monitoring and control introduces benefits that individual tool can not achieve separately. System tool

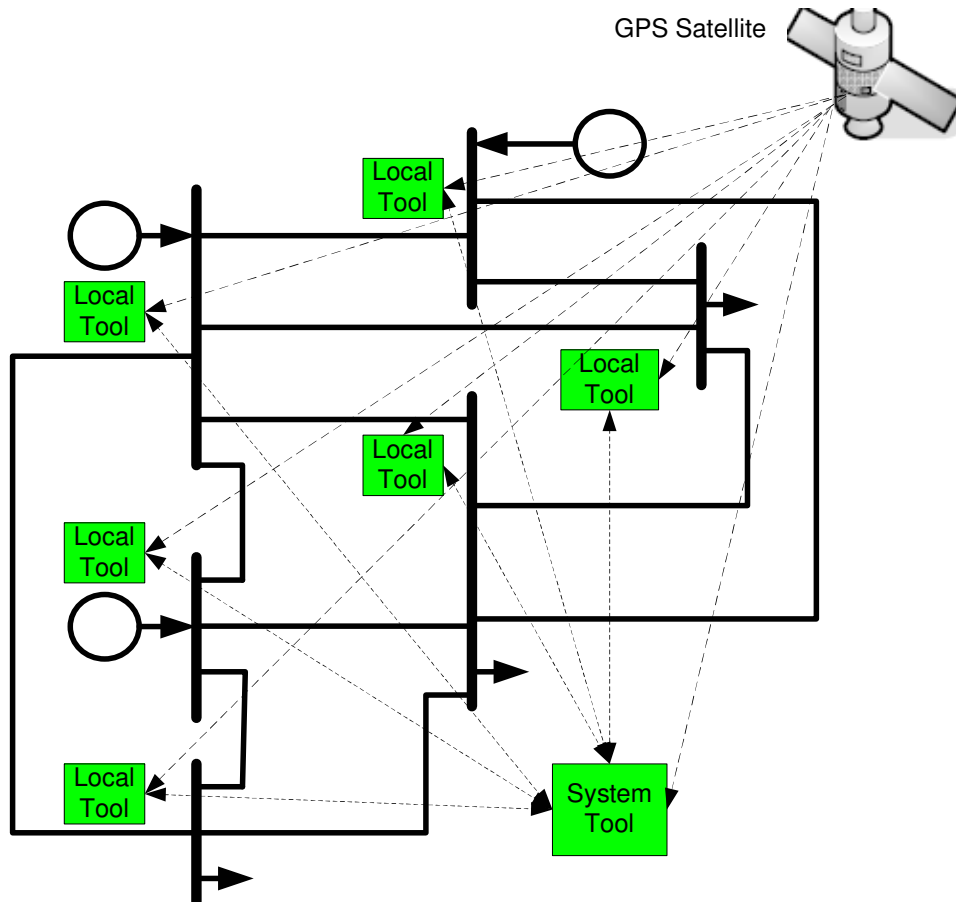


Fig. 25. Potential infrastructure of the interactive scheme

has wide-area information and better view of the system security and vulnerability conditions. It can have a better control decision and notify local substation tool to carefully monitor vulnerable elements during abnormal conditions. Local tool has exact real-time local disturbance information. It has the ability to detect, classify and locate the fault with high accuracy and provide good reference for judging the relay operation. It can also predict some possible events from the local side. Both of the system and local tools work together to fulfill the major task: to help detect, prevent and mitigate cascading outages.

F. Case Study

The IEEE 39-bus New England test system, as shown in Fig. 26, is used to demonstrate this new approach. Data source can be found in [73]. Detailed system data can be found in Appendix C. The transformer branches are taken as transmission lines in those studies.

Case 1. Routine system security analysis

In this case, the system routine security analysis is implemented off-line and the vulnerable lines in the system are found. For those lines, the proposed local analysis tool needs to be installed to monitor protective relays.

From topology processing, we find 11 single-connection lines from the one-line diagram shown in Fig. 26: L22(B19-16), L47(B20-19), and 9 generator branches L37-L45 which connect G30-G38 respectively. There will be one or several buses isolated from the system if any of the above 11 lines are disconnected. The local analysis tools need to be applied on those lines.

From vulnerability analysis for distance relays (we assume all lines have distance relays), we find the top 6 most vulnerable lines according to their vulnerable indices

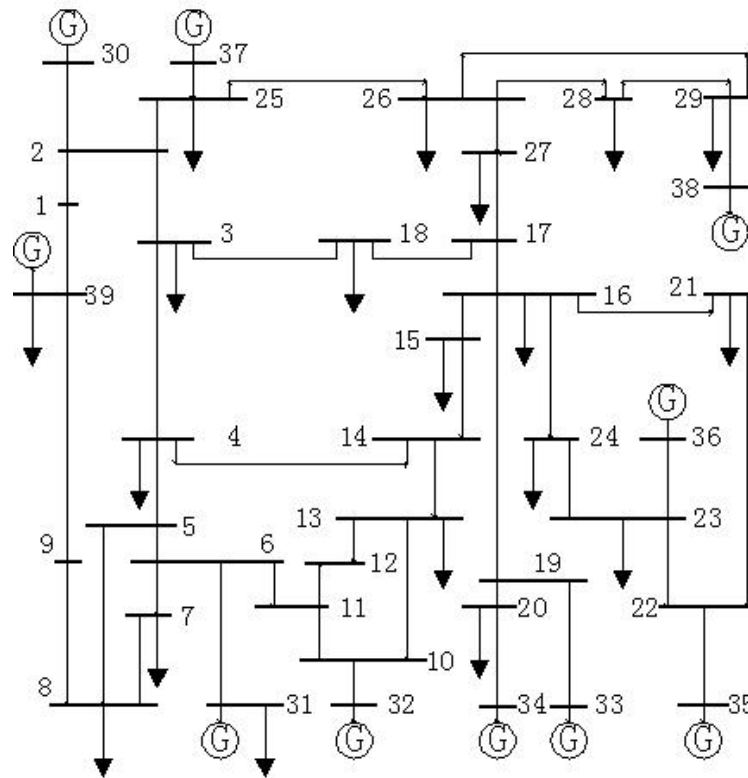


Fig. 26. IEEE 39-bus New England test system

Table VIII. Vulnerable lines and their neighboring lines

Line No	Bus Connection	VI-Relay	Neighboring Lines (contingencies on those lines could influence the vulnerable line)
L37	B6-31	0.0240	L9(B6-5),L11(B7-6),L12(B11-6)
L38	B10-32	0.0206	L16(B11-10),L17(B13-10)
L42	B23-36	0.0191	L28(B23-22),L29(B24-23)
L45	B29-38	0.0157	L33(B29-26),L34(B29-28)
L43	B25-37	0.0149	L4(B25-2),L30(B26-25),L33(B29-26)
L29	B24-23	0.0131	L24(B24-16),L28(B23-22),L42(B23-36)

as shown in Table VIII. For those lines, the fault on the neighboring lines may affect their relay operations. Therefore, those lines also need to be monitored using the local analysis tools.

Case 2. Event-based security analysis

In this case, it will be demonstrated how relay misoperation can cause system cascading outages. Then we describe how to prevent such situation with the benefit of the proposed interactive analysis approach.

The sequence of the scenarios is as follows:

- 1) $t=0s$, a 3-phase fault occurs at middle of line L27(B22-21).
- 2) The fault is cleared at $t=0.11s$ by tripping L27.
- 3) $t=1s$, a second 3-phase fault occurs at middle of line L3(B3-2).
- 4) The second fault is cleared at $t=1.11s$ by tripping L3.
- 5) End simulation at $t=4.0s$.

This contingency may cause distance relay at B24 of L29 (B24-B23) to misoperate at power swing and line overload condition. The trajectory of apparent impedance seen by that relay is shown in Fig. 27. After the first fault is cleared, the apparent impedance seen by the distance relay enters its zone 3 circle at $t=0.242s$ and stays inside till $t=1.008s$. After the second fault is cleared, the apparent impedance enters zone 3 circle again at $t=1.520s$. It may stay at the zone 3 circle longer than the time setting. The distance relay may trip L29 if zone 3 timer expires.

If the distance relay at B24 trips L29 wrongly, buses 22, 23, 35 and 36 will be isolated from the system, including the G35, G36 and load at B23, B24. The rest of the system is unbalanced and cascading outage may happen.

This situation can be prevented by the interactive scheme. From Table VIII, we can see that L29 has already been placed on the vulnerable line list and the local analysis tool needs to be installed on that line. When the first fault occurs, the event-based system security analysis is activated. Through power flow analysis, it is

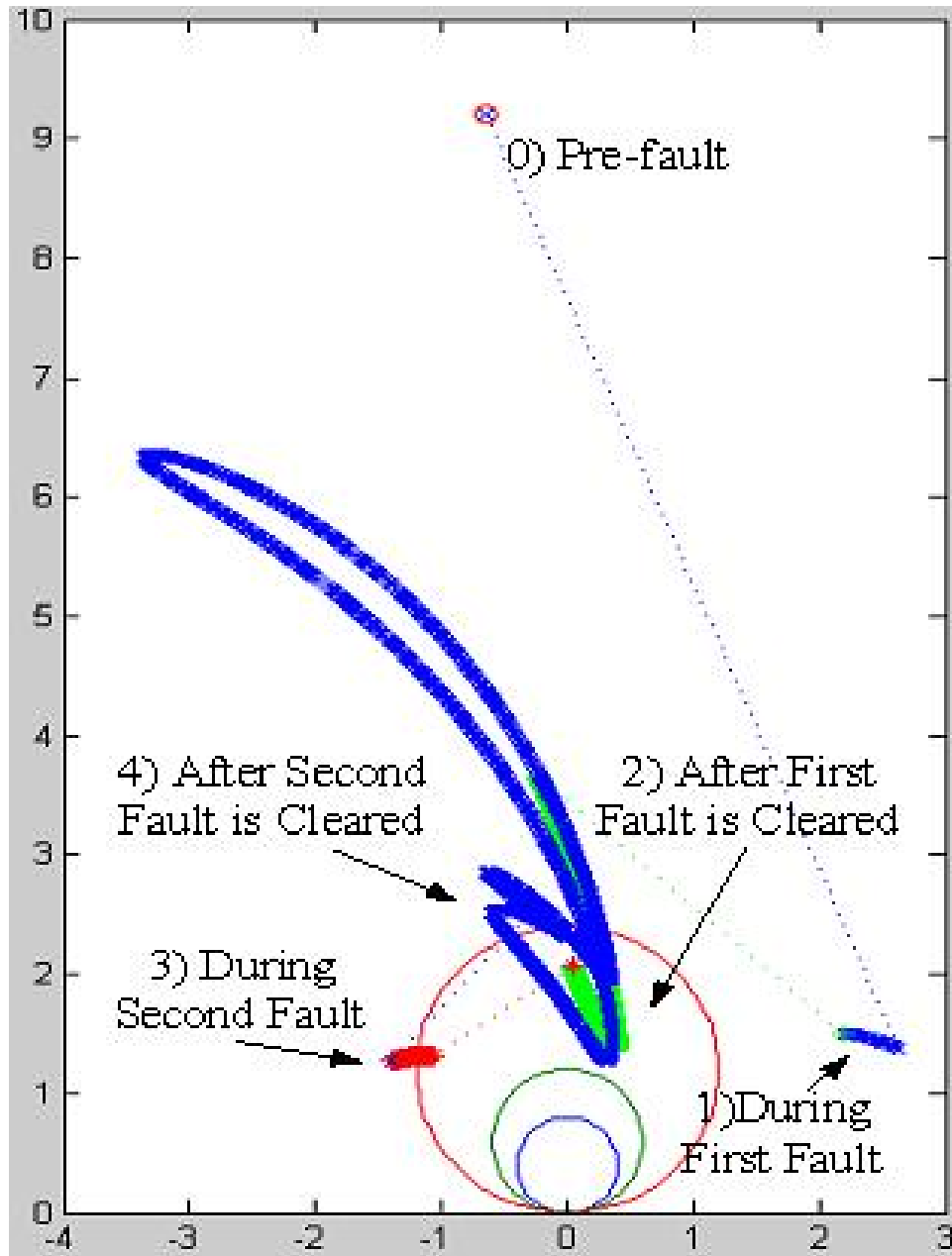


Fig. 27. Apparent impedance seen by distance relay at L29 during simulation

determined that L29 is heavily loaded due to L27 outage. Also from the topology processing, it is determined that L29 and L27 are double-line connections. Loss of L27 and L29 will disconnect buses B22, 23, 35 and 36 from the major system. Therefore, through the system analysis, an alert signal will be sent to the local analysis tool at L29 to increase the security level. When the second fault happens, the local analysis tool draws a conclusion to block the relay from tripping at above mentioned condition. That information will be sent back to the system to initiate appropriate control to mitigate the disturbance and increase system security level.

In reality, it is impossible that one or two contingencies like the ones discussed above can cause large system oscillations and heavy overload condition in bulk power system. Usually there is enough time for proper control actions to mitigate the disturbances and prevent them from unfolding. The proposed interactive scheme between system-wide and local monitoring and control can help detect, prevent and mitigate possible cascading outages.

G. Summary

This chapter presents an interactive scheme between system and local monitoring and control tools. Following conclusions can be drawn from the case studies:

- New approach to help detect, prevent and mitigate cascading outages can be obtained by coordinating the system-wide and local monitoring and control tools.
- The system-wide monitoring and control tool can find the vulnerable elements and send monitoring command to the local tool for detailed monitoring.
- Emergency control means for expected events can be identified by the routine security analysis and activated when such events occur.

- Emergency control means for unexpected events can be identified by event-based security analysis and activated to mitigate the disturbance and help keep the system secure.
- The local monitoring and control tool can find the exact disturbance information and make a correction if there is relay misoperation. Further information can be sent to the system tool for better security control.

CHAPTER VI

EVALUATION OF STEADY STATE CONTROL SCHEME, TRANSIENT
STABILITY CONTROL SCHEME AND INTERACTIVE SCHEME

A. Introduction

Steady state control scheme, transient stability control scheme and interactive scheme have been described in Chapters III, IV and V respectively. Steady state control scheme has the ability to solve steady state problems such as line overload and bus high/low voltage, evaluate the system vulnerability and security information by vulnerability index and margin index during the system normal operation and slow dynamic changing conditions, identify the vulnerable parts in the system, predict some possible successive events and find suitable preventive control to help keep the power system secure if taken properly. It can help prevent the possible cascading outages at its first slow steady state stage. Transient stability control scheme focus on transient stability analysis and control. If the system is judged unstable after the disturbances, stability control means based on potential energy boundary surface (PEBS) method and analytical sensitivity of transient energy margin will be found, verified by time-domain simulation method, and activated to keep the system stable. It can also help prevent or mitigate the possible cascading outages. Interactive scheme considers the interaction between system-wide and local levels, takes the advantages of both system and local information and uses some techniques from steady state control scheme and transient stability control scheme to help detect, prevent and mitigate the cascading outages.

Those three schemes can work separately and jointly. For example, steady state control scheme works during the normal operation and slow steady state changing

conditions after an outage of an element or for the purpose of better economics and more secure operation. Transient stability control scheme studies the system dynamics within a short time period immediately after the disturbances. Security concern is the first priority. Interactive scheme works during both the steady state and dynamic conditions. It monitors the system all the time and takes action when needed.

Lots of case studies have been performed using IEEE 24-bus, 14-bus and 39-bus systems in Chapters III, IV and V respectively. In this Chapter, case studies will be implemented in IEEE 118-bus system for those three schemes. Other references can be found for data sources from [108–110] and modified for future research purpose. Detailed system data is attached in Appendix D. Studies of steady state control scheme, transient stability control scheme and interactive scheme will be provided in Sections B, C and D respectively. Summary will be given in Section E.

B. Study of Steady State Control Scheme

The IEEE 118-bus system configuration is given in Fig. 28.

This is a 118-bus-186-branch system. The power base is 100MVA. System configuration, base power flow data and machine data can be found in [108–110]. 20 generators and 3 areas are given in Fig. 28. Generator at Bus 112 is taken as G20. There are 5 generators at Area 1: G1(B10), G2(B12), G3(B25), G4(B26) and G5(B31). There are 8 generators at Area 2: G6(B45), G7(B49), G8(B54), G9(B59), G10(B61), G11(B65), G12(B66) and G13(B69). And there are 7 generators at Area 3: G14(B80), G15(B87), G16(B89), G17(B100), G18(B103), G19(B111) and G20(B112). G13(B69) is the slack bus. There are 4 tie-lines between Area 1 and Area 2: L30(B23-24), L44(B15-33), L45(B19-34), and L54(B30-38). There are 5 tie-lines between Area 2 and Area 3: L114(B70-74), L115(B70-75), L116(B69-75), L119(B69-77), and

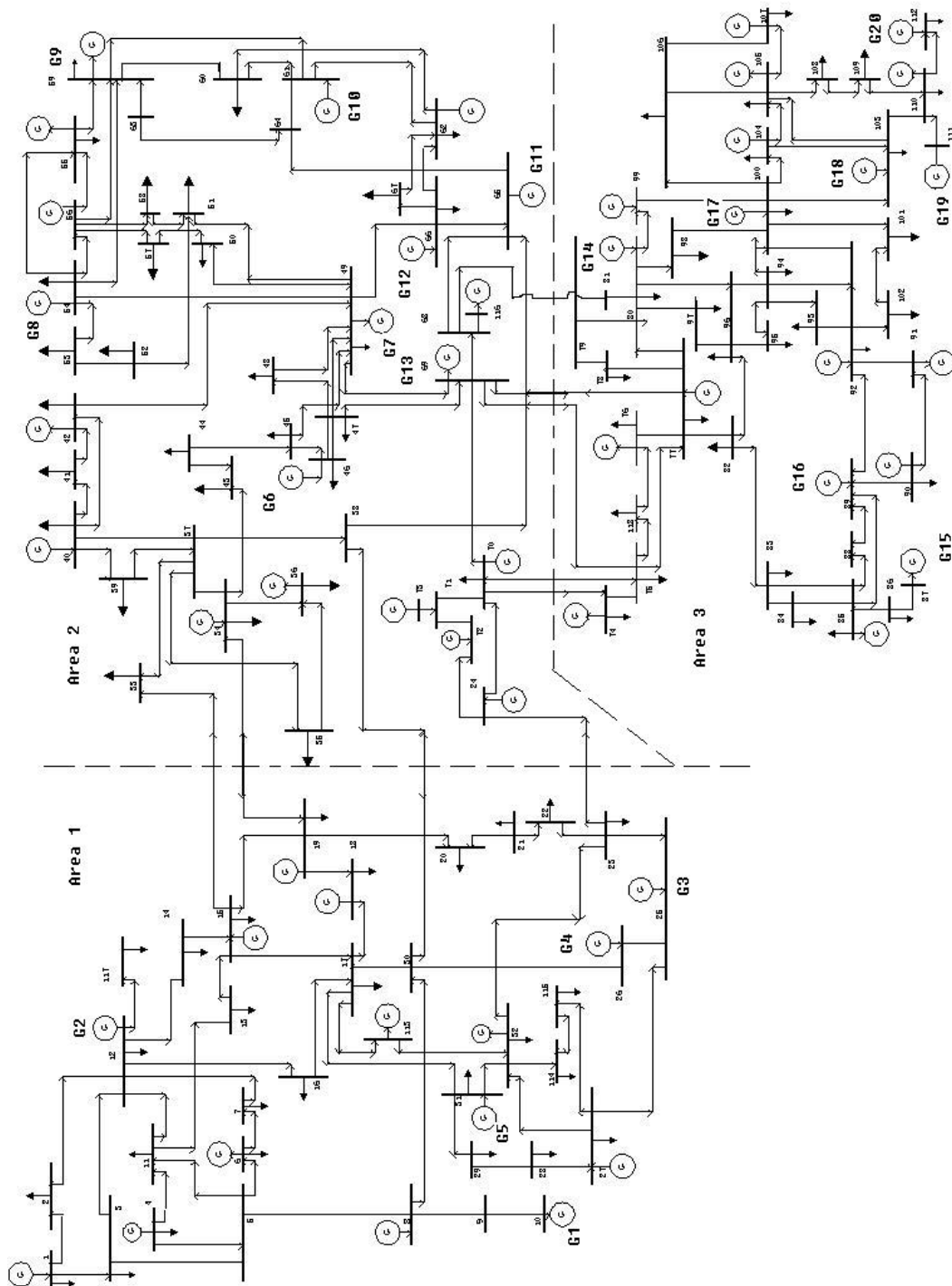


Fig. 28. IEEE 118-bus system

Table IX. Transmission lines and their thermal limits (in MVA value)

Line	L7(B8-9)	L8(B8-5)	L9(B9-10)	L31(B23-25)	L32(B26-25)	L33(B25-27)
Limit	640	510	650	380	380	280
Line	L36(B30-17)	L37(B8-30)	L38(B26-30)	L51(B38-37)	L104(B65-68)	L107(B68-69)
Limit	520	500	380	350	480	500
Line	108(B69-70)	116(B69-75)	119(B69-77)	126(B68-81)	127(B81-80)	183(B68-116)
Limit	300	280	580	560	560	300

L126(B68-81). There are power transfers from Area 1 to Area 2 and from Area 2 to Area 3. The power flow data has been modified from the base case to stress the system conditions as follows: a) to increase real power outputs of generators at Areas 1 and 2, 1.2 times the base case was used, b) to reduce real power outputs of generators at Area 3, 0.6 times the base case was used, and c) to increase load at Area 3, 1.1 times the base case was used.

To make sure there is no line overload for any N-1 contingency analysis, most line thermal limits are set as 250MVA except for those lines in Table IX.

Case 1. N-1 contingency analysis

Take Area 2 as the study area with tie-lines between Area 2 and Area 3 included. Vulnerability index (VI) and margin index (MI) are calculated by network contribution factor (NCF) method and AC power flow (PF) method. Top 6 single line outage contingencies out of 73 contingencies ranked by NCF and PF are given in Table X.

From Table X, we can see that the fast network contribution factor (NCF) method gives similar results as AC power flow method in vulnerability index and margin index. The NCF method can be used as fast contingency screening method to select top ranking contingencies and then use the AC power flow method for detail analysis.

The associated vulnerability index values by NCF and PF methods, and margin

Table X. Top 6 line outages ranked by vulnerability index and margin index

Vulnerability Index		Margin Index	
NCF	PF	NCF	PF
L104(B65-68)	L126(B68-81)	L104(B65-68)	L126(B68-81)
L126(B68-81)	L51(B38-37)	L126(B68-81)	L104(B65-68)
L119(B69-77)	L50(B34-37)	L119(B69-77)	L51(B38-37)
L116(B69-75)	L116(B69-75)	L51(B38-37)	L119(B69-77)
L51(B38-37)	L114(B70-74)	L60(B34-43)	L94(B63-64)
L111(B24-72)	L119(B69-77)	L71(B49-51)	L71(B49-51)

Table XI. Top 6 line outages ranked by vulnerability index based on NCF method
(Part I: Total VI, VI at bus and generator parts)

LineNo	Total VI	VI_V	VI_loadab	VI_Pg	VI_Qg
L104	40.1764	6.2572	5.2130	3.6456	5.3205
L126	34.7011	6.3026	4.9668	3.6456	5.4195
L119	32.8457	6.2557	4.8922	3.6456	5.3165
L116	32.2414	6.2722	5.0858	3.6456	5.7821
L51	31.9812	6.2557	5.0538	3.6456	5.3165
L111	31.6911	6.2609	5.1260	3.6456	5.3168

index values by NCF and PF methods are given in Table XI to Table XVI respectively.

The larger the Vulnerability Index values, the more vulnerable the system conditions.

Table XII. Top 6 line outages ranked by vulnerability index based on NCF method
(Part II: VI at branch part)

LineNo	VI_P1	VI_Q1	VI_Qc	VI_angl	VI_Relay	VI_line_off
L104	12.9921	0.9656	0.0227	2.3687	2.3910	1
L126	9.2021	0.9603	0.0204	1.5628	1.6211	1
L119	8.4579	0.9366	0.0254	1.1193	1.1965	1
L116	7.3236	0.9135	0.0251	1.0597	1.1339	1
L51	7.3722	0.8942	0.0254	1.1713	1.2465	1
L111	7.2800	0.9378	0.0254	1.0089	1.0899	1

Table XIII. Top 6 line outages ranked by vulnerability index based on PF method
(Part I: Total VI, VI at bus and generator parts)

LineNo	Total VI	VI_V	VI_loadab	VI_Pg	VI_Qg
L126	53.4040	6.5208	4.9733	3.8250	24.7608
L51	48.6295	6.4806	5.0594	3.6898	21.3417
L50	40.3328	6.1543	4.9092	3.6485	14.6112
L116	39.8147	6.3581	5.0902	3.6558	13.4622
L114	37.8500	6.2738	5.0067	3.6483	11.8905
L119	36.7172	6.2477	4.8587	3.6461	10.9213

Table XIV. Top 6 line outages ranked by vulnerability index based on PF method
(Part II: VI at branch part)

LineNo	VI_Pl	VI_Ql	VI_Qc	VI_angl	VI_Relay	VI_line.off
L126	8.3997	0.8045	0.0123	1.5227	1.5850	1
L51	7.7818	0.6169	0.0219	1.2833	1.3542	1
L50	7.3176	0.5834	0.0253	1.0003	1.0830	1
L116	7.4240	0.5894	0.0225	1.0687	1.1439	1
L114	7.3276	0.5989	0.0249	0.9992	1.0801	1
L119	7.3447	0.6008	0.0253	0.9957	1.0770	1

Table XV. Top 6 line outages ranked by margin index based on NCF method

LineNo	Total MI	MI_V	MI_loadab	MI_Pg	MI_Qg	MI_Sf	MI_angl
L104	4.5620	0.7476	0.8126	0.5622	0.8371	0.7040	0.8985
L126	4.6096	0.7462	0.8129	0.5622	0.8334	0.7435	0.9114
L119	4.6377	0.7476	0.8130	0.5622	0.8392	0.7580	0.9178
L51	4.6420	0.7476	0.8123	0.5622	0.8392	0.7641	0.9166
L60	4.6483	0.7458	0.8124	0.5622	0.8393	0.7669	0.9218
L71	4.6490	0.7469	0.8128	0.5622	0.8393	0.7666	0.9211

Table XVI. Top 6 line outages ranked by margin index based on PF method

LineNo	Total MI	MI_V	MI_loadab	MI_Pg	MI_Qg	MI_Sf	MI_angl
L126	4.5882	0.7425	0.8129	0.5493	0.8097	0.7594	0.9144
L104	4.6126	0.7485	0.8126	0.5573	0.8283	0.7537	0.9122
L51	4.6241	0.7431	0.8123	0.5588	0.8329	0.7631	0.9139
L119	4.6373	0.7461	0.8130	0.5617	0.8332	0.7642	0.9190
L94	4.6376	0.7452	0.8130	0.5615	0.8222	0.7745	0.9211
L71	4.6385	0.7329	0.8128	0.5619	0.8391	0.7711	0.9206

The smaller the margin index values, the less secure the system conditions. Margin index method does not give the same contingency rankings as vulnerability index method because they do not model the same parameters.

Case 2. Successive study after the most vulnerable contingency

From Table X, we know that L104(B65-68) outage is identified as the most vulnerable contingency by network contribution factor (NCF) method both in vulnerability index and margin index values, because it increases the loading conditions of other transmission lines by NCF approximation. We can see the largest line real power vulnerability index (VI.PI) value is 12.9921. The AC power flow method identifies L126 (B68-81) outage as the most vulnerable contingency because it has the largest generator reactive power output vulnerability index (VI.Qg) value as 24.7608. We can further study the vulnerability index and margin index values after line L104 or L126 outage.

From Table XVII and Table XVIII, we can see that the results of network contribution factor (NCF) method for contingency analysis and vulnerability and security evaluation are very similar to AC power flow method. Thus, NCF method can be used for a fast screening method for security analysis.

Case 3. Steady state control after double-line outage

Suppose that tie-line L116 (B69-75) has a permanent fault and is tripped by pro-

Table XVII. Top 6 line outages ranked by vulnerability index and margin index after L104(B65-68) is out-of-service

Vulnerability Index		Margin Index	
NCF	PF	NCF	PF
L106(B49-69)	L107(B68-69)	L126(B68-81)	L107(B68-69)
L119(B69-77)	L126(B68-81)	L106(B49-69)	L126(B68-81)
L126(B68-81)	L51(B38-37)	L119(B69-77)	L51(B38-37)
L105(B47-69)	L116(B69-75)	L105(B47-69)	L96(B38-65)
L107(B68-69)	L119(B69-77)	L51(B38-37)	L119(B69-77)
L51(B38-37)	L50(B34-37)	L107(B68-69)	L94(B63-64)

Table XVIII. Top 6 line outages ranked by vulnerability index and margin index after L126(B68-81) is out-of-service

Vulnerability Index		Margin Index	
NCF	PF	NCF	PF
L119(B69-77)	L116(B69-75)	L119(B69-77)	L104(B65-68)
L104(B65-68)	L114(B70-74)	L104(B65-68)	L51(B38-37)
L116(B69-75)	L51(B38-37)	L107(B68-69)	L116(B69-75)
L115(B70-75)	L50(B34-37)	L51(B38-37)	L94(B63-64)
L51(B38-37)	L47(B35-37)	L116(B69-75)	L71(B49-51)
L114(B70-74)	L104(B65-68)	L71(B49-51)	L96(B38-65)

Table XIX. Line flow before and after L116(B69-75) and L119(B69-77) outage (in p.u.)

LineNo	Apparent flow before outage	Apparent flow after outage	Flow after outage	Line limit
L126(B68-81)	3.7897	6.5442	6.5005+j0.7545	5.6000
L127(B81-80)	3.7778	6.4618	6.4617-j0.0308	5.6000

Table XX. Generator contribution factors for L126(B68-81) and L127(B81-80)

	G11	G12	G13	Others
A_Gen(126,:)	0.5206	0.1288	0.4282	0
A_Gen(127,:)	0.5175	0.1280	0.4256	0

tective relay. Assume another tie-line L119(B69-77) is also tripped by protective relay because of relay misoperation which is a possible case. This is a double-line outage contingency. We only consider the steady state condition in this case study. After this contingency, two lines have overload conditions: L126(B68-81) and L127(B81-80) as shown in Table XIX.

If there are no effective overload relieving method, the overloaded L126 and L127 will be tripped successively. Then tie-lines L114 (B70-74) and L115 (B70-75) will also be tripped because of the overload conditions. Cascading outage may occur.

Assume that there are no other transmission network control means and load control means. Only generator control means is available. L126 (B68-81) is the tie-line between Area 2 and Area 3. The power is transmitted first through L126 and then through L127(B81-80) from Area 2 to Area 3 besides the other two tie-lines L114 and L115. The generator contribution factor for L126 and L27 is given in Table XX.

G11 and G13 are two generators which contribute most to L126 and L127 overload. G14 (B80) is one least contributing generator and the closest generator to L126 and L127. The steady state control scheme picks up two generator pairs to relieve

Table XXI. Generator contribution factors for L126(B68-81) and L127(B81-80) after adjustment

	G11	G12	G13	Others
A_Gen(126,:)	0.4867	0.1202	0.4119	0
A_Gen(127,:)	0.4842	0.1195	0.4097	0

the overload, to decrease G11 (B65) and increase G4 (B80) to relieve L126 overload, to decrease G13 (B69) and increase G14 (B80) to relieve L127 overload,

Step 1. The amount of real power at L126 that needs to be reduced is $6.5005 - 5.6 = 0.9005$ p.u.. For G11, the reduced amount is $0.5206 / (0.5206 + 0.4282) * 0.9005 = 0.4941$ p.u. For G13, the reduced amount is $0.9005 - 0.4941 = 0.4064$ p.u. The increased amount of G14 is 0.9005 p.u.

Step 2. After the generator real power outputs adjustment, AC power flow is run. New line flow at L126 is $5.7347 + j0.6336$ p.u. and new line flow at L127 is $5.7048 + j0.1175$ p.u. The apparent powers are 5.7696 p.u. and 5.7060 p.u. respectively, still larger than the thermal limit 5.6 p.u. The generator contribution factor for L126 and L27 is given in Table XXI.

The amount of real power at L126 that needs to be reduced is $5.7347 - 5.6 = 0.1347$ p.u. For G11, the reduced amount is $0.4867 / (0.4867 + 0.4119) * 0.1347 = 0.073$ p.u. For G13, the reduced amount is $0.1347 - 0.073 = 0.0617$ p.u. The increased amount of G14 is 0.1347 p.u.

Step 3. After the new generator real power outputs adjustment, AC power flow is run. New line flow at L126 is $5.6204 + j0.6173$ p.u. and new line flow at L127 is $5.5916 + j0.1382$ p.u. The apparent powers are 5.6542 p.u. and 5.5933 p.u. respectively. L127 overload is solved. L126 overload is remaining but much

Table XXII. Solution methods for L126(B68-81) and L127(B81-80) overload

	Procedure	Result
Base condition	L126 & L127 overload (6.5442 p.u. & 6.4618 p.u. vs. their 5.6 p.u. limit)	Outage of L126 & 127, cascading outage and system islanding may occur
Step 1	Down G11 with 0.4941 p.u., down G13 with 0.4064 p.u., and Up G14 with 0.9005 p.u.;	L126 and L127 overload relieved but not solved
Step 2	Down G11 with 0.073 p.u., down G13 with 0.0617 p.u., and Up G14 with 0.1347 p.u.;	L126 overload relieved but not solved, L127 overload solved
Step 3	Down G11 with 0.0542 p.u., and Up G14 with 0.0542 p.u.;	L126 overload solved
Step 4	Verified with AC load flow	Solve, no violation.

smaller than the original case. G11 is still the most contributing generator. Thus G11 and G14 pair is chosen. 0.0542 p.u. is the amount for G11 to decrease and for G14 to increase.

Step 4. New AC power flow is run. New line flow at L126 is $5.5734 + j0.6108$ p.u. and new line flow at L127 is $5.5451 + j0.1466$ p.u. The apparent power are 5.6 p.u. and 5.547 p.u. respectively. Overload problem is solved.

The above procedure can be summarized in Table XXII.

From this study case, we can see that steady state control scheme is very effective in preventing possible cascading outages.

C. Study of Transient Stability Control Scheme

Assume there is a 3-phase fault at 50% of line L119(B69-77) at $t = 0s$, the critical clearing time (CCT) for this fault is 0.147s within a 3s simulation period. The stability criteria in time domain simulation is maximum phase angle difference of 180° between two machines. If the angle difference between any two machines after the simulation is larger than 180° , the system is unstable. Otherwise, the system is

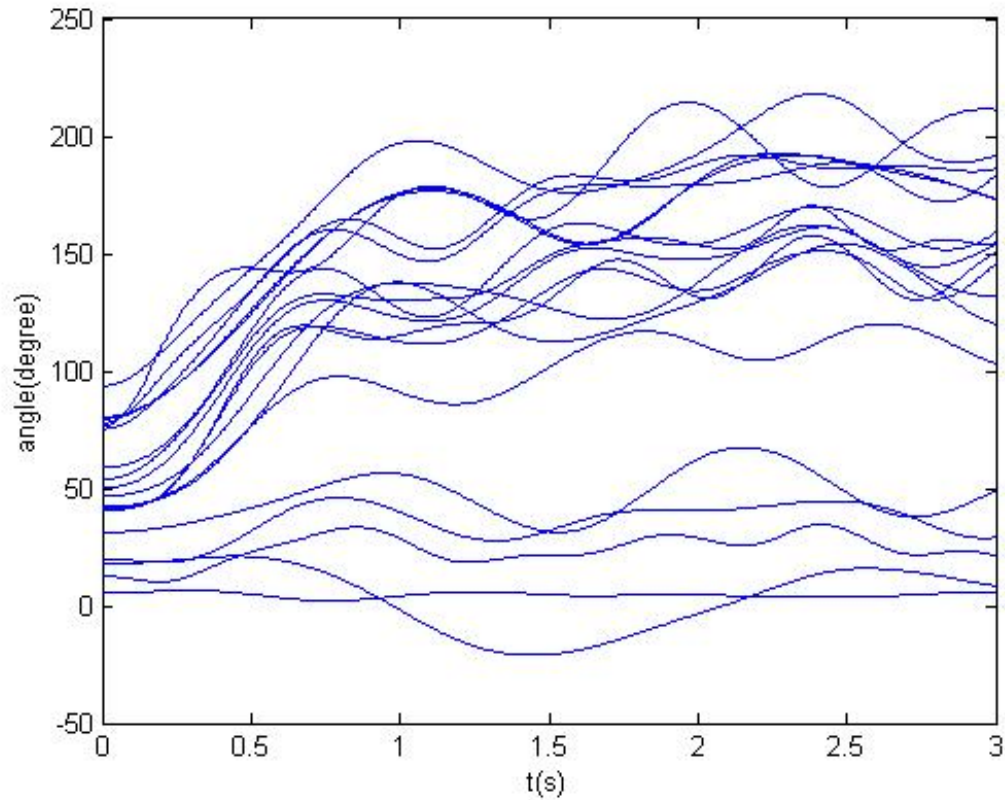


Fig. 29. Machine angles with fault clearing time at $t=0.149s$

stable. If the fault is cleared at $t = 0.149s$, the power system loses stability at $t = 0.799s$ in time domain simulation. The transient energy margin is -0.8997 from the potential energy boundary surface (PEBS) method. We can see the unstable swing in Fig. 29.

Assume the stability control means can be activated at $t = 0.25s$. We can use the method from the transient stability control scheme. From Chapter IV, we know that the transient stability control means can be classified in two groups: generator-input-based control (GIBC) and admittance-based control (ABC). Following case studies are those two kinds of control.

Case 1. Transient stability control by generator-input-based control (GIBC)

Table XXIII. Sensitivity analysis and fast-valving for stability control

GenNo	$\partial E/\partial P_m$	P_{m0} (p.u.)	ΔP_m (p.u.)	ratio
1	-2.9863	5.4000	0.3013	0.0558
2	-3.0353	1.0200	0.2964	0.2906
3	-2.9748	2.6400	0.3024	0.1146
4	-2.9937	3.7680	0.3005	0.0798
5	-2.9215	0.0840	0.3079	3.6660
6	-3.0028	0.2280	0.2996	1.3141
7	-2.9714	2.4480	0.3028	0.1237
8	-3.0092	0.5760	0.2990	0.5190
9	-2.9829	1.8600	0.3016	0.1622
10	-3.0162	1.9200	0.2983	0.1554
11	-2.9217	4.6920	0.3079	0.0656
12	-2.9639	4.7040	0.3035	0.0645
13	-2.7592	7.9879	0.3261	0.0408
14	-2.6624	2.8620	0.3379	0.1181
15	-1.7415	0.0240	0.5166	21.5254
16	-2.1993	3.6420	0.4091	0.1123
17	-2.3161	1.5120	0.3884	0.2569
18	-2.2980	0.2400	0.3915	1.6312
19	-2.1241	0.2160	0.4235	1.9609
20	-2.1354	0.0001	0.4213	7021.8

Generator fast-valving is an effective generator-input-based control (GIBC). It uses mechanism of rapid opening and closing steam valves to reduce the generator accelerating power after the disturbance [53]. We can get the generator input (mechanical power P_m) part of analytical sensitivity of energy margin from Eq. 4.25 in Chapter IV. Table XXIII gives the P_m part of sensitivity of energy margin, variance of P_m to make the energy margin positive and the fast-valving ratio compared with machine original mechanical power P_m .

From Table XXIII we can see that to stabilize the system, generator fast-valving amount from 0.2964 p.u. (G2) to 0.5166 p.u. (G15) of different generators is needed. In addition, fast-valving of G5, G6, G15, G18, G19 and G20 are impossible because they need the reduced amount larger than their original mechanical power input.

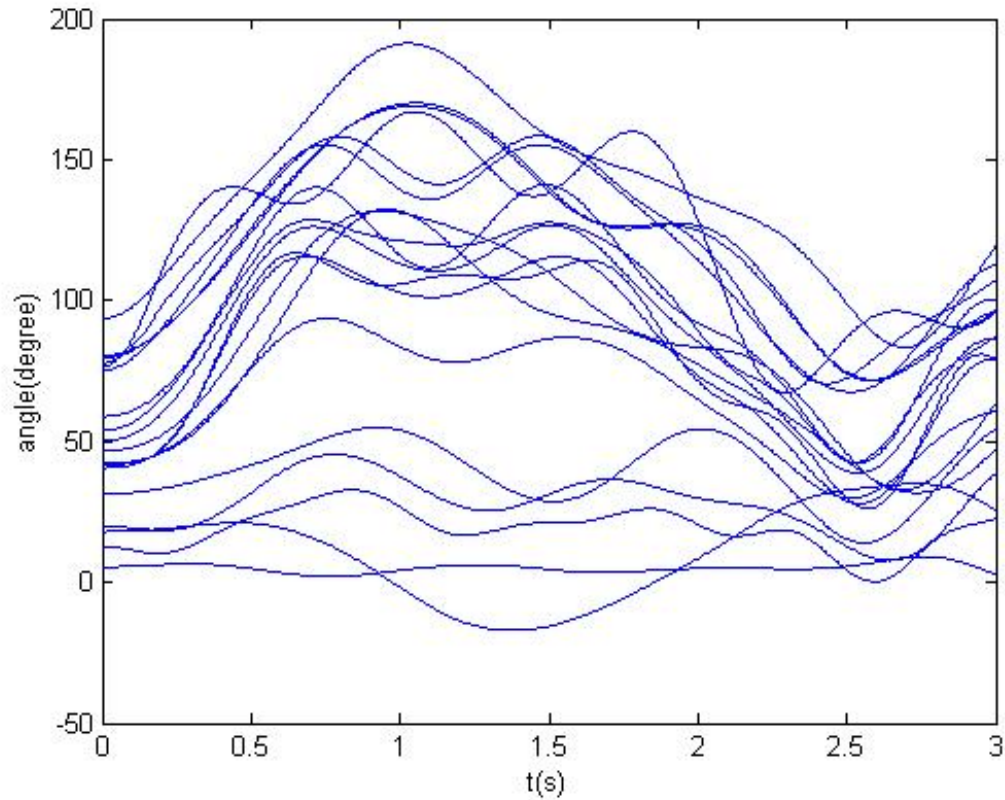


Fig. 30. Machine angles with G13 fast-valving at $t=0.25s$

If we check the varying ratio compared with original mechanical power input P_m , G13(B69) and G1(B10) are two least varying generators with ratios of 4.08% and 5.58% respectively. G13 is the nearest generator to the disturbance in electrical distance thus the most disturbed and accelerating one. Therefore, G13 is the optimal one chosen for stability control. G1 is also a good choice because of the small fast-valving ratio.

Let us use G13 fast-valving with 4.08% (0.3261 p.u.) at $t = 0.25s$. From the time-domain simulation analysis, it can be seen that it stabilizes the system. We can see this from Fig. 30.

Let us use G1 fast-valving with 5.58% (0.3013 p.u.) at $t = 0.25s$. From the

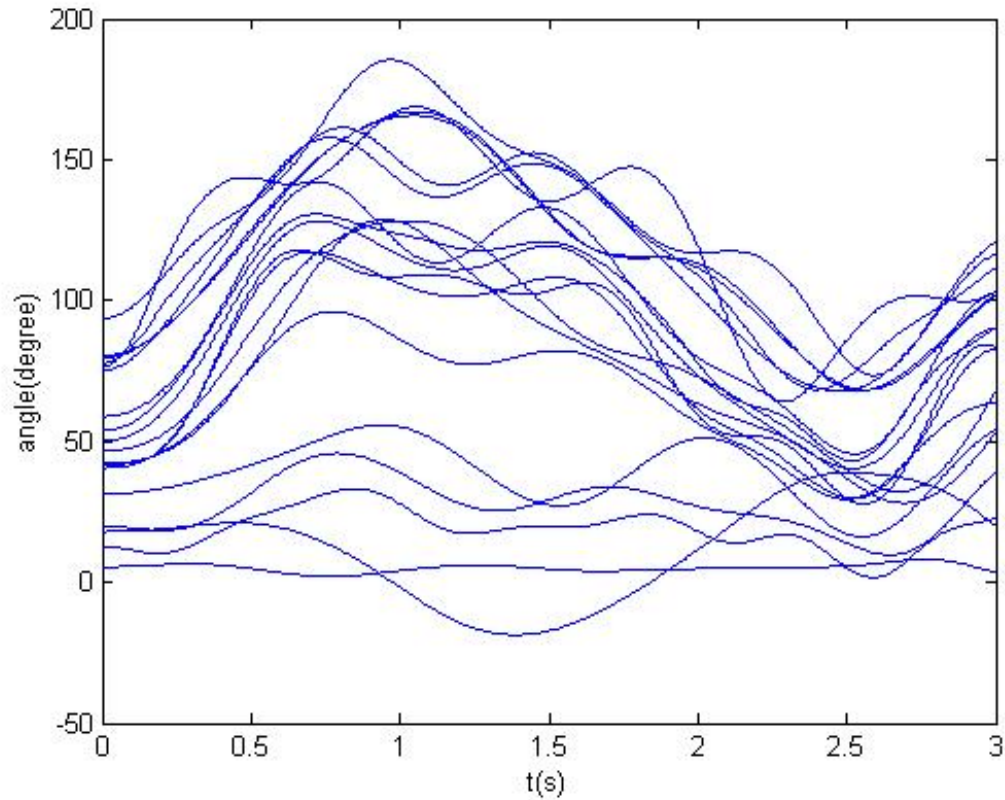


Fig. 31. Machine angles with G1 fast-valving at $t=0.25s$

time-domain simulation analysis, it can be seen that it stabilizes the system. We can see this from Fig. 31.

Case 2. Transient stability control by admittance-based control (ABC)

Generator dynamic braking, shunt reactor switching, shunt capacitor switching, line switching, TCSC inserting, SVC inserting, etc. are all admittance-based controls (ABC) because they change the system admittance parameters. Here we only consider the generator dynamic braking, shunt reactor switching and shunt capacitor switching at B69 to stabilize G13 because it is the most accelerating one. Assume we have such kinds of control means at B69. For certain amount of generator dynamic braking, shunt reactor switching and shunt capacitor switching, we can calculate the

Table XXIV. Stability control means at B69 and their contribution to transient energy margin

Control Means	Amount(MVA)	Energy Margin	Amount(MVA)	Energy Margin
Braking resistor	30	-0.024	31	0.006
Shunt capacitor	100	-0.025	104	0.011
Shunt reactor	100	-1.707	10	-0.9833

admittance matrix variance by Eq. 4.22 and then get the transient energy margin variance by Eq. 4.24. By adjusting the varying amount of generator braking resistor, shunt reactor or shunt capacitor, we can make the new energy margin positive. Then we verify the result in the time-domain simulation analysis. If it can stabilize the system, we can use this control. If it can not, we continue adjusting the control amount to stabilize the system.

Table XXIV is a summary table of control means and their contribution to transient energy margin based on potential energy boundary surface (PEBS) method and sensitivity analysis.

Shunt reactor switching contributes negative to the transient energy margin. We verify the results of dynamic braking with 31MVA capacity and shunt capacitor switching with 104MVA capacity at B69 in time-domain simulation and find they can stabilize the system, as we can see from Fig. 32 and Fig. 33.

D. Study of Interactive Scheme

Interaction between system-wide and local levels needs to be considered to assure the secure operation of the power system. A simple example is given to show the advantage of this interactive scheme. From the system point of view, tie-lines are important lines because they transfer power among different sub-systems or areas

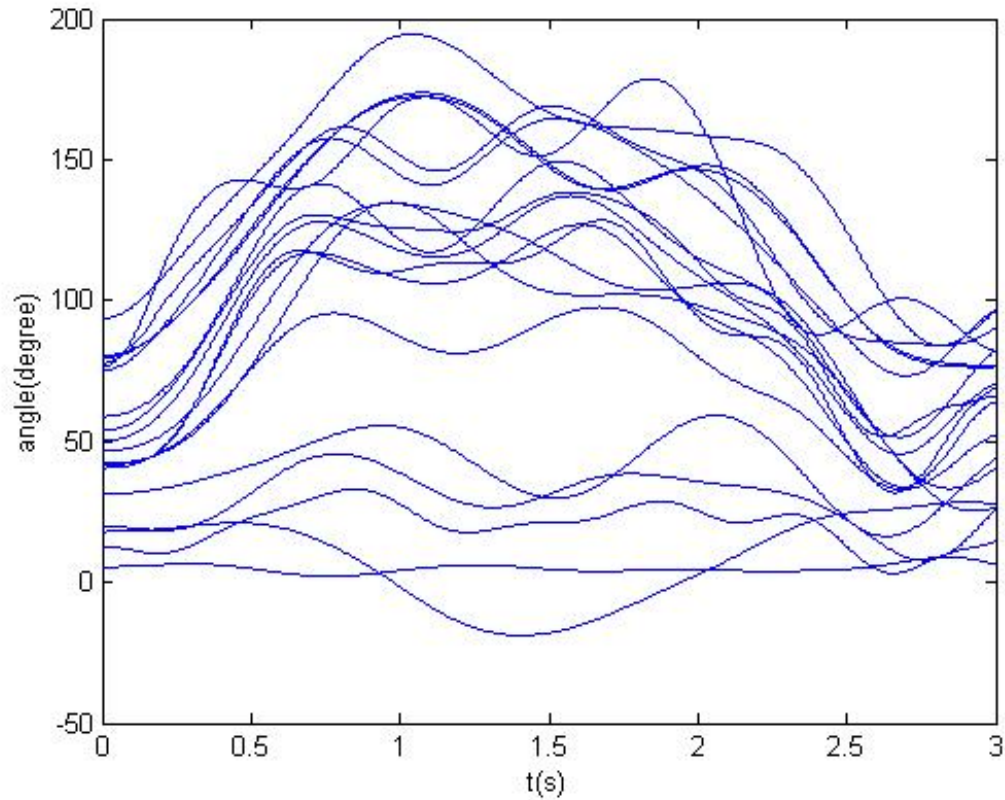


Fig. 32. Machine angles with dynamic braking at G13 at $t=0.25s$

to fulfill the important transaction. Assume there is a 3-phase fault at 50% of line L119(B69-77) at $t = 0s$, the critical clearing time (CCT) for this fault is $0.147s$ within a $3s$ simulation period. This fault is cleared at $t = 0.05s$. We consider for the next contingency. The vulnerability analysis by AC power flow method after this line outage ranks L107 (B68-69) outage as the most vulnerable case both in total vulnerability index value and relay vulnerability index value. Then we assume another 3-phase fault occurs at $t = 1s$. The critical clearing time (CCT) for this fault is $0.0117s$. We clear this fault at $t = 1.0117s$. The scenario goes as follows:

- 1) $t = 0s$, first 3-phase fault occurs at 50% at L119 (B69-77);

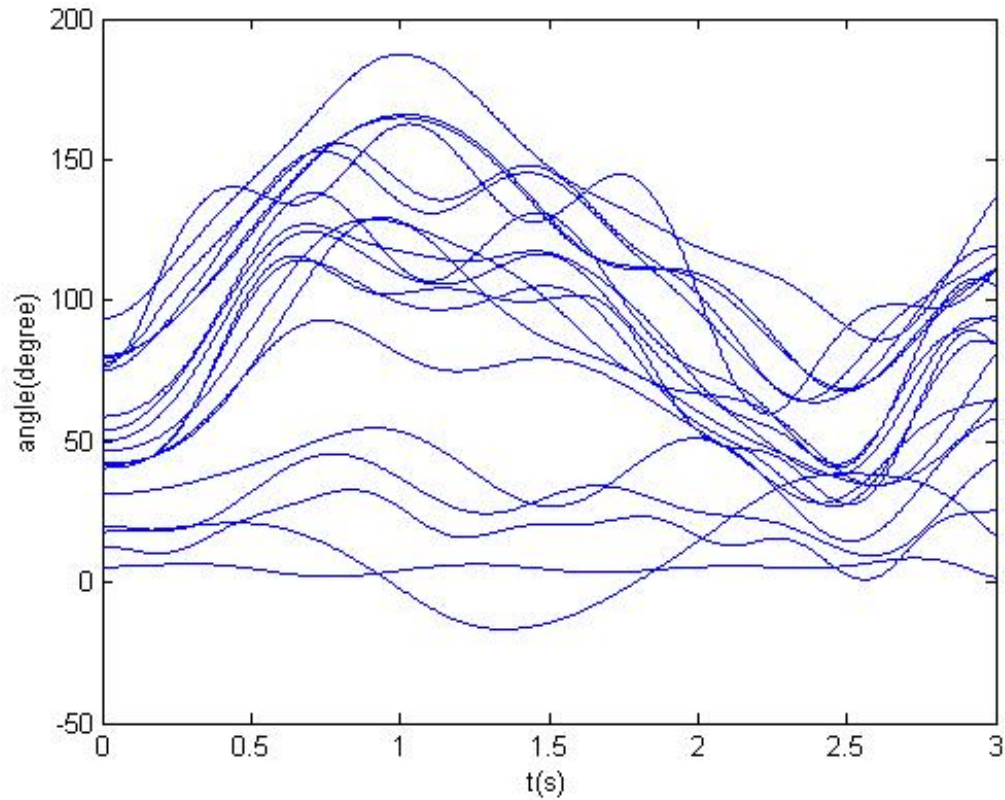


Fig. 33. Machine angles with shunt capacitor switching at B69 at $t=0.25s$

- 2) $t = 0.05s$, the fault is cleared by tripping breakers at two ends of L119 and no breaker re-closing;
- 3) $t = 1.0s$, second 3-phase fault occurs at 50% at L107 (B68-69);
- 4) $t = 1.0117s$, the fault is cleared by tripping breakers at two ends of L106 and no breaker re-closing;
- 5) $t = 3s$, stop the time-domain simulation.

The time-domain simulation finds that distance relay at B69 of L108 (B69-70) sees apparent impedance falling into its zone 3 from $t = 1.365s$ to $2.024s$ with the

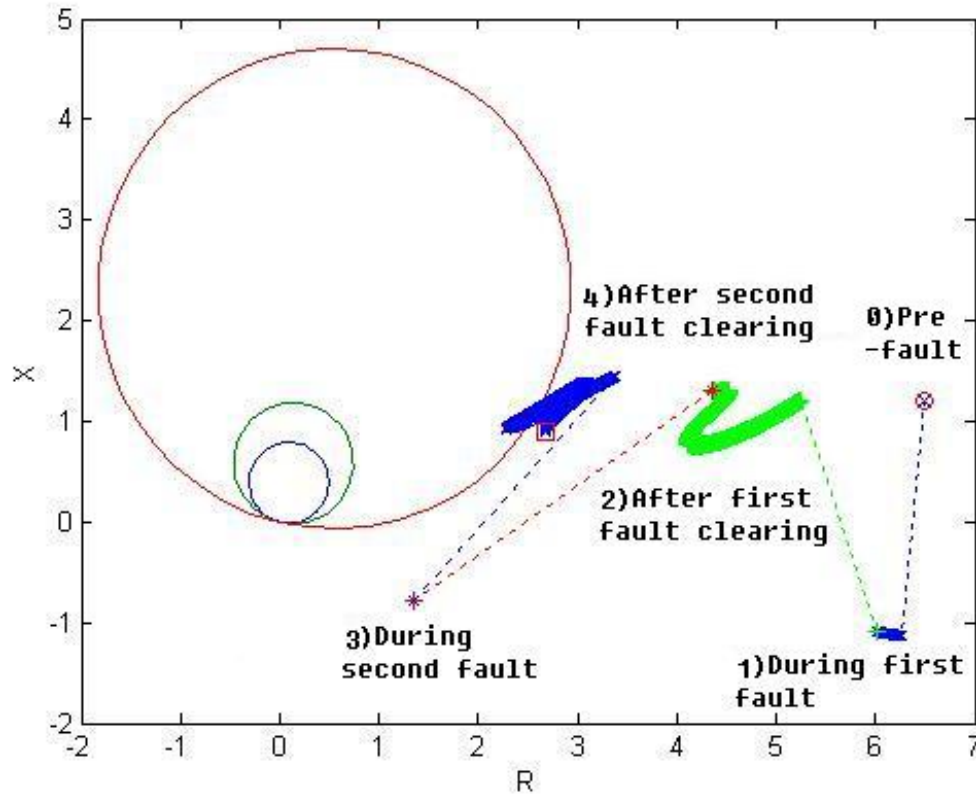


Fig. 34. Normalized apparent impedance seen by distance relay at B69 of L108

lasting time as long as 0.659s. Distance relay at B69 of L116(B69-75) sees apparent impedance falling into its zone 3 from $t = 1.277s$ to $t = 2.177s$ with the lasting time as long as 0.9s. We can see this from Fig. 34 and Fig. 35.

For distance relay settings, zone 1 and zone 2 are chosen to be 0.8 and 1.2 respectively. Zone 3 is used to protect the 120% of the next longest neighboring line.

If any of those two relays misoperates, the system will lose stability and cascading outages will occur. If such an interactive scheme is installed in the system, the system tool can identify the vulnerable condition after L119 outage. Thus it can notify local tools to monitor distance relays at L108 and L116 carefully. After the next fault occurs at L107, the local tool can conclude that there are no faults at L108 and L116

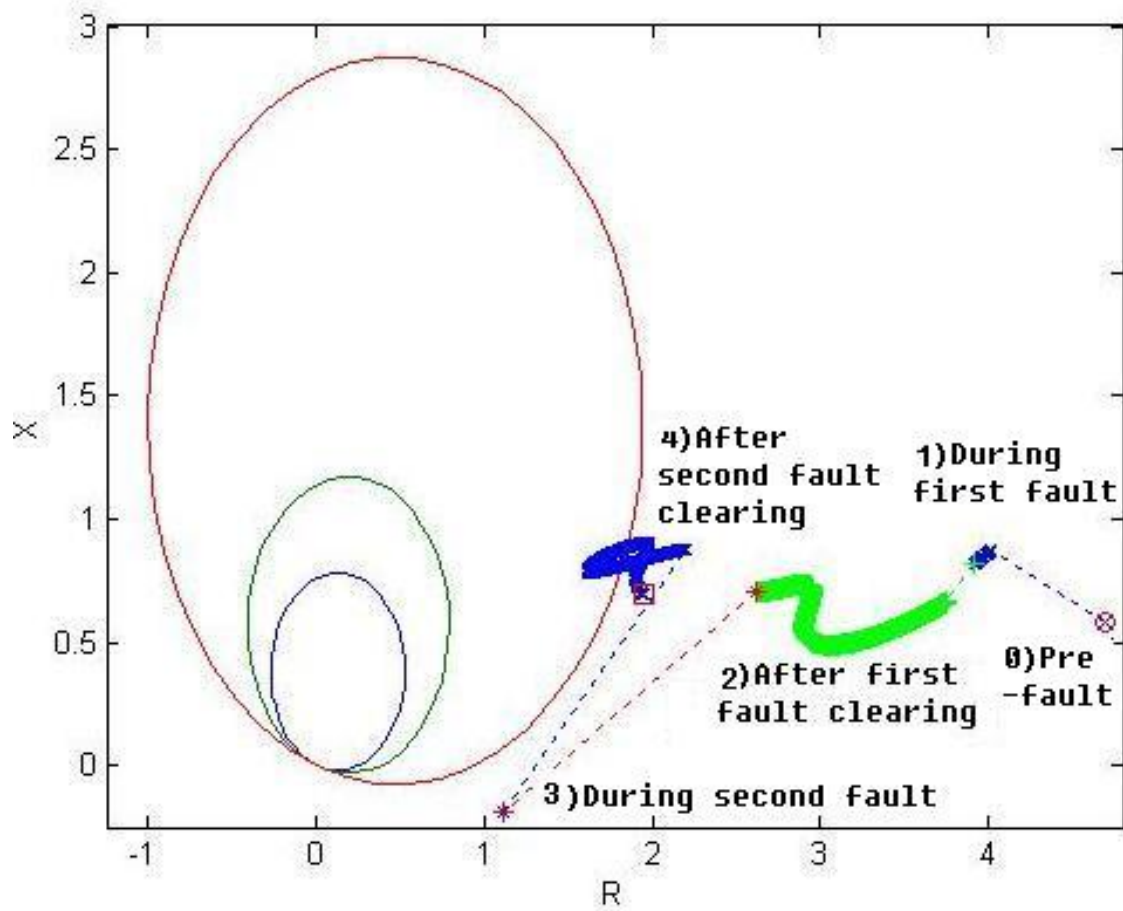


Fig. 35. Normalized apparent impedance seen by distance relay at B69 of L116

during the power swing condition so that it can block the possible misoperations of those two relays. Thus the possible cascading outages may be prevented by this interactive scheme.

E. Summary

This chapter describes the relationship among steady state control scheme, transient stability control scheme and interactive scheme and evaluates their performance by case studies implemented in the IEEE 118-bus system. Promising simulation results show that those control schemes can help detect, prevent and mitigate the cascading outages.

CHAPTER VII

CONCLUSIONS

A. Summary of Achievements

The purpose of this dissertation is to understand the mechanism of power system cascading outages and develop some effective methods and tools to help detect, prevent and mitigate them. Catastrophic power system cascading outages worldwide in recent years urge power system researchers and engineers to try their best to understand cascading outages and find ways to detect, prevent and mitigate them. The research in this area is far from being mature. This dissertation presents three effective schemes: steady state control scheme, transient stability control scheme and interactive scheme to help detect, prevent and mitigate power system cascading outages.

Steady state control scheme can help detect and prevent a possible cascading outage at its first slow evolving steady state stage. New tools such as vulnerability index (VI), margin index (MI), network contribution factor (NCF) method, topology processing method and selected minimum load shedding (SMLS), and new controls such as transmission network control based on NCF method, generator control based on generator distribution factor (GDF) and load control based on load distribution factor (LDF) to solve the overload or congestion have been proposed and developed. Transient stability control scheme can help prevent and mitigate the possible cascading outage at its transient progress stage. It uses a Lyapunov direct method, potential energy boundary surface (PEBS) method, and analytical sensitivity of transient energy margin for fast stabilizing control. Its results are verified by the accurate time-domain transient stability analysis method. Interactive scheme takes advantages of accurate system and local information and analysis results, uses some techniques from

both steady state control and transient stability control and works all the time at the system-wide level and local level. Detailed system-wide monitoring and control tool has been developed. Lots of simulation studies have been tested in the IEEE 14-bus, 24-bus, 39-bus and 118-bus systems and the promising results show their ability to help detect, prevent and mitigate cascading outages.

In Chapter II, the fundamentals of the proposed approach have been presented. The mechanism of cascading outages are studied. The proposed solutions based on the assumed mechanism are introduced. Chapter III has provided the steady state control scheme for early detection and prevention of cascading outages. With the aid of new tools and new controls, the whole new procedure has been proposed as follows: evaluation of the system operating condition, identification of vulnerable parts and conditions, prediction of possible successive events, and prevention of cascading outages with appropriate control. The transient stability control scheme has been introduced in Chapter IV. It aims at solving the transient stability problem and finding effective transient stability control means to stabilize the system. New classification of transient stability control means has been given: generator-input-based control (GIBC) and admittance-based control (ABC). For each control means available in the system, its contribution to transient stability has been calculated based on the sensitivity analysis of transient energy margin and parameter variance. Such control means can make the transient energy margin to move from negative to positive, which allows the system to go from unstable to stable state. This will be verified in the more accurate time-domain transient stability analysis. If it is true, based on the time-domain simulation, an optimal transient stability control will be found and activated. If it is not true, adjustment of the control amount will be made and final solution will be found. Chapter V has developed an interactive scheme between system-wide and local monitoring and control to help detect, prevent and mitigate

cascading outages. The interaction between system-wide and local levels, especially the system transient stability analysis and relay action, has been studied. Effective tools in the system-wide monitoring and control, such as routine security analysis including vulnerability analysis, static and dynamic contingency analysis for expected events, event-based security analysis for unexpected real-time events, security control based on steady state control and transient stability control for expected events and unexpected events, have been implemented. An interactive scheme between system-wide and local levels has been described. Evaluation of those three schemes has been studied in the IEEE 118-bus system and reported in Chapter VI. The simulation results in this chapter show the ability of those three schemes to help detect, prevent and mitigate the cascading outages.

B. Research Contribution

The contributions of this dissertation are both the theoretical research and practical applications in detection, prevention and mitigation of power system cascading outages. The conventional research and operating practice in this area are not sufficient to fulfill this task. This dissertation has studied the causes and mechanism of cascading outages and developed three effective schemes: steady state control scheme, transient stability control scheme, and interactive scheme to help detect, prevent and mitigate the cascading outages. New tools and new techniques have been implemented. They can also serve as operator training tool and decision support tool for better system situational awareness and better system security analysis and control. The proposed approach can be added into the current EMS functionality at control center or serve as an additional security control tool. The benefits from using those schemes have been demonstrated clearly in the dissertation.

C. Suggestions for Future Research

The research and study in this dissertation may be continued. Extensive transient stability analysis and control should be continued because fast approximate potential energy boundary surface (PEBS) method is not as accurate as time-domain simulation method. Voltage stability analysis can also be included because several large area cascading outages are related to voltage collapse issue. All software modules are programmed in Matlab and they can be implemented in Visual C++ or Java for faster speed and better user interface.

REFERENCES

- [1] U.S.-Canada Power System Outage Task Force, “Final Report on the August 14, 2003 Blackout in the United States and Canada: Causes and Recommendations,” Tech. Rep., Apr. 2004, [Online] Available: <http://www.nerc.com>.
- [2] NERC Disturbance Analysis Working Group, “NERC Disturbance Reports,” Tech. Rep., Princeton, New Jersey, 1996–2002, [Online] Available: <http://www.nerc.com>.
- [3] C. S. Joseph, D. S. Black, R. Charles, L. J. Connor, and C. E. Bagge, “Report to the President by the Federal Power Commission on the Power Failure in the Northeastern United States and the Province of Ontario on November 9-10, 1965,” Tech. Rep., Washington, D.C., Dec. 1965, [Online] Available: http://blackout.gmu.edu/archive/a_1965.html.
- [4] Federal Power Commission U.S. Department of Energy, “The Con Edison Power Failure of July 13 and 14, 1977,” Tech. Rep., Washington, D.C., June 1978, [Online] Available: http://blackout.gmu.edu/archive/a_1977.html.
- [5] C. W. Taylor, *Power system voltage stability*, New York: McGraw-Hill, 1994.
- [6] E. Agneholm, “The Restoration Process Following a Major Breakdown in a Power System,” Tech. Rep., Goteborg, Sweden, May 1996, [Online] Available: <http://www.elkraft.chalmers.se/Publikationer/EKS.publ/Abstract/Agneholm.Lic.pdf>.
- [7] G. Doorman, G. Kjolle, K. Uhlen, E. S. Huse, and N. Flatubo, “Report to the Nordic Council of Ministers: Vulnerability of the

- Nordic Power System,” Tech. Rep. TRA5962, May 2004, [Online] Available: <http://www.ksg.harvard.edu/hepg/Papers/Door-man.vul.nordic.system.0504.pdf>.
- [8] A. Kurita and T. Sakurai, “The power system failure on July 23, 1987 in Tokyo,” in *Proc. 27th conf. on Decision and Control*, 1988, pp. 2093–2097.
- [9] V.X. Filho, L.A.S. Pilotto, N. Martins, A.R.C. Carvalho, and A. Bianco, “Brazilian defense plan against extreme contingencies,” in *Proc. of IEEE 2001 Power Engineering Society Summer Meeting*, July 2001, vol. 2, pp. 834–839.
- [10] NERC Disturbance Analysis Working Group, “NERC Disturbance Reports,” Tech. Rep., Princeton, New Jersey, 1996, [Online] Available: <http://www.nerc.com>.
- [11] H. R. O’Leary, “DOE’s Report to the President: The Electric Power Outages in the Western United States, July 2-3, 1996,” Tech. Rep., Washington, D.C., Aug. 1996, [Online] Available: <http://www.nerc.com>.
- [12] E. System, “Power Failure in Eastern Denmark and Southern Sweden on 23 September 2003, Final Report on the Course of Events,” Tech. Rep., Nov. 2003, [Online] Available: <http://www.pserc.org>.
- [13] Union for the Co-ordination of Transmission of Electricity, “Interim Report of the Investigation Committee on the 28 September 2003 Blackout in Italy,” Tech. Rep., Oct. 2003, [Online] Available: <http://www.pserc.org>.
- [14] U. Knight, *Power systems in emergencies*, Chicester, England: John Wiley and Sons, Inc., 2004.

- [15] Costas Vournas, “Technical Summary on the Athens and Southern Greece Blackout of July 12, 2004,” Tech. Rep., School of Electrical & Computer Engineering, National Technical University of Athens, July 2004, [Online] Available: <http://www.pserc.org>.
- [16] “Resources for understanding the Moscow blackout of 2005,” Power Systems Engineering Research Center (PSerc) Website, [Online] Available: <http://www.pserc.org>.
- [17] J.J. Paserba, “How FACTS controllers benefit AC transmission systems,” in *Proc. of IEEE 2003 PES Transmission and Distribution Conference and Exposition*, Sep. 2003, vol. 3, pp. 949–956.
- [18] Y.L. Kang, G.B. Shrestha, and T.T. Lie, “Application of an NLPID controller on a UPFC to improve transient stability of a power system,” *IEE Proc.-Gener. Trans. Distrib.*, vol. 148, no. 6, pp. 523–529, Nov. 2001.
- [19] Y. Wang, Y.L. Tan, and G. Guo, “Robust nonlinear co-ordinated excitation and TCSC control for power systems,” *IEEE Proc.*, vol. 149, no. 3, pp. 367–372, May 2002.
- [20] P. M. Anderson, B. L. Agrawal, and J. E. V. Ness, *Subsynchronous resonance in power systems*, New York: IEEE Press, 1990.
- [21] R. Piwko, D. Osborn, R. Gramlich, G. Jordan, and D. Hawkins et al., “Wind energy delivery issues [transmission planning and competitive electricity market operation],” *IEEE Power and Energy Magazine*, vol. 3, no. 6, pp. 47–56, Nov./Dec. 2005.

- [22] P. Bak, *How Nature Works: The science of self-organized criticality*, Copernicus, New York, 1996.
- [23] A. G. Phadke and J. S. Thorp, “Expose hidden failures to prevent cascading outages,” *IEEE Computer Applications in Power*, vol. 9, no. 3, pp. 20–23, July 1996.
- [24] D. Novosel, M. M. Begovic, and V. Madani, “Shedding light on blackouts: Studying the causes of system blackouts in an effort to better protect against and lessen the impact of future disturbances and speed up restoration,” *IEEE Power and Energy Magazine*, vol. 1, no. 1, pp. 32–43, Jan./Feb. 2004.
- [25] W.V. Hassenzahl, D.W. Hazelton, B.K. Johnson, P. Komarek, and M. Noe, “Electric power applications of superconductivity,” *Proceedings of the IEEE*, vol. 92, no. 10, pp. 1655–1674, Oct. 2004.
- [26] W.V. Hassenzahl, “Superconductivity, an enabling technology for 21st century power systems?,” *IEEE Trans. Applied Superconductivity*, vol. 11, no. 1, pp. 1447–1453, Mar. 2001.
- [27] C. Rehtanz, “Systemic use of multifunctional SMES in electric power systems,” *IEEE Trans. Power Systems*, vol. 14, no. 4, pp. 1422–1427, Nov. 1999.
- [28] B.A. Carreras, V.E. Lynch, and I. Dobson, “Dynamical and probabilistic approaches to the study of blackout vulnerability of the power transmission grid,” in *Proc. 37th Annual Hawaii International Conference on System Sciences*, Jan. 2004, pp. 55–61.
- [29] D. C. Elizondo, J. D. L. Ree, A. G. Phadke, and S. Horowitz, “Hidden failures in protection systems and their impact on wide-area disturbances,” in *Proc.*

- IEEE 2001 Power Engineering Society Winter Meeting*, Jan/Feb 2001, vol. 2, pp. 710–714.
- [30] A. G. Phadke, “Hidden failures in electric power systems,” *Int. J. Critical Infrastructures*, vol. 1, no. 1, pp. 64–75, 2004.
- [31] J. C. Tan, P. A. Crossley, P. G. McLaren, P. F. Gale, and I. Hall et al., “Application of a wide area backup protection expert system to prevent cascading outages,” *IEEE Trans. Power Delivery*, vol. 17, no. 2, pp. 375–380, Apr. 2002.
- [32] I. Kamwa, R. Grondin, and Y. Hebert, “Wide-area measurement based stabilizing control of large power systems—a decentralized/hierarchical approach,” *IEEE Trans. Power Systems*, vol. 16, no. 1, pp. 136–153, Feb. 2001.
- [33] Working Group C6 of the System Protection Subcommittee of the IEEE Power System Relaying Committee, “Wide Area Protection and Emergency Control,” Tech. Rep., 2002, [Online] Available: <http://www.pes-psrc.org>.
- [34] M. Begovic, D. Novosel, D. Karlsson, C. Henville, and G. Michel et al., “Wide-area protection and emergency control,” *Proceedings of the IEEE*, vol. 93, no. 5, pp. 876–891, May 2005.
- [35] C.W. Taylor, D.C. Erickson, K.E. Martin, R.E. Wilson, and V. Venkatasubramanian et al., “WACS-wide-area stability and voltage control system: R&D and online demonstration,” *Proceedings of the IEEE*, vol. 93, no. 5, pp. 892–906, May 2005.
- [36] M. Zima, M. Larsson, P. Korba, C. Rehtanz, and G. Andersson, “Design aspects for wide-area monitoring and control systems,” *Proceedings of the IEEE*, vol. 93, no. 5, pp. 980–996, May 2005.

- [37] J. Bertsch, C. Carnal, D. Karlson, J. McDaniel, and K. Vu, “Wide-area protection and power system utilization,” *Proceedings of the IEEE*, vol. 93, no. 5, pp. 997–1003, May 2005.
- [38] W. R. Lachs, “Area-wide system protection scheme against extreme contingencies,” *Proceedings of the IEEE*, vol. 93, no. 5, pp. 1004–1027, May 2005.
- [39] Q. Chen, K. Zhu, and J.D. McCalley, “Dynamic decision-event trees for rapid response to unfolding events in bulk transmission systems,” in *Proc. of IEEE 2001 Power Tech Proceedings*, Porto, Portugal, Sep. 2001, pp. 1–5.
- [40] Y. Sun and T. J. Overbye, “Visualization for power system contingency analysis data,” *IEEE Trans. Power System*, vol. 19, no. 4, pp. 1859–1866, Nov. 2004.
- [41] P. M. Anderson and B. K. LeReverend, “Industry experience with special protection schemes,” *IEEE Trans. Power Systems*, vol. 11, no. 3, pp. 1166–1179, Aug. 1996.
- [42] C.-C. Liu, J. Jung, G.T. Heydt, V. Vittal, and A.G. Phadke et al., “The strategic power infrastructure defense (SPID) system: A conceptual design,” *IEEE Control Systems Magazine*, vol. 20, no. 4, pp. 40–52, Aug. 2000.
- [43] M. Amin, “Toward self-healing energy infrastructure systems,” *IEEE Computer Applications in Power*, vol. 14, no. 1, pp. 20–28, Jan. 2001.
- [44] Inc. Commonwealth Associates, “White Paper: A Scenario Describing the August 14, 2003 Blackout,” Tech. Rep., 2003, [Online] Available: <http://www.caiengr.com/Scenariofor081403Release0.pdf>.
- [45] J. Salmeron, K. Wood, and R. Baldick, “Analysis of electric grid security under terrorist threat,” *IEEE Trans. Power System*, vol. 19, no. 2, pp. 905–912, May

2004.

- [46] J. MacCalley, “Operational defense of power system cascading sequences: Probability, prediction & mitigation,” Power Systems Engineering Research Center (PSerc) Seminars (Tele-Seminar), Oct. 2003, [Online] Available: <http://www.pserc.org>.
- [47] F. Dobraca, M. A. Pai, and P. W. Sauer, “Relay margins as a tool for dynamical security analysis,” *Int. J. Electr. Power Energy Syst*, vol. 12, no. 4, pp. 226–234, Oct. 1990.
- [48] C. Singh and I.A. Hiskens, “Direct assessment of protection operation and non-viable transients,” *IEEE Trans. Power System*, vol. 16, no. 3, pp. 427–434, Aug. 2001.
- [49] M. Jonsson, “Line protection and power system collapse,” M.S. thesis, Chalmers University of Technology, Goteborg, Sweden, 2001.
- [50] H. Wang and J. S. Thorp, “Optimal locations for protection system enhancement: A simulation of cascading outages,” *IEEE Trans. Power Delivery*, vol. 16, no. 4, pp. 528–533, Oct. 2001.
- [51] S. A. Soman, T. B. Nguyen, M. A. Pai, and R. Vaidyanathan, “Analysis of angle stability problems: A transmission protection systems perspective,” *IEEE Trans. Power Delivery*, vol. 19, no. 3, pp. 1024–1033, July 2004.
- [52] N. Zhang, H. Song, and M. Kezunovic, “New monitoring and control scheme for preventing cascading outage,” in *Proc. 37th Annual North American Power Symposium (NAPS2005)*, Ames, Iowa, Oct. 2005, pp. 37–42.

- [53] P. Kundur, *Power system stability and control*, New York: McGraw Hill Inc., 1994.
- [54] H. Song and M. Kezunovic, "Static analysis of vulnerability and security margin of the power system," in *Proc. IEEE PES Transmission & Distribution Conference & Exposition*, Dallas, Texas, May. 2006, pp. 147–152.
- [55] G.C. Ejebe and B.F. Wollenberg, "Automatic contingency selection," *IEEE Trans. Power Apparatus and Systems*, vol. 98, no. 1, pp. 97–109, Jan/Feb 1979.
- [56] Y. Dai, J. D. McCalley, and V. Vittal, "Simplification, expansion and enhancement of direct interior point algorithm for power system maximum loadability," *IEEE Trans. Power Systems*, vol. 15, no. 3, pp. 1014 – 1021, Aug. 2000.
- [57] M. Larsson, C. Rehtanz, and J. Bertsch, "Monitoring and operation of transmission corridors," in *Proceedings of the IEEE Power Tech Conference*, June 2003, vol. 3, pp. 1–8.
- [58] H. Song and M. Kezunovic, "Relieving overload and improving voltage by the network contribution factor (NCF) method," in *Proc. 36th Annual North American Power Symposium (NAPS2004)*, Moscow, Idaho, Aug. 2004, pp. 1–5.
- [59] B. Stott and O. Alsac, "Fast decoupled load flow," *IEEE Trans. Power Apparatus and Systems*, vol. 93, pp. 859–869, 1974.
- [60] A. P. S. Meliopoulos, C. S. Cheng, and F. Xia, "Performance evaluation of static security analysis methods," *IEEE Trans. Power Systems*, vol. 3, no. 4, pp. 1441–1449, Aug. 1994.
- [61] J. Bialek, "Topological generation and load distribution factors for supplement charge allocation in transmission open access," *IEEE Trans. Power Systems*,

- vol. 12, no. 3, pp. 1185–1193, Aug. 1997.
- [62] E.B. Makram, K.P. Thorton, and H.E. Brown, “Selection of lines to be switched to eliminate overloaded lines using a z-matrix method,” *IEEE Trans. Power Systems*, vol. 4, no. 2, pp. 653–661, May 1989.
- [63] N. Muller and V. H. Quintana, “Line and shunt switching to alleviate overloads and voltage violations in power networks,” *Generation, Transmission and Distribution, IEE Proceedings C*, vol. 136, no. 4, pp. 246–253, July 1989.
- [64] N.S. Rau, “Transmission loss and congestion cost allocation - an approach based on responsibility,” *IEEE Trans. Power Systems*, vol. 15, no. 4, pp. 1401–1409, Nov. 2000.
- [65] T. Niimura and Y. Niu, “Transmission congestion relief by economic load management,” in *Proc. of IEEE Power Engineering Society 2002 Summer Meeting*, 2002, vol. 3, pp. 1645–1649.
- [66] C. Grigg, P. Wong, P. Albrecht, R. Allan, and M. Bhavaraju et al., “The IEEE reliability test system - 1996, a report prepared by the reliability test system task force of the application of probability methods subcommittee,” *IEEE Trans. Power Systems*, vol. 14, no. 3, pp. 1010–1020, Aug. 1999.
- [67] V. Vittal, E.Z. Zhou, C. Hwang, and A.-A. Fouad, “Derivation of stability limits using analytical sensitivity of the transient energy margin,” *IEEE Trans. Power Systems*, vol. 4, no. 4, pp. 1363–1372, Nov. 1989.
- [68] J. Tong, H.-D. Chang, and T.P. Conneen, “A sensitivity-based BCU method for fast derivation of stability limits in electric power systems,” *IEEE Trans. Power Systems*, vol. 8, no. 4, pp. 1418–1428, Nov. 1993.

- [69] V. Chadalavada and V. Vittal, “Transient stability assessment for network topology changes: application of energy margin analytical sensitivity,” *IEEE Trans. Power Systems*, vol. 9, no. 3, pp. 1658–1664, Aug. 1994.
- [70] P. Kundur, J. Paserba, V. Ajjarapu, G. Andersson, and A. Bose et al., “Definition and classification of power system stability,” *IEEE Trans. Power System*, vol. 19, no. 2, pp. 1387–1401, May 2004.
- [71] E. W. Kimbark, *Power system stability*, vol. 1&2, New York: John Wiley and Sons, Inc., 1950.
- [72] P. M. Anderson and A. A. Fouad, *Power system control and stability*, vol. I, Ames, Iowa: The Iowa State University Press, 1977.
- [73] M. A. Pai, *Energy function analysis for power system stability*, Norwell, MA: Kluwer Academic Publishers, 1989.
- [74] M. Pavella and P. G. Murthy, *Transient stability of power systems, theory and practice*, New York: J.Wiley & Sons, 1994.
- [75] P. W. Sauer and M. A. Pai, *Power system dynamics and stability*, Upper Saddle River, N.J.: Prentice Hall, 1998.
- [76] H.-D. Chiang, F.F. Wu, and P.P. Varaiya, “Foundations of the potential energy boundary surface method for power system transient stability analysis,” *IEEE Trans. Circuits and Systems*, vol. 35, no. 6, pp. 712–728, June 1988.
- [77] P. Omahen, “Fast transient stability assessment using corrective PEBS method,” in *Proc. of the 6th Mediterranean Electrotechnical Conference*, 1991, vol. 2, pp. 1408–1411.

- [78] M.H. Haque and A.H.M.A. Rahim, “An efficient method of identifying coherent generators using Taylor series expansion,” *IEEE Trans. Power System*, vol. 3, no. 3, pp. 1112–1118, Aug. 1988.
- [79] M.A. Pai and P.W. Sauer, “Stability analysis of power systems by Lyapunov’s direct method,” *IEEE Control Systems Magazine*, vol. 9, no. 1, pp. 23–27, Jan. 1989.
- [80] P.W. Sauer, A.K. Behera, M.A. Pai, J.R. Winkelman, and J.H. Chow, “Trajectory approximations for direct energy methods that use sustained faults with detailed power system models,” *IEEE Trans. Power System*, vol. 4, no. 2, pp. 499–506, May 1989.
- [81] T.L. Baldwin, L. Mili, and A.G. Phadke, “Dynamic Ward equivalents for transient stability analysis,” *IEEE Trans. Power System*, vol. 9, no. 1, pp. 59–67, Feb. 1994.
- [82] H.-D. Chiang, F.F. Wu, and P.P. Varaiya, “A BCU method for direct analysis of power system transient stability,” *IEEE Trans. Power System*, vol. 9, no. 3, pp. 1194–1208, Aug. 1994.
- [83] E. Chiodo and D. Lauria, “Transient stability evaluation of multimachine power systems: a probabilistic approach based upon the extended equal area criterion,” *IEE Proceedings Generation, Transmission and Distribution*, vol. 141, no. 6, pp. 545–553, Nov. 1994.
- [84] C.-W. Liu and J. Thorp, “Application of synchronised phasor measurements to real-time transient stability prediction,” *IEE Proceedings Generation, Transmission and Distribution*, vol. 142, no. 4, pp. 355–360, July 1995.

- [85] H.D. Chiang, C.C. Chu, and G. Cauley, “Direct stability analysis of electric power systems using energy functions: Theory, applications, and perspective,” *IEEE Proceedings*, vol. 83, no. 11, pp. 1497–1529, Nov. 1995.
- [86] V. Vittal, J.D. McCalley, V. Van Acker, W. Fu, and N. Abi-Samra, “Transient instability risk assessment,” in *Proc. of 1999 IEEE PES Summer Meeting*, July 1999, vol. 1, pp. 206–211.
- [87] K.W. Chan, R.W. Dunn, and A.R. Daniels, “Transient and dynamic stability constraint assessment using hybrid TEF and clustering analysis,” in *Proc. of 2000 IEEE PES Winter Meeting*, 2000, vol. 2, pp. 1383–1388.
- [88] P.S. Karunadsa, U.D. Annakkage, and B.A. MacDonald, “Dynamic security control using secure regions derived from a decision tree technique,” in *Proc. of 2000 IEEE PES Summer Meeting*, 2000, vol. 3, pp. 1861–1865.
- [89] E. Vaahedi, W. Li, T. Chia, and H. Dommel, “Large scale probabilistic transient stability assessment using BC Hydro’s on-line tool,” *IEEE Trans. Power System*, vol. 15, no. 2, pp. 661–667, May 2000.
- [90] X.P. Gu and S.K. Tso, “Applying rough-set concept to neural-network-based transient stability classification of power systems,” in *Proc. of 2000 Intl. Conf. Advances in Power System Control, Operation and Management, APSCOM-00*, 2000, vol. 2, pp. 400–404.
- [91] D. Sutanto and W.R. Lachs, “Improving transient stability by containing accelerating energy,” in *Proc. of 2000 Intl. Conf. Advances in Power System Control, Operation and Management, APSCOM-00*, 2000, vol. 2, pp. 395–399.
- [92] L.F.C. Alberto, F.H.J.R. Silva, and N.G. Bretas, “Direct methods for transient

- stability analysis in power systems: State of art and future perspectives,” in *Proc. of 2001 IEEE Power Tech*, Porto, 2001, vol. 2, pp. 1–6.
- [93] CIGRE Study Committee 32, “Aids for the emergency control of power systems, Parts I and II,” in *Proc. of 1980 IEEE PES Winter Meeting*, New York, Feb. 1980, vol. A80, pp. 3–4.
- [94] E. W. Kimbark, “Improvement of power system stability by changes in the network,” *IEEE Trans. on Power Apparatus and Systems*, vol. PAS-88, no. 5, pp. 773–781, May 1969.
- [95] A.A. Grobovoy and N.N. Lizalek, “Multiple dynamic brake and power system emergency control,” in *Proc. of 1998 International Conference on Power System Technology*, 1998, vol. 2, pp. 1351–1355.
- [96] Y. Wang, A.A. Hashmani, and T.T. Lie, “Nonlinear co-ordinated excitation and TCPS controller for multimachine power system transient stability enhancement,” *IEE Proc.-Gener. Trans. Distrib.*, vol. 148, no. 2, pp. 133–141, Mar. 2001.
- [97] M. Tsuda, Y. Mitani, and K. Tsuji, “Application of resistor based superconducting fault current limiter to enhancement of power system transient stability,” *IEEE Trans. on Applied Superconductivity*, vol. 11, no. 1, pp. 2122–2125, Mar. 2001.
- [98] K. Sedraoui, K. Al-haddad, and G. Oliver, “A new approach for the dynamic control unified power flow controller (UPFC),” in *Proc. of 2001 IEEE PES Summer Meeting*, 2001, vol. 2, pp. 955–960.
- [99] A.C.M. Valle and A.O. Borges, “Fuzzy Logic controller simulating an SVC

- device in power system transient stability analysis,” in *Proc. of 2001 IEEE Porto Power Tech Conference*, Porto, Sep. 2001, vol. 1, pp. 1–4.
- [100] K. Duangkamol, Y. Mitani, and K. Tsuji, “Evaluation on fault current limiting and power system stabilization by a SMES with a series phase compensater,” in *Proc. of 2001 IEEE Porto Power Tech Conference*, Porto, Sep. 2001, vol. 1, pp. 1–6.
- [101] M. Ghandhari, G. Anderson, and I.A. Hiskens, “Control Lyapunov Functions for controllable series devices,” *IEEE Trans. Power System*, vol. 16, no. 4, pp. 689–694, Nov. 2001.
- [102] M.A. Pai, P.W. Sauer, and F. Dobraca, “A new approach to transient stability evaluation in power systems,” in *Proc. of the 27th IEEE Conference on Decision and Control*, Dec. 1988, vol. 1, pp. 676–680.
- [103] M. Jonsson and J. E. Daalder, “An adaptive scheme to prevent undesirable distance protection operation during voltage instability,” *IEEE Trans. Power Delivery*, vol. 18, no. 4, pp. 1174–1180, Oct. 2003.
- [104] IEEE PES Power Systems Relaying Committee, “Power Swing and Out-of-step Considerations on Transmission Lines,” Tech. Rep. Draft 7, Feb. 2005.
- [105] S. Tamronglak, “Analysis of power system disturbances due to relay hidden failures,” Ph.D. dissertation, Virginia Polytechnic Institute and State University, Blacksburg, Virginia, 1994.
- [106] M. Kezunovic, H. Song, and N. Zhang, “Detection, Prevention and Mitigation of Cascading Events: Part I of Final Project Report,” Tech. Rep. 05-59, Power Systems Engineering Research Center, 2005, [Online] Available:

<http://www.pserc.org>.

- [107] N. Zhang and M. Kezunovic, "Improving real-time fault analysis and validating relay operations to prevent or mitigate cascading blackouts," in *Proc. IEEE PES Transmission & Distribution Conference & Exposition*, Dallas, Texas, May. 2006, pp. 847–852.
- [108] T. Athay, R. Podmore, and S. Virmani, "A practical method for the direct analysis of transient stability," *IEEE Trans. on Power Apparatus and Systems*, vol. PAS-98, no. 2, pp. 573–584, March/April 1979.
- [109] M. H. Haque and A. H. M. A. Rahim, "Determination of first swing stability limit of multimachine power systems through taylor series expansions," *Generation, Transmission and Distribution, IEE Proceedings C*, vol. 136, no. 6, pp. 373–379, Nov. 1989.
- [110] R. D. Christie, "Power systems test case archive," Website of EE Dept. of University of Washington, Aug. 1999, [Online] Available: <http://www.ee.washington.edu/research/pstca/>.
- [111] S. K. M. Kodsi and C. A. Canizares, "Modeling and Simulation of IEEE 14 Bus System with FACTS Controllers," Tech. Rep. 2003-3, Waterloo, Canada, 2003, [Online] Available: <http://www.power.uwaterloo.ca/~claudio/papers/IEEEBenchmarkTFreport.pdf>.

APPENDIX A

IEEE 14-BUS TEST SYSTEM DATA

There are five tables for this test system data: Bus data, PV bus data, Line data, Generator data, Exciter data. People can find some data sources from [110,111] and modify them for their own research purpose.

Follows are some descriptions for data meaning.

Bus Type: 1: PQ bus; 2: PV bus; 3: Swing bus.

P_L, Q_L : real and reactive parts of the load at buses, in MVA value.

B_s : shunt capacitor at buses, in MVA value.

V_m : bus voltage magnitudes, in p.u. value. PQ bus voltage magnitudes will be set as 0 for power flow flat start.

Area: control area.

P_g : real power output of generators, in MVA value.

Q_g : reactive power output of PV buses, in MVA value. Some PV buses are not generators.

Q_{max} : Maximum reactive power output of PV buses, in MVA value.

Q_{min} : Minimum reactive power output of PV buses, in MVA value.

V_{sp} : Scheduled PV bus voltage magnitudes, in p.u. value.

P_{max} : Maximum real power output of generators, in MVA value.

fBus: from bus, the beginning bus of the line.

tBus: to bus, the ending bus of the line.

r : line resistance, in p.u. value.

x : line reactance, in p.u. value.

b : line charging capacitance, in p.u. value.

limit: transmission line limits, in MVA value.

tap-ratio: Non-nominal transformer ratios. 1 for lines and nominal transformers.

angle: phase-shifter angles.

H : generator inertial constant, in value of s at its own MVA rating.

D : damping, in value of s at its own MVA rating.

X_d : d-axis synchronous reactance, in value of p.u. at its own MVA rating.

X'_d : d-axis transient reactance, in value of p.u. at its own MVA rating.

X_q : q-axis synchronous reactance, in value of p.u. at its own MVA rating.

X'_q : q-axis transient reactance, in value of p.u. at its own MVA rating.

τ'_{d0} : d-axis open circuit transient time constant, in value of s.

τ'_{q0} : q-axis open circuit transient time constant, in value of s.

K_A : regulator gain.

K_E : exciter constant related to self-excited field.

K_F : regulator stabilizing circuit gain.

τ_A : regulator amplifier time constant.

τ_E : exciter time constant.

τ_F : regulator stabilizing circuit time constant.

K_{Se} : saturation parameter.

τ_{Se} : saturation parameter.

Table XXV. Bus data of IEEE 14-bus system

BusNo	Type	P_L (MVA)	Q_L (MVA)	B_s (MVA)	V_m	Area
1	3	0.00	0.00	0.00	1.060	1
2	2	21.70	12.70	0.00	1.045	1
3	2	94.20	19.00	0.00	1.010	1
4	1	47.80	-3.90	0.00	1.018	1
5	1	7.60	1.60	0.00	1.020	1
6	2	11.20	7.50	0.00	1.070	1
7	1	0.00	0.00	0.00	1.062	1
8	2	0.00	0.00	0.00	1.090	1
9	1	39.50	16.60	19.00	1.056	1
10	1	9.00	5.80	0.00	1.051	1
11	1	3.50	1.80	0.00	1.057	1
12	1	6.10	1.60	0.00	1.055	1
13	1	13.50	5.80	0.00	1.050	1
14	1	14.90	5.00	0.00	1.035	1

Table XXVI. PV bus data of IEEE 14-bus system

BusNo	P_g (MVA)	Q_g (MVA)	Q_{max} (MVA)	Q_{min} (MVA)	V_{sp} (p.u.)	P_{max} (MVA)
1	232.39	-16.89	300.00	-300.00	1.060	332.39
2	40.00	42.40	50.00	-40.00	1.045	140.00
3	20.00	23.39	40.00	0.00	1.010	100.00
6	18.00	12.24	24.00	-6.00	1.070	100.00
8	15.00	17.36	24.00	-6.00	1.090	100.00

Table XXVII. Line data of IEEE 14-bus system

LineNo	fBus	tBus	$r(\text{p.u.})$	$x(\text{p.u.})$	$b(\text{p.u.})$	limit(MVA)	tap-ratio	angle
1	5	6	0.00000	0.25202	0.00000	250	0.930	0.000
2	4	7	0.00000	0.20912	0.00000	250	0.970	0.000
3	4	9	0.00000	0.55618	0.00000	250	0.960	0.000
4	1	2	0.01938	0.05917	0.05280	250	1.000	0.000
5	2	3	0.04699	0.19797	0.04380	250	1.000	0.000
6	2	4	0.05811	0.17632	0.03740	250	1.000	0.000
7	1	5	0.05403	0.22304	0.04920	250	1.000	0.000
8	2	5	0.05695	0.17388	0.03400	250	1.000	0.000
9	3	4	0.06701	0.17103	0.03460	250	1.000	0.000
10	4	5	0.01335	0.04211	0.01280	250	1.000	0.000
11	7	8	0.00000	0.17615	0.00000	250	1.000	0.000
12	7	9	0.00000	0.11001	0.00000	250	1.000	0.000
13	9	10	0.03181	0.08450	0.00000	250	1.000	0.000
14	6	11	0.09498	0.19890	0.00000	250	1.000	0.000
15	6	12	0.12291	0.25581	0.00000	250	1.000	0.000
16	6	13	0.06615	0.13027	0.00000	250	1.000	0.000
17	9	14	0.12711	0.27038	0.00000	250	1.000	0.000
18	10	11	0.08205	0.19207	0.00000	250	1.000	0.000
19	12	13	0.22092	0.19988	0.00000	250	1.000	0.000
20	13	14	0.17093	0.34802	0.00000	250	1.000	0.000

Table XXVIII. Generator data of IEEE 14-bus system

GenNo	BusNo	MVA	$H(\text{s})$	$D(\text{s})$	$X_d(\text{p.u.})$	$X'_d(\text{p.u.})$	$X_q(\text{p.u.})$	$X'_q(\text{p.u.})$	$\tau'_{d0}(\text{s})$	$\tau'_{q0}(\text{s})$
1	1	615	5.148	0.00	0.8979	0.2995	0.646	0.646	7.40	0.00
2	2	60	6.540	0.00	1.0500	0.1850	0.980	0.360	6.10	0.30
3	3	60	6.540	0.00	1.0500	0.1850	0.980	0.360	6.10	0.30
4	6	25	5.060	0.00	1.2500	0.2320	1.220	0.715	4.75	1.50
5	8	25	5.060	0.00	1.2500	0.2320	1.220	0.715	4.75	1.50

Table XXIX. Exciter data of IEEE 14-bus system

GenNo	BusNo	K_A	K_E	K_F	τ_A (s)	τ_E (s)	τ_F (s)	K_{Se}	τ_{Se} (s)
1	1	200	1.00	0.0012	0.0250	0.000	1.00	0.0039	1.555
2	2	20	1.00	0.0010	0.0250	0.314	1.00	0.0039	1.555
3	3	20	1.00	0.0010	0.0250	0.314	1.00	0.0039	1.555
4	6	20	1.00	0.0010	0.0250	0.314	1.00	0.0039	1.555
5	8	20	1.00	0.0010	0.0250	0.314	1.00	0.0039	1.555

APPENDIX B

IEEE 24-BUS TEST SYSTEM DATA

There are five tables for this test system data: Bus data, PV bus data, Line data, Generator data, Exciter data. Data descriptions are the same as those in Appendix A. Data source can be found at [66]. The generators at the same bus have been combined into one generator. The generator data and exciter data have been changed accordingly into p.u. value at the system 100MVA base.

Table XXX. Bus data of IEEE 24-bus system

BusNo	Type	P_L (MVA)	Q_L (MVA)	B_s (MVA)	V_m	Area
1	2	108.00	22.00	0.00	1.035	1
2	2	97.00	20.00	0.00	1.035	1
3	1	180.00	37.00	0.00	0.977	1
4	1	74.00	15.00	0.00	1.040	1
5	1	71.00	14.00	0.00	0.975	1
6	1	136.00	28.00	-100	0.950	1
7	2	125.00	25.00	0.00	1.025	1
8	1	171.00	35.00	0.00	1.009	1
9	1	175.00	36.00	19.00	1.000	1
10	1	195.00	40.00	0.00	1.007	1
11	1	0.00	0.00	0.00	1.000	1
12	1	0.00	0.00	0.00	1.020	1
13	3	265.00	54.00	0.00	1.020	1
14	2	194.00	39.00	0.00	0.980	1
15	2	317.00	64.00	0.00	1.014	1
16	2	100.00	20.00	0.00	1.017	1
17	1	0.00	0.00	0.00	1.055	1
18	2	333.00	68.00	0.00	1.050	1
19	1	181.00	37.00	0.00	1.000	1
20	1	128.00	26.00	0.00	1.056	1
21	2	0.00	0.00	0.00	1.050	1
22	2	0.00	0.00	0.00	1.050	1
23	2	0.00	0.00	0.00	1.050	1
24	1	0.00	0.00	0.00	1.025	1

Table XXXI. PV bus data of IEEE 24-bus system

BusNo	P_g (MVA)	Q_g (MVA)	Q_{max} (MVA)	Q_{min} (MVA)	V_{sp} (p.u.)	P_{max} (MVA)
1	172.00	28.20	80.00	-50.00	1.035	192.00
2	172.00	14.00	80.00	-50.00	1.035	192.00
7	240.00	51.60	180.00	0.00	1.025	300.00
13	285.30	122.10	240.00	0.00	1.020	591.00
14	0.00	13.70	200.00	-50.00	0.980	200.00
15	215.00	0.05	110.00	-50.00	1.014	215.00
16	155.00	25.22	180.00	-50.00	1.017	155.00
18	400.00	137.40	200.00	-50.00	1.050	400.00
21	400.00	108.20	200.00	-50.00	1.050	400.00
22	300.00	-29.76	96.00	-60.00	1.050	300.00
23	660.00	135.36	310.00	-125.00	1.050	600.00

Table XXXII. Line data of IEEE 24-bus system

LineNo	fBus	tBus	$r(\text{p.u.})$	$x(\text{p.u.})$	$b(\text{p.u.})$	limit(MVA)	tap-ratio	angle
1	1	2	0.003	0.014	0.461	175	0.930	0.000
2	1	3	0.055	0.211	0.057	175	0.970	0.000
3	1	5	0.022	0.085	0.023	175	0.960	0.000
4	2	4	0.033	0.127	0.034	175	1.000	0.000
5	2	6	0.050	0.192	0.052	175	1.000	0.000
6	3	9	0.031	0.119	0.032	175	1.000	0.000
7	3	24	0.002	0.084	0.000	400	1.015	0.000
8	4	9	0.027	0.104	0.028	175	1.000	0.000
9	5	10	0.023	0.088	0.024	175	1.000	0.000
10	6	10	0.014	0.061	2.459	175	1.000	0.000
11	7	8	0.016	0.061	0.017	175	1.000	0.000
12	8	9	0.043	0.165	0.045	175	1.000	0.000
13	8	10	0.043	0.165	0.045	175	1.000	0.000
14	9	11	0.002	0.084	0.000	400	1.030	0.000
15	9	12	0.002	0.084	0.000	400	1.030	0.000
16	10	11	0.002	0.084	0.000	400	1.015	0.000
17	10	12	0.002	0.084	0.000	400	1.015	0.000
18	11	13	0.006	0.048	0.100	500	1.000	0.000
19	11	14	0.005	0.042	0.088	500	1.000	0.000
20	12	13	0.006	0.048	0.100	500	1.000	0.000
21	12	23	0.012	0.097	0.203	500	1.000	0.000
22	13	23	0.011	0.087	0.182	500	1.000	0.000
23	14	16	0.005	0.059	0.082	500	1.000	0.000
24	15	16	0.002	0.017	0.036	500	1.000	0.000
25	15	21	0.006	0.049	0.103	500	1.000	0.000
26	15	21	0.006	0.049	0.103	500	1.000	0.000
27	15	24	0.007	0.052	0.109	500	1.000	0.000
28	16	17	0.003	0.026	0.055	500	1.000	0.000
29	16	19	0.003	0.023	0.049	500	1.000	0.000
30	17	18	0.002	0.014	0.030	500	1.000	0.000
31	17	22	0.014	0.105	0.221	500	1.000	0.000
32	18	21	0.003	0.026	0.055	500	1.000	0.000
33	18	21	0.003	0.026	0.055	500	1.000	0.000
34	19	20	0.005	0.040	0.083	500	1.030	0.000
35	19	20	0.005	0.040	0.083	500	1.030	0.000
36	20	23	0.003	0.022	0.046	500	1.015	0.000
37	20	23	0.003	0.022	0.046	500	1.015	0.000
38	21	22	0.009	0.068	0.142	500	1.000	0.000

Table XXXIII. Generator data of IEEE 24-bus system

GenNo	BusNo	MVA	$H(s)$	$D(s)$	$X_d(p.u.)$	$X'_d(p.u.)$	$X_q(p.u.)$	$X'_q(p.u.)$	$\tau'_{d0}(s)$	$\tau'_{q0}(s)$
1	1	192	6.684	0.00	0.0298	0.0298	1.780	0.453	3.90	0.54
2	2	192	6.684	0.00	0.0298	0.0298	1.780	0.453	3.90	0.54
3	7	300	9.912	0.00	0.1259	0.1259	1.580	0.485	8.40	0.46
4	13	591	19.488	0.00	0.2475	0.2475	1.650	0.500	4.50	0.50
5	14	155	5.460	0.00	0.5460	0.5460	1.680	0.400	4.20	0.60
6	15	215	7.420	0.00	0.0090	0.0090	1.850	0.567	8.20	0.48
7	16	155	5.460	0.00	0.5460	0.5460	0.610	0.453	3.80	0.49
8	18	400	23.550	0.00	1.8840	1.8840	0.600	0.60	8.00	0.00
9	21	400	23.550	0.00	1.8840	1.8840	1.780	0.440	4.60	0.37
10	22	300	11.130	0.00	0.0247	0.0247	1.990	0.490	4.10	0.56
11	23	670	23.280	0.00	0.2236	0.2236	0.568	0.568	10.8	0.00

Table XXXIV. Exciter data of IEEE 24-bus system

GenNo	BusNo	K_A	K_E	K_F	$\tau_A(s)$	$\tau_E(s)$	$\tau_F(s)$	K_{Se}	$\tau_{Se}(s)$
1	1	20.00	1.00	0.0010	0.0250	0.3140	1.00	0.0039	1.5550
2	2	20.00	1.00	0.0010	0.0250	0.3140	1.00	0.0039	1.5550
3	7	20.00	1.00	0.0010	0.0250	0.3140	1.00	0.0039	1.5550
4	13	20.00	1.00	0.0010	0.0250	0.3140	1.00	0.0039	1.5550
5	14	20.00	1.00	0.0010	0.0250	0.3140	1.00	0.0039	1.5550
6	15	20.00	1.00	0.0010	0.0250	0.3140	1.00	0.0039	1.5550
7	16	20.00	1.00	0.0010	0.0250	0.3140	1.00	0.0039	1.5550
8	18	20.00	1.00	0.0010	0.0250	0.3140	1.00	0.0039	1.5550
9	21	20.00	1.00	0.0010	0.0250	0.3140	1.00	0.0039	1.5550
10	22	20.00	1.00	0.0010	0.0250	0.3140	1.00	0.0039	1.5550
11	23	20.00	1.00	0.0010	0.0250	0.3140	1.00	0.0039	1.5550

APPENDIX C

IEEE 39-BUS TEST SYSTEM DATA

There are five tables for this test system data: Bus data, PV bus data, Line data, Generator data, Exciter data. Data descriptions are the same as those in Appendix A. Data source can be found at [73]. People can modify them for their own research purpose.

Table XXXV. PV bus data of IEEE 39-bus system

BusNo	P_g (MVA)	Q_g (MVA)	Q_{max} (MVA)	Q_{min} (MVA)	V_{sp} (p.u.)	P_{max} (MVA)
30	250.00	144.92	99990	-99990	1.0475	350.00
31	572.83	207.04	99990	-99990	0.9820	1145.00
32	650.00	205.73	99990	-99990	0.9831	750.00
33	632.00	108.94	99990	-99990	0.9972	732.00
34	508.00	166.99	99990	-99990	1.0123	608.00
35	650.00	211.11	99990	-99990	1.0493	750.00
36	560.00	100.44	99990	-99990	1.0635	660.00
37	540.00	0.65	99990	-99990	1.0278	640.00
38	830.00	22.66	99990	-99990	1.0265	930.00
39	1000.00	87.88	99990	-99990	1.0300	1100.00

Table XXXVI. Bus data of IEEE 39-bus system

BusNo	Type	P_L (MVA)	Q_L (MVA)	B_s (MVA)	V_m	Area
1	1	0.00	0.00	0.00	1.047	1
2	1	0.00	0.00	0.00	1.049	1
3	1	322.00	2.40	0.00	1.030	1
4	1	500.00	184.00	0.00	1.003	1
5	1	0.00	0.00	0.00	1.005	1
6	1	0.00	0.00	0.00	1.007	1
7	1	233.80	84.00	0.00	0.996	1
8	1	522.00	176.00	0.00	0.995	1
9	1	0.00	0.00	0.00	1.028	1
10	1	0.00	0.00	0.00	1.017	1
11	1	0.00	0.00	0.00	1.012	1
12	1	8.50	88.00	0.00	1.000	1
13	1	0.00	0.00	0.00	1.014	1
14	1	0.00	0.00	0.00	1.011	1
15	1	320.00	153.00	0.00	1.015	1
16	1	329.00	32.30	0.00	1.032	1
17	1	0.00	0.00	0.00	1.034	1
18	1	158.00	30.00	0.00	1.031	1
19	1	0.00	0.00	0.00	1.050	1
20	1	680.00	103.00	0.00	0.991	1
21	1	274.00	115.00	0.00	1.032	1
22	1	0.00	0.00	0.00	1.050	1
23	1	247.50	84.60	0.00	1.045	1
24	1	308.60	-92.20	0.00	1.037	1
25	1	224.00	47.20	0.00	1.057	1
26	1	139.00	17.00	0.00	1.052	1
27	1	281.00	75.50	0.00	1.037	1
28	1	206.00	27.60	0.00	1.050	1
29	1	283.50	26.90	0.00	1.050	1
30	2	0.00	0.00	0.00	1.047	1
31	3	9.20	4.60	0.00	0.982	1
32	2	0.00	0.00	0.00	0.983	1
33	2	0.00	0.00	0.00	0.997	1
34	2	0.00	0.00	0.00	1.012	1
35	2	0.00	0.00	0.00	1.049	1
36	2	0.00	0.00	0.00	1.063	1
37	2	0.00	0.00	0.00	1.028	1
38	2	0.00	0.00	0.00	1.026	1
39	2	1104.00	250.00	0.00	1.030	1

Table XXXVII. Line data of IEEE 39-bus system

LineNo	fBus	tBus	r (p.u.)	x (p.u.)	b (p.u.)	limit(MVA)	tap-ratio	angle
1	2	1	0.00350	0.04110	0.69870	1000	0.930	0.000
2	39	1	0.00100	0.02500	0.75000	1000	0.970	0.000
3	3	2	0.00130	0.01510	0.25720	1000	0.960	0.000
4	25	2	0.00700	0.00860	0.14600	1000	1.000	0.000
5	4	3	0.00130	0.02130	0.22140	1000	1.000	0.000
6	18	3	0.00110	0.01330	0.21380	1000	1.000	0.000
7	5	4	0.00080	0.01280	0.13420	1000	1.000	0.000
8	14	4	0.00080	0.01290	0.13820	1000	1.000	0.000
9	6	5	0.00020	0.00260	0.04340	1000	1.000	0.000
10	4	5	0.01335	0.04211	0.01280	1000	1.000	0.000
11	7	8	0.00000	0.17615	0.00000	1000	1.000	0.000
12	7	9	0.00000	0.11001	0.00000	1000	1.000	0.000
13	9	10	0.03181	0.08450	0.00000	1000	1.000	0.000
14	6	11	0.09498	0.19890	0.00000	1000	1.000	0.000
15	6	12	0.12291	0.25581	0.00000	1000	1.000	0.000
16	6	13	0.06615	0.13027	0.00000	1000	1.000	0.000
17	9	14	0.12711	0.27038	0.00000	1000	1.000	0.000
18	10	11	0.08205	0.19207	0.00000	1000	1.000	0.000
19	12	13	0.22092	0.19988	0.00000	1000	1.000	0.000
20	13	14	0.17093	0.34802	0.00000	1000	1.000	0.000
21	7	8	0.00000	0.17615	0.00000	1000	1.000	0.000
22	7	9	0.00000	0.11001	0.00000	1000	1.000	0.000
23	9	10	0.03181	0.08450	0.00000	1000	1.000	0.000
24	6	11	0.09498	0.19890	0.00000	1000	1.000	0.000
25	6	12	0.12291	0.25581	0.00000	1000	1.000	0.000
26	6	13	0.06615	0.13027	0.00000	1000	1.000	0.000
27	9	14	0.12711	0.27038	0.00000	1000	1.000	0.000
28	10	11	0.08205	0.19207	0.00000	1000	1.000	0.000
29	12	13	0.22092	0.19988	0.00000	1000	1.000	0.000
30	13	14	0.17093	0.34802	0.00000	1000	1.000	0.000
31	7	8	0.00000	0.17615	0.00000	1000	1.000	0.000
32	7	9	0.00000	0.11001	0.00000	1000	1.000	0.000
33	9	10	0.03181	0.08450	0.00000	1000	1.000	0.000
34	6	11	0.09498	0.19890	0.00000	1000	1.000	0.000
35	6	12	0.12291	0.25581	0.00000	1000	1.000	0.000
36	6	13	0.06615	0.13027	0.00000	1000	1.000	0.000
37	9	14	0.12711	0.27038	0.00000	1000	1.000	0.000
38	10	11	0.08205	0.19207	0.00000	1000	1.000	0.000
39	12	13	0.22092	0.19988	0.00000	1000	1.000	0.000
40	13	14	0.17093	0.34802	0.00000	1000	1.000	0.000
41	7	8	0.00000	0.17615	0.00000	1000	1.000	0.000
42	7	9	0.00000	0.11001	0.00000	1000	1.000	0.000
43	9	10	0.03181	0.08450	0.00000	1000	1.000	0.000
44	6	11	0.09498	0.19890	0.00000	1000	1.000	0.000
45	6	12	0.12291	0.25581	0.00000	1000	1.000	0.000
46	6	13	0.06615	0.13027	0.00000	1000	1.000	0.000

Table XXXVIII. Generator data of IEEE 39-bus system

GenNo	BusNo	MVA	H (s)	D (s)	X_d (p.u.)	X'_d (p.u.)	X_q (p.u.)	X'_q (p.u.)	τ'_{d0} (s)	τ'_{g0} (s)
1	30	1000	3.50	0.00	0.310	0.310	0.310	0.310	8.96	0.310
2	31	1000	2.53	0.00	0.697	0.697	0.697	0.697	6.00	0.535
3	32	1000	2.98	0.00	0.531	0.531	0.531	0.531	5.89	0.600
4	33	1000	2.38	0.00	0.436	0.436	0.436	0.436	6.00	0.535
5	34	1000	2.17	0.00	1.320	1.320	1.320	1.320	6.00	0.535
6	35	1000	2.90	0.00	0.500	0.500	0.500	0.500	6.00	0.535
7	36	1000	2.20	0.00	0.490	0.490	0.490	0.490	6.00	0.535
8	37	1000	2.03	0.00	0.570	0.570	0.570	0.570	6.00	0.535
9	38	1000	2.88	0.00	0.570	0.570	0.570	0.570	6.00	0.535
10	39	1000	41.67	0.00	0.060	0.060	0.060	0.060	6.00	0.535

Table XXXIX. Exciter data of IEEE 39-bus system

GenNo	BusNo	K_A	K_E	K_F	τ_A (s)	τ_E (s)	τ_F (s)	K_{Se}	τ_{Se} (s)
1	30	20	1.00	0.0630	0.2500	0.3140	0.3500	0.0039	1.5550
2	31	20	1.00	0.0630	0.2500	0.3140	0.3500	0.0039	1.5550
3	32	20	1.00	0.0630	0.2500	0.3140	0.3500	0.0039	1.5550
4	33	20	1.00	0.0630	0.2500	0.3140	0.3500	0.0039	1.5550
5	34	20	1.00	0.0630	0.2500	0.3140	0.3500	0.0039	1.5550
6	35	20	1.00	0.0630	0.2500	0.3140	0.3500	0.0039	1.5550
7	36	20	1.00	0.0630	0.2500	0.3140	0.3500	0.0039	1.5550
8	37	20	1.00	0.0630	0.2500	0.3140	0.3500	0.0039	1.5550
9	38	20	1.00	0.0630	0.2500	0.3140	0.3500	0.0039	1.5550
10	39	20	1.00	0.0630	0.2500	0.3140	0.3500	0.0039	1.5550

APPENDIX D

IEEE 118-BUS TEST SYSTEM DATA

There are five tables for this test system data: Bus data, PV bus data, Line data, Generator data, Exciter data. Data descriptions are the same as those in Appendix A. People can find some data sources from [108–110] and modify for their own research purpose.

Table XL.: Bus data of IEEE 118-bus system

BusNo	Type	P_L (MVA)	Q_L (MVA)	B_s (MVA)	V_m	Area
1	2	51.00	27.00	0.00	0.955	1
2	1	20.00	9.00	0.00	0.971	1
3	1	39.00	10.00	0.00	0.968	1
4	2	39.00	12.00	0.00	0.998	1
5	1	0.00	0.00	-40.0	1.002	1
6	2	52.00	22.00	0.00	0.990	1
7	1	19.00	2.00	0.00	0.989	1
8	2	28.00	0.00	0.00	1.015	1
9	1	0.00	0.00	0.00	1.043	1
10	2	0.00	0.00	0.00	1.050	1
11	1	70.00	23.00	0.00	0.985	1
12	2	47.00	10.00	0.00	0.990	1
13	1	34.00	16.00	0.00	0.968	1
14	1	14.00	1.00	0.00	0.984	1
15	2	90.00	30.00	0.00	0.970	1
16	1	25.00	10.00	0.00	0.984	1
17	1	11.00	3.00	0.00	0.995	1
18	2	60.00	34.00	0.00	0.973	1
19	2	45.00	25.00	0.00	0.963	1
20	1	18.00	3.00	0.00	0.958	1
21	1	14.00	8.00	0.00	0.959	1
22	1	10.00	5.00	0.00	0.970	1
23	1	7.00	3.00	0.00	1.000	1
24	2	13.00	0.00	0.00	0.992	2
25	2	0.00	0.00	0.00	1.050	1
26	2	0.00	0.00	0.00	1.015	1
27	2	71.00	13.00	0.00	0.968	1
28	1	17.00	7.00	0.00	0.962	1
29	1	24.00	4.00	0.00	0.963	1

Continued on next page

Table XL – continued from previous page

BusNo	Type	P_L (MVA)	Q_L (MVA)	B_s (MVA)	V_m	Area
30	1	0.00	0.00	0.00	0.968	1
31	2	43.00	27.00	0.00	0.967	1
32	2	59.00	23.00	0.00	0.964	1
33	1	23.00	9.00	0.00	0.972	2
34	2	59.00	26.00	14.00	0.986	2
35	1	33.00	9.00	0.00	0.981	2
36	2	31.00	17.00	0.00	0.980	2
37	1	0.00	0.00	-25.0	0.992	2
38	1	0.00	0.00	0.00	0.962	2
39	1	27.00	11.00	0.00	0.970	2
40	2	66.00	23.00	0.00	0.970	2
41	1	37.00	10.00	0.00	0.967	2
42	2	96.00	23.00	0.00	0.985	2
43	1	18.00	7.00	0.00	0.978	2
44	1	16.00	8.00	10.00	0.985	2
45	1	53.00	22.00	10.00	0.987	2
46	2	28.00	10.00	10.00	1.005	2
47	1	34.00	0.00	0.00	1.017	2
48	1	20.00	11.00	15.00	1.021	2
49	2	87.00	30.00	0.00	1.025	2
50	1	17.00	4.00	0.00	1.001	2
51	1	17.00	8.00	0.00	0.967	2
52	1	18.00	5.00	0.00	0.957	2
53	1	23.00	11.00	0.00	0.946	2
54	2	113.00	32.00	0.00	0.955	2
55	2	63.00	22.00	0.00	0.952	2
56	2	84.00	18.00	0.00	0.954	2
57	1	12.00	3.00	0.00	0.971	2
58	1	12.00	3.00	0.00	0.959	2
59	2	277.00	113.00	0.00	0.985	2
60	1	78.00	3.00	0.00	0.993	2
61	2	0.00	0.00	0.00	0.995	2
62	2	77.00	14.00	0.00	0.998	2
63	1	0.00	0.00	0.00	0.969	2
64	1	0.00	0.00	0.00	0.984	2
65	2	0.00	0.00	0.00	1.005	2
66	2	39.00	18.00	0.00	1.050	2
67	1	28.00	7.00	0.00	1.020	2
68	1	0.00	0.00	0.00	1.003	2
69	3	0.00	0.00	0.00	1.035	2
70	2	66.00	20.00	0.00	0.984	2
71	1	0.00	0.00	0.00	0.987	2
72	2	12.00	0.00	0.00	0.980	2
73	2	6.00	0.00	0.00	0.991	2
74	2	68.00	27.00	12.00	0.958	3

Continued on next page

Table XL – continued from previous page

BusNo	Type	P_L (MVA)	Q_L (MVA)	B_s (MVA)	V_m	Area
75	1	47.00	11.00	0.00	0.967	3
76	2	68.00	36.00	0.00	0.943	3
77	2	61.00	28.00	0.00	1.006	3
78	1	71.00	26.00	0.00	1.003	3
79	1	39.00	32.00	20.00	1.009	3
80	2	130.00	26.00	0.00	1.040	3
81	1	0.00	0.00	0.00	0.997	3
82	1	54.00	27.00	20.00	0.989	3
83	1	20.00	10.00	10.00	0.985	3
84	1	11.00	7.00	0.00	0.980	3
85	2	24.00	15.00	0.00	0.985	3
86	1	21.00	10.00	0.00	0.987	3
87	2	0.00	0.00	0.00	1.015	3
88	1	48.00	10.00	0.00	0.987	3
89	2	0.00	0.00	0.00	1.005	3
90	2	163.00	42.00	0.00	0.985	3
91	2	10.00	0.00	0.00	0.980	3
92	2	65.00	10.00	0.00	0.993	3
93	1	12.00	7.00	0.00	0.987	3
94	1	30.00	16.00	0.00	0.991	3
95	1	42.00	31.00	0.00	0.981	3
96	1	38.00	15.00	0.00	0.993	3
97	1	15.00	9.00	0.00	1.011	3
98	1	34.00	8.00	0.00	1.024	3
99	2	42.00	0.00	0.00	1.010	3
100	2	37.00	18.00	0.00	1.017	3
101	1	22.00	15.00	0.00	0.993	3
102	1	5.00	3.00	0.00	0.991	3
103	2	23.00	16.00	0.00	1.001	3
104	2	38.00	25.00	0.00	0.971	3
105	2	31.00	26.00	20.00	0.965	3
106	1	43.00	16.00	0.00	0.962	3
107	2	50.00	12.00	6.00	0.952	3
108	1	2.00	1.00	0.00	0.967	3
109	1	8.00	3.00	0.00	0.967	3
110	2	39.00	30.00	6.00	0.973	3
111	2	0.00	0.00	0.00	0.980	3
112	2	68.00	13.00	0.00	0.975	3
113	2	6.00	0.00	0.00	0.993	1
114	1	8.00	3.00	0.00	0.960	1
115	1	22.00	7.00	0.00	0.960	1
116	2	184.00	0.00	0.00	1.005	2
117	1	20.00	8.00	0.00	0.974	1
118	1	33.00	15.00	0.00	0.949	3

Table XLI.: PV bus data of IEEE 118-bus system

BusNo	P_g (MVA)	Q_g (MVA)	Q_{max} (MVA)	Q_{min} (MVA)	V_{sp} (p.u.)	P_{max} (MVA)
1	0.00	0.00	15.00	-5.00	0.955	100.00
4	0.00	0.00	300.00	-300.00	0.998	100.00
6	0.00	0.00	50.00	-13.00	0.990	100.00
8	0.00	0.00	300.00	-300.00	1.015	100.00
10	450.00	0.00	250.00	-147.00	1.050	650.00
12	85.00	0.00	120.00	-35.00	0.990	185.00
15	0.00	0.00	30.00	-10.00	0.970	100.00
18	0.00	0.00	50.00	-16.00	0.973	100.00
19	0.00	0.00	24.00	-8.00	0.962	100.00
24	0.00	0.00	300.00	-300.00	0.992	100.00
25	220.00	0.00	140.00	-47.00	1.050	320.00
26	314.00	0.00	1000.00	-1000.00	1.015	414.00
27	0.00	0.00	300.00	-300.00	0.968	100.00
31	7.00	0.00	300.00	-300.00	0.967	107.00
32	0.00	0.00	42.00	-14.00	0.963	100.00
34	0.00	0.00	24.00	-8.00	0.984	100.00
36	0.00	0.00	24.00	-8.00	0.980	100.00
40	0.00	0.00	300.00	-300.00	0.970	100.00
42	0.00	0.00	300.00	-300.00	0.985	100.00
46	19.00	0.00	100.00	-100.00	1.005	119.00
49	204.00	0.00	210.00	-85.00	1.025	304.00
54	48.00	0.00	300.00	-300.00	0.955	148.00
55	0.00	0.00	23.00	-8.00	0.952	100.00
56	0.00	0.00	15.00	-8.00	0.954	100.00
59	155.00	0.00	180.00	-60.00	0.985	255.00
61	160.00	0.00	300.00	-100.00	0.995	260.00
62	0.00	0.00	20.00	-20.00	0.998	100.00
65	391.00	0.00	250.00	-67.00	1.005	591.00
66	392.00	0.00	250.00	-67.00	1.050	592.00
69	516.40	0.00	300.00	-300.00	1.035	805.20
70	0.00	0.00	32.00	-10.00	0.984	100.00
72	0.00	0.00	100.00	-100.00	0.980	100.00
73	0.00	0.00	100.00	-100.00	0.991	100.00
74	0.00	0.00	9.00	-6.00	0.958	100.00
76	0.00	0.00	23.00	-8.00	0.943	100.00
61	160.00	0.00	300.00	-100.00	0.995	260.00
77	0.00	0.00	70.00	-20.00	1.006	100.00
80	477.00	0.00	280.00	-165.00	1.040	677.00
85	0.00	0.00	23.00	-8.00	0.985	100.00
87	4.00	0.00	1000.00	-100.00	1.015	104.00
89	607.00	0.00	300.00	-210.00	1.005	807.00
90	0.00	0.00	300.00	-300.00	0.985	100.00
91	0.00	0.00	100.00	-100.00	0.980	100.00
92	0.00	0.00	9.00	-3.00	0.990	100.00
99	0.00	0.00	100.00	-100.00	1.010	100.00
100	252.00	0.00	155.00	-50.00	1.017	352.00
103	40.00	0.00	40.00	-15.00	1.010	140.00
104	0.00	0.00	23.00	-8.00	0.971	100.00
105	0.00	0.00	23.00	-8.00	0.965	100.00
107	0.00	0.00	250.00	-250.00	0.952	100.00
110	0.00	0.00	23.00	-8.00	0.973	100.00
111	36.00	0.00	1000.00	-100.00	0.980	136.00
112	0.01	0.00	1000.00	-100.00	0.975	100.00
113	0.00	0.00	250.00	-100.00	0.993	100.00
116	0.00	0.00	1000.00	-1000.00	1.005	100.00

Table XLII.: Line data of IEEE 118-bus system

LineNo	fBus	tBus	$r(\text{p.u.})$	$x(\text{p.u.})$	$b(\text{p.u.})$	limit(MVA)	tap-ratio	angle
1	1	2	0.03030	0.09990	0.02540	250	1.000	0.000
2	1	3	0.01290	0.04240	0.01082	250	1.000	0.000
3	4	5	0.00176	0.00798	0.00210	250	1.000	0.000
4	3	5	0.02410	0.10800	0.02840	250	1.000	0.000
5	5	6	0.01190	0.05400	0.01426	250	1.000	0.000
6	6	7	0.00459	0.02080	0.00550	250	1.000	0.000
7	8	9	0.00244	0.03050	1.16200	640	1.000	0.000
8	8	5	0.00000	0.02670	0.00000	510	0.985	0.000
9	9	10	0.00258	0.03220	1.23000	650	1.000	0.000
10	4	11	0.02090	0.06880	0.01748	250	1.000	0.000
11	5	11	0.02030	0.06820	0.01738	250	1.000	0.000
12	11	12	0.00595	0.01960	0.00502	250	1.000	0.000
13	2	12	0.01870	0.06160	0.01572	250	1.000	0.000
14	3	12	0.04840	0.16000	0.04060	250	1.000	0.000
15	7	12	0.00862	0.03400	0.00874	250	1.000	0.000
16	11	13	0.02225	0.07310	0.01876	250	1.000	0.000
17	12	14	0.02150	0.07070	0.01816	250	1.000	0.000
18	13	15	0.07440	0.24440	0.06268	250	1.000	0.000
19	14	15	0.05950	0.19500	0.05020	250	1.000	0.000
20	12	16	0.02120	0.08340	0.02140	250	1.000	0.000
21	15	17	0.01320	0.04370	0.04440	250	1.000	0.000
22	16	17	0.04540	0.18010	0.04660	250	1.000	0.000
23	17	18	0.01230	0.05050	0.01298	250	1.000	0.000
24	18	19	0.01119	0.04930	0.01142	250	1.000	0.000
25	19	20	0.02520	0.11700	0.02980	250	1.000	0.000
26	15	19	0.01200	0.03940	0.01010	250	1.000	0.000
27	20	21	0.01830	0.08490	0.02160	250	1.000	0.000
28	21	22	0.02090	0.09700	0.02460	250	1.000	0.000
29	22	23	0.03420	0.15900	0.04040	250	1.000	0.000
30	23	24	0.01350	0.04920	0.04980	250	1.000	0.000
31	23	25	0.01560	0.08000	0.08640	380	1.000	0.000
32	26	25	0.00000	0.03820	0.00000	380	0.960	0.000
33	25	27	0.03180	0.16300	0.17640	280	1.000	0.000
34	27	28	0.01913	0.08550	0.02160	250	1.000	0.000
35	28	29	0.02370	0.09430	0.02380	250	1.000	0.000
36	30	17	0.00000	0.03880	0.00000	520	0.960	0.000
37	8	30	0.00431	0.05040	0.51400	500	1.000	0.000
38	26	30	0.00799	0.08600	0.90800	380	1.000	0.000
39	17	31	0.04740	0.15630	0.03990	250	1.000	0.000
40	29	31	0.01080	0.03310	0.00830	250	1.000	0.000
41	23	32	0.03170	0.11530	0.11730	250	1.000	0.000
42	31	32	0.02980	0.09850	0.02510	250	1.000	0.000
43	27	32	0.02290	0.07550	0.01926	250	1.000	0.000
44	15	33	0.03800	0.12440	0.03194	250	1.000	0.000
45	19	34	0.07520	0.24700	0.06320	250	1.000	0.000
46	35	36	0.00224	0.01020	0.00268	250	1.000	0.000
47	35	37	0.01100	0.04970	0.01318	250	1.000	0.000
48	33	37	0.04150	0.14200	0.03660	250	1.000	0.000
49	34	36	0.00871	0.02680	0.00568	250	1.000	0.000
50	34	37	0.00256	0.00940	0.00984	250	1.000	0.000
51	38	37	0.00000	0.03750	0.00000	350	0.935	0.000
52	37	39	0.03210	0.10600	0.02700	250	1.000	0.000
53	37	40	0.05930	0.16800	0.04200	250	1.000	0.000
54	30	38	0.00464	0.05400	0.42200	250	1.000	0.000
55	39	40	0.01840	0.06050	0.01552	250	1.000	0.000
56	40	41	0.01450	0.04870	0.01222	250	1.000	0.000
57	40	42	0.05550	0.18300	0.04660	250	1.000	0.000
58	41	42	0.04100	0.13500	0.03440	250	1.000	0.000

Continued on next page

Table XLII – continued from previous page

LineNo	fBus	tBus	r(p.u.)	x(p.u.)	b(p.u.)	limit(MVA)	tap-ratio	angle
59	43	44	0.06080	0.24540	0.06068	250	1.000	0.000
60	34	43	0.04130	0.16810	0.04226	250	1.000	0.000
61	44	45	0.02240	0.09010	0.02240	250	1.000	0.000
62	45	46	0.04000	0.13560	0.03320	250	1.000	0.000
63	46	47	0.03800	0.12700	0.03160	250	1.000	0.000
64	46	48	0.06010	0.18900	0.04720	250	1.000	0.000
65	47	49	0.01910	0.06250	0.01604	250	1.000	0.000
66	42	49	0.07150	0.32300	0.08600	250	1.000	0.000
67	42	49	0.07150	0.32300	0.08600	250	1.000	0.000
68	45	49	0.06840	0.18600	0.04440	250	1.000	0.000
69	48	49	0.01790	0.05050	0.01258	250	1.000	0.000
70	49	50	0.02670	0.07520	0.01874	250	1.000	0.000
71	49	51	0.04860	0.13700	0.03420	250	1.000	0.000
72	51	52	0.02030	0.05880	0.01396	250	1.000	0.000
73	52	53	0.04050	0.16350	0.04058	250	1.000	0.000
74	53	54	0.02630	0.12200	0.03100	250	1.000	0.000
75	49	54	0.07300	0.28900	0.07380	250	1.000	0.000
76	49	54	0.07300	0.28900	0.07380	250	1.000	0.000
77	54	55	0.01690	0.07070	0.02020	250	1.000	0.000
78	54	56	0.00275	0.00955	0.00732	250	1.000	0.000
79	55	56	0.00488	0.01510	0.00374	250	1.000	0.000
80	56	57	0.03430	0.09660	0.02420	250	1.000	0.000
81	50	57	0.04740	0.13400	0.03320	250	1.000	0.000
82	56	58	0.03430	0.09660	0.02420	250	1.000	0.000
83	51	58	0.02550	0.07190	0.01788	250	1.000	0.000
84	54	59	0.05030	0.22930	0.05980	250	1.000	0.000
85	56	59	0.08250	0.25100	0.05690	250	1.000	0.000
86	56	59	0.08250	0.25100	0.05690	250	1.000	0.000
87	55	59	0.04739	0.21580	0.05646	250	1.000	0.000
88	59	60	0.03170	0.14500	0.03760	250	1.000	0.000
89	59	61	0.03280	0.15000	0.03880	250	1.000	0.000
90	60	61	0.00264	0.01350	0.01456	250	1.000	0.000
91	60	62	0.01230	0.05610	0.01468	250	1.000	0.000
92	61	62	0.00824	0.03760	0.00980	250	1.000	0.000
93	63	59	0.00000	0.03860	0.00000	250	0.960	0.000
94	63	64	0.00172	0.02000	0.21600	250	1.000	0.000
95	64	61	0.00000	0.02680	0.00000	250	0.985	0.000
96	38	65	0.00901	0.09860	1.04600	250	1.000	0.000
97	64	65	0.00269	0.03020	0.38000	250	1.000	0.000
98	49	66	0.01800	0.09190	0.02480	250	1.000	0.000
99	49	66	0.01800	0.09190	0.02480	250	1.000	0.000
100	62	66	0.04820	0.21800	0.05780	250	1.000	0.000
101	62	67	0.02580	0.11700	0.03100	250	1.000	0.000
102	65	66	0.00000	0.03700	0.00000	250	0.935	0.000
103	66	67	0.02240	0.10150	0.02682	250	1.000	0.000
104	65	68	0.00138	0.01600	0.63800	480	1.000	0.000
105	47	69	0.08440	0.27780	0.07092	250	1.000	0.000
106	49	69	0.09850	0.32400	0.08280	250	1.000	0.000
107	68	69	0.00000	0.03700	0.00000	500	0.935	0.000
108	69	70	0.03000	0.12700	0.12200	300	1.000	0.000
109	24	70	0.00221	0.41150	0.10198	250	1.000	0.000
110	70	71	0.00882	0.03550	0.00878	250	1.000	0.000
111	24	72	0.04880	0.19600	0.04880	250	1.000	0.000
112	71	72	0.04460	0.18000	0.04444	250	1.000	0.000
113	71	73	0.00866	0.04540	0.01178	250	1.000	0.000
114	70	74	0.04010	0.13230	0.03368	250	1.000	0.000
115	70	75	0.04280	0.14100	0.03600	250	1.000	0.000
116	69	75	0.04050	0.12200	0.12400	280	1.000	0.000
117	74	75	0.01230	0.04060	0.01034	250	1.000	0.000

Continued on next page

Table XLII – continued from previous page

LineNo	fBus	tBus	r(p.u.)	x(p.u.)	b(p.u.)	limit(MVA)	tap-ratio	angle
118	76	77	0.04440	0.14800	0.03680	250	1.000	0.000
119	69	77	0.03090	0.10100	0.10380	580	1.000	0.000
120	75	77	0.06010	0.19990	0.04978	250	1.000	0.000
121	77	78	0.00376	0.01240	0.01264	250	1.000	0.000
122	78	79	0.00546	0.02440	0.00648	250	1.000	0.000
123	77	80	0.01700	0.04850	0.04720	250	1.000	0.000
124	77	80	0.02940	0.10500	0.02280	250	1.000	0.000
125	79	80	0.01560	0.07040	0.01870	250	1.000	0.000
126	68	81	0.00175	0.02020	0.80800	560	1.000	0.000
127	81	80	0.00000	0.03700	0.00000	560	0.935	0.000
128	77	82	0.02980	0.08530	0.08174	250	1.000	0.000
129	82	83	0.01120	0.03665	0.03796	250	1.000	0.000
130	83	84	0.06250	0.13200	0.02580	250	1.000	0.000
131	83	85	0.04300	0.14800	0.03480	250	1.000	0.000
132	84	85	0.03020	0.06410	0.01234	250	1.000	0.000
133	85	86	0.03500	0.12300	0.02760	250	1.000	0.000
134	86	87	0.02828	0.20740	0.04450	250	1.000	0.000
135	85	88	0.02000	0.10200	0.02760	250	1.000	0.000
136	85	89	0.02390	0.17300	0.04700	250	1.000	0.000
137	88	89	0.01390	0.07120	0.01934	250	1.000	0.000
138	89	90	0.05180	0.18800	0.05280	250	1.000	0.000
139	89	90	0.02380	0.09970	0.10600	250	1.000	0.000
140	90	91	0.02540	0.08360	0.02140	250	1.000	0.000
141	89	92	0.00990	0.05050	0.05480	250	1.000	0.000
142	89	92	0.03930	0.15810	0.04140	250	1.000	0.000
143	91	92	0.03870	0.12720	0.03268	250	1.000	0.000
144	92	93	0.02580	0.08480	0.02180	250	1.000	0.000
145	92	94	0.04810	0.15800	0.04060	250	1.000	0.000
146	93	94	0.02230	0.07320	0.01876	250	1.000	0.000
147	94	95	0.01320	0.04340	0.01110	250	1.000	0.000
148	80	96	0.03560	0.18200	0.04940	250	1.000	0.000
149	82	96	0.01620	0.05300	0.05440	250	1.000	0.000
150	94	96	0.02690	0.08690	0.02300	250	1.000	0.000
151	80	97	0.01830	0.09340	0.02540	250	1.000	0.000
152	80	98	0.02380	0.10800	0.02860	250	1.000	0.000
153	80	99	0.04540	0.20600	0.05460	250	1.000	0.000
154	92	100	0.06480	0.29500	0.04720	250	1.000	0.000
155	94	100	0.01780	0.05800	0.06040	250	1.000	0.000
156	95	96	0.01710	0.05470	0.01474	250	1.000	0.000
157	96	97	0.01730	0.08850	0.02400	250	1.000	0.000
158	98	100	0.03970	0.17900	0.04760	250	1.000	0.000
159	99	100	0.01800	0.08130	0.02160	250	1.000	0.000
160	100	101	0.02770	0.12620	0.03280	250	1.000	0.000
161	92	102	0.01230	0.05590	0.01464	250	1.000	0.000
162	101	102	0.02460	0.11200	0.02940	250	1.000	0.000
163	100	103	0.01600	0.05250	0.05360	250	1.000	0.000
164	100	104	0.04510	0.20400	0.05410	250	1.000	0.000
165	103	104	0.04660	0.15840	0.04070	250	1.000	0.000
166	103	105	0.05350	0.16250	0.04080	250	1.000	0.000
167	100	106	0.06050	0.22900	0.06200	250	1.000	0.000
168	104	105	0.00994	0.03780	0.00986	250	1.000	0.000
169	105	106	0.01400	0.05470	0.01434	250	1.000	0.000
170	105	107	0.05300	0.18300	0.04720	250	1.000	0.000
171	105	108	0.02610	0.07030	0.01844	250	1.000	0.000
172	106	107	0.05300	0.18300	0.04720	250	1.000	0.000
173	108	109	0.01050	0.02880	0.00760	250	1.000	0.000
174	103	110	0.03906	0.18130	0.04610	250	1.000	0.000
175	109	110	0.02780	0.07620	0.02020	250	1.000	0.000
176	110	111	0.02200	0.07550	0.02000	250	1.000	0.000

Continued on next page

Table XLII – continued from previous page

LineNo	fBus	tBus	r (p.u.)	x (p.u.)	b (p.u.)	limit(MVA)	tap-ratio	angle
177	110	112	0.02470	0.06400	0.06200	250	1.000	0.000
178	17	113	0.00913	0.03010	0.00768	250	1.000	0.000
179	32	113	0.06150	0.20300	0.05180	250	1.000	0.000
180	32	114	0.01350	0.06120	0.01628	250	1.000	0.000
181	27	115	0.01640	0.07410	0.01972	250	1.000	0.000
182	114	115	0.00230	0.01040	0.00276	250	1.000	0.000
183	68	116	0.00034	0.00405	0.16400	300	1.000	0.000
184	12	117	0.03290	0.14000	0.03580	250	1.000	0.000
185	75	118	0.01450	0.04810	0.01198	250	1.000	0.000
186	76	118	0.01640	0.05440	0.01356	250	1.000	0.000

Table XLIII. Generator data of IEEE 118-bus system

GenNo	BusNo	MVA	H (s)	D (s)	X_d (p.u.)	X'_d (p.u.)	X_q (p.u.)	X'_q (p.u.)	τ'_{d0} (s)	τ'_{q0} (s)
1	10	800	8.00	0.00	0.0875	0.0875	0.0875	0.0875	7.40	0.000
2	12	800	22.00	0.00	0.0636	0.0636	0.0636	0.0636	6.10	0.300
3	25	800	8.00	0.00	0.1750	0.1750	0.1750	0.1750	6.10	0.300
4	26	800	14.00	0.00	0.1000	0.1000	0.1000	0.1000	4.75	1.500
5	31	800	26.00	0.00	0.0538	0.0538	0.0538	0.0538	4.75	1.500
6	46	800	8.00	0.00	0.0875	0.0875	0.0875	0.0875	7.40	0.000
7	49	800	8.00	0.00	0.0875	0.0875	0.0875	0.0875	6.10	0.300
8	54	800	8.00	0.00	0.0875	0.0875	0.0875	0.0875	6.10	0.300
9	59	800	8.00	0.00	0.0875	0.0875	0.0875	0.0875	4.75	1.500
10	61	800	12.00	0.00	0.1167	0.1167	0.1167	0.1167	4.75	1.500
11	65	800	10.00	0.00	0.1400	0.1400	0.1400	0.1400	7.40	0.000
12	66	800	12.00	0.00	0.1167	0.1167	0.1167	0.1167	6.10	0.300
13	69	800	20.00	0.00	0.0700	0.0700	0.0700	0.0700	6.10	0.300
14	80	800	20.00	0.00	0.0700	0.0700	0.0700	0.0700	4.75	1.500
15	87	800	30.00	0.00	0.0467	0.0467	0.0467	0.0467	4.75	1.500
16	89	800	38.148	0.00	0.0500	0.0500	0.0500	0.0500	7.40	0.000
17	100	800	32.00	0.00	0.0438	0.0438	0.0438	0.0438	6.10	0.300
18	103	800	8.00	0.00	0.0875	0.0875	0.0875	0.0875	6.10	0.300
19	111	800	16.00	0.00	0.0875	0.0875	0.0875	0.0875	4.75	1.500
20	112	800	15.00	0.00	0.0467	0.0467	0.0467	0.0467	4.75	1.500

Table XLIV. Exciter data of IEEE 118-bus system

GenNo	BusNo	K_A	K_E	K_F	τ_A (s)	τ_E (s)	τ_F (s)	K_{Se}	τ_{Se} (s)
1	10	20	1.00	0.0012	0.0250	0.000	1.00	0.0039	1.555
2	12	20	1.00	0.0010	0.0250	0.314	1.00	0.0039	1.555
3	25	20	1.00	0.0010	0.0250	0.314	1.00	0.0039	1.555
4	26	20	1.00	0.0010	0.0250	0.314	1.00	0.0039	1.555
5	31	20	1.00	0.0010	0.0250	0.314	1.00	0.0039	1.555
6	46	20	1.00	0.0012	0.0250	0.000	1.00	0.0039	1.555
7	49	20	1.00	0.0010	0.0250	0.314	1.00	0.0039	1.555
8	54	20	1.00	0.0010	0.0250	0.314	1.00	0.0039	1.555
9	59	20	1.00	0.0010	0.0250	0.314	1.00	0.0039	1.555
10	61	20	1.00	0.0010	0.0250	0.314	1.00	0.0039	1.555
11	65	20	1.00	0.0012	0.0250	0.000	1.00	0.0039	1.555
12	66	20	1.00	0.0010	0.0250	0.314	1.00	0.0039	1.555
13	69	20	1.00	0.0010	0.0250	0.314	1.00	0.0039	1.555
14	80	20	1.00	0.0010	0.0250	0.314	1.00	0.0039	1.555
15	87	20	1.00	0.0010	0.0250	0.314	1.00	0.0039	1.555
16	89	20	1.00	0.0012	0.0250	0.000	1.00	0.0039	1.555
17	100	20	1.00	0.0010	0.0250	0.314	1.00	0.0039	1.555
18	103	20	1.00	0.0010	0.0250	0.314	1.00	0.0039	1.555
19	111	20	1.00	0.0010	0.0250	0.314	1.00	0.0039	1.555
20	112	20	1.00	0.0010	0.0250	0.314	1.00	0.0039	1.555

VITA

Hongbiao Song received his B.S. and M.S. degrees in electrical engineering from North China Electric Power University, Baoding and Beijing, China, in 1999 and 2002 respectively. Since Aug. 2002, he has been with Texas A&M University pursuing his Ph.D. degree under the supervision of Dr. Mladen Kezunovic in the Department of Electrical and Computer Engineering. His research interests are power system analysis, simulation, stability, control, cascading events, protection, substation automation, data integration and information exchange, intelligent systems.

His permanent address is Ya He Dian Chang Yun Xing Bu, Nanyang, Henan, 473001, China.

The typist for this thesis was Hongbiao Song.